frontiers in Built Environment

REVIEW
published: 16 March 2022
doi: 10.3389/fbuil.2022.811460

Applications of Machine Learning to Wind Engineering

Teng Wu[1]* *and Reda Snaiki*[2]

[1]Department of Civil, Structural and Environmental Engineering, University at Buffalo, Buffalo, NY, United States, [2]Department of Construction Engineering, École de Technologie Supérieure, University of Quebec, Montreal, QC, Canada

Advances of the analytical, numerical, experimental and field-measurement approaches in wind engineering offers unprecedented volume of data that, together with rapidly evolving learning algorithms and high-performance computational hardware, provide an opportunity for the community to embrace and harness full potential of machine learning (ML). This contribution examines the state of research and practice of ML for its applications to wind engineering. In addition to ML applications to wind climate, terrain/topography, aerodynamics/aeroelasticity and structural dynamics (following traditional Alan G. Davenport Wind Loading Chain), the review also extends to cover wind damage assessment and wind-related hazard mitigation and response (considering emerging performance-based and resilience-based wind design methodologies). This state-of-the-art review suggests to what extend ML has been utilized in each of these topic areas within wind engineering and provides a comprehensive summary to improve understanding how learning algorithms work and when these schemes succeed or fail. Moreover, critical challenges and prospects of ML applications in wind engineering are identified to facilitate future research efforts.

Keywords: machine learning, wind engineering, wind climate, terrain and topography, aerodynamics and aeroelasticity, structural dynamics, wind damage assessment, hazard mitigation and response

OPEN ACCESS

Edited by:
Forrest J. Masters, University of Florida, United States

Reviewed by:
Girma Bitsuamlak, Western University, Canada
Pedro L. Fernández-Cabán, Clarkson University, United States
Muhammad Hajj, Stevens Institute of Technology, United States

***Correspondence:**
Teng Wu
tengwu@buffalo.edu

Specialty section:
This article was submitted to Wind Engineering and Science, a section of the journal Frontiers in Built Environment

Received: *08 November 2021*
Accepted: *27 January 2022*
Published: *16 March 2022*

Citation:
Wu T and Snaiki R (2022) Applications of Machine Learning to Wind Engineering. Front. Built Environ. 8:811460. doi: 10.3389/fbuil.2022.811460

1 INTRODUCTION

Wind engineering is an interdisciplinary field to provide rational treatment of interaction between the atmospheric boundary-layer winds and human activities (Cermak 1975). There is a long and significant history for machine learning (ML) applications in several subfields involved in wind engineering, such as fluid mechanics (Brunton et al., 2020), meteorology (Chen et al., 2020) and mechanics of structures (Salehi and Burgueño 2018). The application of statistical learning to turbulence modeling in early 1940s (Kolmogorov 1941) and perceptron learning to structural design in late 1980s (Adeli and Yeh 1989) are representative examples. On the other hand, it seems similar passions have not been shared by researchers in the wind engineering community. Actually, ML-based wind engineering is still in its infancy stage and the full-capacity of ML has not been leveraged yet. However, the exceptional performance of ML to extract hidden informative features from data shows great promise for addressing unresolved complexities and issues originated from first principles investigations in the field of wind engineering. In addition, recent advances in performance-/resilience-based wind engineering have placed new demands on wind characterization, aerodynamics modeling and structural analysis that need powerful simulation tools such as ML to overcome the emerging challenges by simultaneously achieving high computational efficiency and accuracy. It is reasonable to expect the revitalization of ML within the wind engineering field that is fueled by 1) rapidly evolving learning algorithms and

high-performance computational hardware, 2) unprecedented volume of data generated with improved wind engineering techniques and methodologies, and 3) urgent needs for more accurate and efficient learning and modeling of complex phenomena in wind-related problems.

As a key subfield of artificial intelligence (AI) [that together with natural intelligence plays a role of the computational part of the ability to achieve goals in the world (McCarthy 2007)], ML develops learning algorithms that use inputs from a sample generator and observations from a system to generate an approximation of its outputs (Cherkassky and Mulier 2007). The evolution of learning algorithms started when McCulloch and Pitts (1943) invented the first mathematical model of a neural network. In 1952, Arthur Samuel from IBM introduced the first self-learning computer program to play the game of checkers (Wiederhold et al., 1990). Then, Rosenblatt (1957) designed the first neural network for computers (the perceptron) that set the foundation of deep neural networks (DNNs). Kelley (1960) presented the method of gradients (or method of steepest descent) in his analytical development of flight performance optimization, which was used to develop the basics of a continuous backpropagation model for training feedforward neural networks (Rumelhart et al., 1986). On the other hand, Hopfield (1982) created a feedback neural network that was considered as the first recurrent neural network (RNN). LeCun et al. (1989) combined convolutional neural network (CNN) and backpropagation algorithm to recognize handwritten digits. Watkins (1989) introduced the concept of Q-learning based on Markov process to significantly enhance the practicability and feasibility of reinforcement learning. Later, Cortes and Vapnik (1995) designed a support-vector network considered as a new learning machine for two-group classification problems with high generalization ability. Hochreiter and Schmidhuber (1997) introduced a long short-term memory cell to address the long-term dependency issue in RNN. To overcome the learning difficulty in DNNs, Hinton et al. (2006) derived a fast, greedy algorithm that can learn deep, directed belief networks one layer at a time and hence facilitate the rapid development of deep learning. Recently, Goodfellow et al. (2014) proposed a generative adversarial network consisting of two models (i.e., generative and discriminative models) that compete with each other in a zero-sum game. The sophisticated ML algorithm needs the help of advanced computational hardware [e.g., graphics processing unit (GPU) and tensor processing unit (TPU)] to unlock its full potential (Berggren et al., 2020). For example, the great success of AlexNet (a deep CNN on GPU) is essentially attributed to its ability to leverage GPU for training (Krizhevsky et al., 2012).

Equipped with both sophisticated algorithms and advanced computational hardware, the learning machine (LM) is driven by data. Both the quantity (data rich and comprehensive) and quality of the training/testing data are important to ensure good performance of ML applications. Wind engineering by nature is a data-rich field (e.g., high spatial and temporal resolution), and it is rapidly becoming a data-comprehensive domain due to recent advances of analytical, numerical, experimental and field-measurement methods (Kareem and Wu 2013; Hangan et al., 2017). The data of spatiotemporally varying wind flows are extended from synoptic events measured by airport wind observation system with traditional anemometers to non-synoptic events measured by several field campaigns with advanced doppler radars and Lidars (Light Detection and Ranging) [e.g., Verification of the Origins of Rotation in Tornadoes Experiment (VORTEX) and Radar Observations of Tornadoes and Thunderstorms Experiment (ROTATE) campaigns for tornado events and Severe Convective OUtflow in Thunderstorms (SCOUT) and Wind Ports and Sea (WPS) campaigns for thunderstorm downburst events]. Massive wind data over complex terrain/topography are collected by continuous-wave short-range WindScanner systems (e.g., Berg et al., 2013). The low Reynolds-number, straight-line-wind, stationary aerodynamics data generated in conventional boundary-layer wind tunnels are extended to 1) high-Reynolds-number aerodynamics data resulting from recently built large-scale facilities [e.g., windstorm simulation facility at Insurance Institute for Business and Home Safety (IBHS), Wall of Wind (WOW) at Florida International University and Wind Engineering Energy and Environment (WindEEE) at Western University], 2) vortex-flow aerodynamics data produced by tornado simulators (e.g., tornado-like vortex simulator at Iowa State University and VorTECH at Texas Tech University), and 3) transient aerodynamics data generated in emerging actively controlled wind tunnels (e.g., individually-controlled multi-fan wind tunnels at Tongji University, University at Buffalo and University of Florida). Also, significant nonlinear and inelastic structural dynamics data under strong winds are being created in laboratories due to advances in performance-based wind design methodology (Abdullah et al., 2020). In addition to the experimental and field-measurement approaches the comprehensive data are further enriched by high-fidelity large-scale simulation tools that are advanced by theoretical developments in wind engineering field (Blocken 2014; Kareem 2020), such as computational fluid dynamics/computational structural dynamics (CFS/CSI)-based hybrid modeling of transient structural response (Hao and Wu 2018) and statistics-based synthesis of nonstationary wind field (Wang and Wu 2021). The Computational Modeling and Simulation Center (SimCenter) of the Natural Hazards Engineering Research Infrastructure (NHERI) program provides an effective way to integrate various simulation tools (Deierlein and Zsarnóczay 2021). Furthermore, novel real-time aerodynamics hybrid simulation techniques are emerging to effectively generate nonlinear and full-scale data in wind engineering by seamlessly stitching the numerical modeling in computer and physical testing in wind tunnel (Wu et al., 2019; Wu and Song 2019). Data quality is essential to facilitate curation and reuse of the diverse and large datasets generated in the field of wind engineering. There are numerous methods and criteria specified by various wind engineering research groups/centers to ensure the high data quality, and the NHERI DesignSafe cyberinfrastructure platform recently suggested the best practices for detailed data quality assessment in terms of metadata quality, data content quality, data completeness and representation and data publications review (Rathje et al., 2017).

The improved understanding concerning the complex nature of wind fields (e.g., nonstationary and non-Gaussian features), the

associated structural aerodynamics/aeroelasticity (e.g., transient and nonlinear features) and the resulting load effects (e.g., nonlinear and inelastic structural response), as well as the necessary shift from a prescriptive design approach to performance-based design methodology and further to resilience-based design philosophy (i.e., improving the rapidity, robustness, resourcefulness and redundancy), poses new challenges in wind engineering field. Hence, there is an urgent need of more accurate and efficient learning and modeling tools for effective solutions. The conventional stationary and linear analysis framework for wind-structure interactions established by Robert H. Scanlan (1914–2001) and Alan G. Davenport (1932–2009) has been very successful due to its simplicity and applicability, however, its shortcomings have begun to surface since the underlying complexities associated with many wind engineering problems clearly show a departure from implicit assumptions of stationarity, Gaussianity and linear features. A number of semi-empirical nonlinear reduced-order models have been developed in this context and improvement in their efficiency and robustness is a topic of cutting-edge research in the wind engineering community (Wu 2013). Unfortunately, these reduced-order models do not always have a satisfactory representation of the full nonlinear equations which govern the complex phenomena in wind-related problems. An alternate way is to utilize the CFD techniques, however, their computational effort is too high considering the three-dimensional nature of winds and associated bluff-body aerodynamics. While CFD plays a significant role in generating high-fidelity data of complex wind-structure interactions, its high computational cost makes it not easy to be used either in an informational mode to enhance wind hazard-related planning and development activities (e.g., risk mitigation that needs to quickly run thousands of scenarios at minimal computational expense) or in an operational mode to support emergency management and response associated with a wind hazard (e.g., decision making that needs real-time prediction capability under an uncertain environment). To address the emerging challenges, data-driven machine learning offers a promising approach that is capable of processing big data in wind engineering field as well as modeling associated complex phenomena with high computational efficiency and simulation accuracy.

With the rapid development of ML applications in wind engineering due to the confluence of advanced learning algorithms, high-performance computational hardware and big data, it is believed that a systematic review on this subject is important to suggest to what extend ML has been utilized in each of the topic areas within wind engineering and provide a comprehensive summary to improve understanding how learning algorithms work and when these schemes succeed or fail. Specifically, a total of 65 ML algorithms (**Appendix A**) are identified for their applications in the five topic areas of wind climate, terrain/topography, aerodynamics/aeroelasticity, structural dynamics and damage assessment, and mitigation and response. This review first presents technical background of typical ML approaches in terms of supervised learning, unsupervised learning, semi-supervised learning and reinforcement learning (RL), followed by the state of research and practice of ML applications to each topic area within wind engineering field, and concluded with critical research gaps and future prospects. While ML can augment the analytical approaches [e.g., data-driven discovery of closure models (Raissi et al., 2019)], numerical schemes [e.g., data-driven turbulence modeling (Duraisamy et al., 2019)], experimental tests [e.g., data-driven active control of transient wind simulation (Li et al., 2021a)] and field measurements [e.g., data-driven sparse sensor placement (Manohar et al., 2018)] in wind engineering, the review only focuses on its role to complement existing methodologies and hence potentially extend/transform current lines of wind engineering research and practice.

2 BACKGROUND OF MACHINE LEARNING

Machine learning (ML) is a subclass of artificial intelligence (AI) that extracts the underlying pattern within a set of data (e.g., Murphy 2012; Goodfellow et al., 2016; Mohri et al., 2018). To acquire the hidden pattern and knowledge of a problem, the learning process involves in general five important steps, namely data collection, data preparation, training, evaluation and parameters tuning. Once the learning machine is trained based on the available data (usually retrieved from analytical solutions, numerical simulations, experimental tests or full-scale measurements), it can predict future or unseen events. Based on the data fed into the learning machine, ML algorithms can be classified into four categories, namely supervised learning, unsupervised learning, semi-supervised learning and reinforcement learning (**Figure 1**).

To train the algorithm, the supervised learning fully depends on labeled data, the unsupervised learning relies purely on unlabeled data and the semi-supervised learning combines limited labeled data with a large amount of unlabeled data. For reinforcement learning (RL), there is essentially no predefined data. Although RL is occasionally treated as semi-supervised learning considering the agent learns from its own experiences in terms of infrequent and partial rewards, it is classified here into separate category to highlight there is no explicit, external supervisory information provided to the learning agent. It is noted the kriging and polynomial chaos expansions as two widely-used, data-driven statistical interpolation approaches are not reviewed in this study.

2.1 Supervised Learning

Supervised learning models are a set of algorithms that learn the mapping, from given labeled training data, between known inputs and outputs. The trainable parameters of these models are determined based on the minimization of the loss function. Supervised learning models usually require a large amount of reliable and unbiased data for training which might not be always available. These algorithms can be employed for two important tasks, namely regression and classification.

2.1.1 Regression

Regression is a type of supervised learning in which the output is a numeric variable. Among many regression models, feed-forward

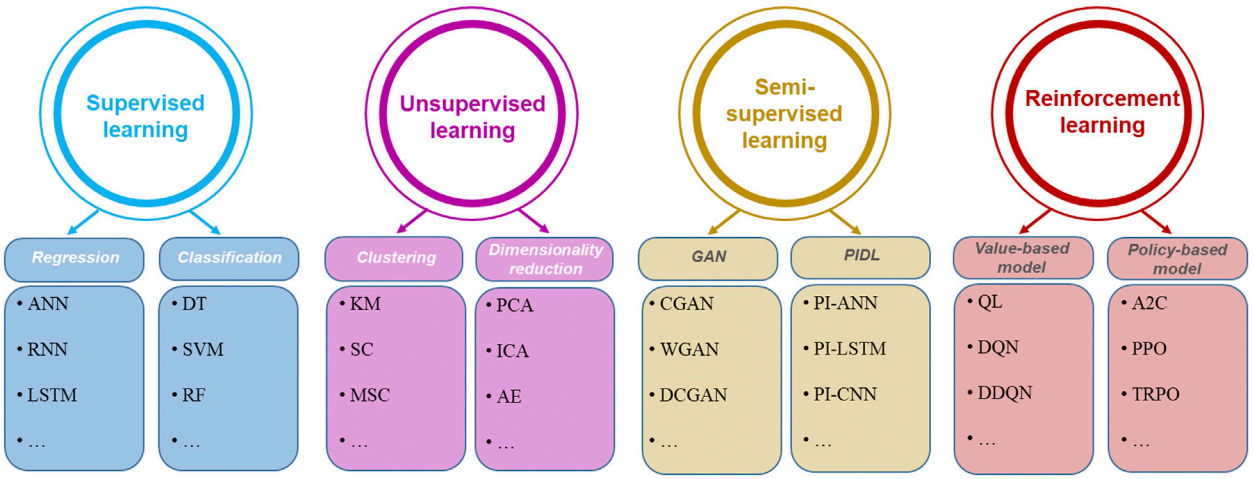

FIGURE 1 | Machine learning categories.

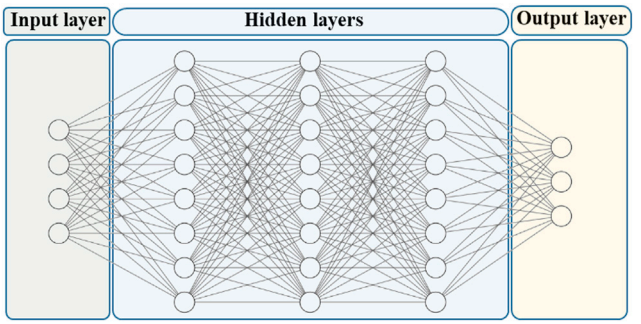

FIGURE 2 | Architecture of a typical FFNN.

neural networks (FFNN) are widely utilized in wind engineering field [**Figure 2**]. They are statistical models inspired by biological learning (McCulloch and Pitts 1943) and characterized by adaptive weights between neurons which are tuned using a learning algorithm from observed training data. For simplicity, the FFNN is also denoted as artificial neural network (ANN) in this study.

Deep neural networks (DNN) are also a type of FFNN characterized by a deep architecture equipped with multiple layers, and hence allows for better generalization and accuracy (Deng and Yu 2014; Pouyanfar et al., 2018). The convolutional neural networks (CNN) is another important FFNN with sparse convolutional matrices that are usually employed for pattern recognition and image classification (Krizhevsky et al., 2012; Goodfellow et al., 2016). Recurrent neural networks (RNN) are a class of feedback neural networks that allow previous outputs to be used as inputs while having hidden states and are suited to model time-dependent regression problems (e.g., Medsker and Jain 1999; Mandic and Chambers 2001). Long short-term memory (LSTM) are an advanced version of RNN to alleviate the gradient vanishing and exploding issue by only keeping necessary past information in future model states (Bengio et al., 1994).

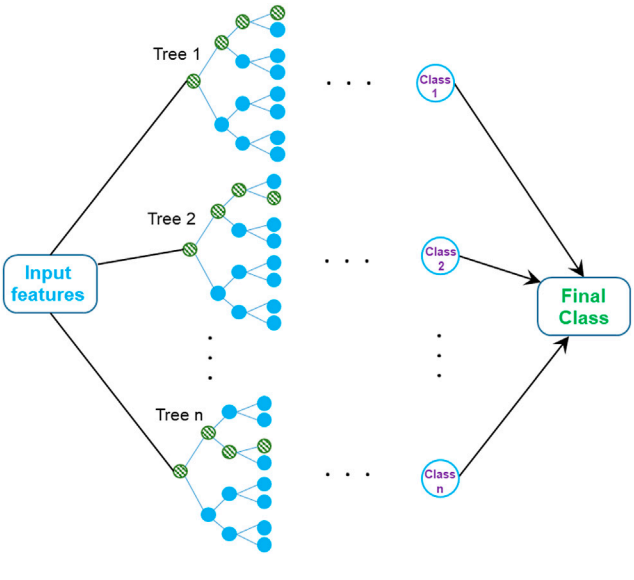

FIGURE 3 | Architecture of a typical random forest classifier.

2.1.2 Classification

Classification is another type of supervised learning in which the output is a categorical variable or a class. Support vector machines (SVM) (Scholkopf and Smola 2018) and random forest (RF) (Breiman 2001) are two classical examples of classification algorithms. SVM classifier identifies a hyperplane in a high-dimensional space in which a simple linear classification can be performed. RF classifier, on the other hand, fits a number of decision tree classifiers on various sub-samples of the dataset, then averages the results to improve outcome accuracy [**Figure 3**].

2.2 Unsupervised Learning

Unsupervised learning models draw inferences from datasets to describe hidden structures from unlabeled data based on

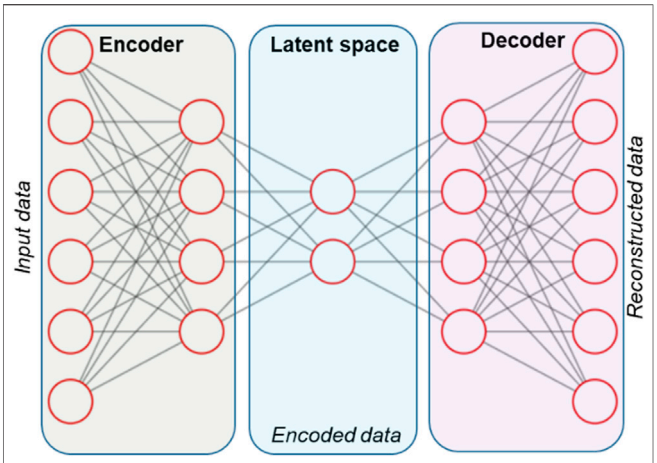

FIGURE 4 | Architecture of a typical autoencoder model.

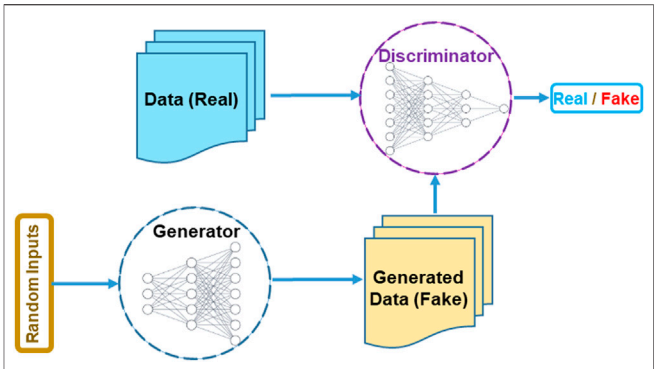

FIGURE 5 | Architecture of a typical GAN model.

inherent characteristics (Russell and Norvig 2016). These models usually group instances of input data using a defined similarity index (global criterion). Clustering and dimensionality reduction are two standard examples of unsupervised learning applications.

2.2.1 Clustering

Clustering is an unsupervised learning task used for pattern recognition that automatically discovers natural groups or clusters in data. A cluster refers to a collection of data points aggregated together with similar features (Maulik and Bandyopadhyay 2002). The k-means clustering is one of the simplest unsupervised ML models. It is a centroid-based algorithm that partitions the data into k clusters. Mean-shift clustering is another unsupervised model with a sliding-window-based algorithm to identify dense areas of data points. Other clustering algorithms such as the density-based spatial clustering of applications with noise, the expectation–maximization clustering using gaussian mixture models and the agglomerative hierarchical clustering are also popularly used for statistical data analysis.

2.2.2 Dimensionality Reduction

Dimensionality reduction aims to find the most important features within the dataset by identifying lower-dimensional representations for high-dimensional data. It minimizes the storage space, reduces the computation time and avoids overfitting. The ML-based dimensionality reduction can be divided into linear and nonlinear algorithms. The principal component analysis (PCA) is a commonly used linear technique that can be regarded as a two-layer neural network with a linear activation function. It essentially provides new uncorrelated variables, also denoted as principal components, which maximize the variance. The nonlinear autoencoder is a specific type of FFNN that compresses the initial input space into a reduced dimensional space using the encoder and then decompresses the obtained latent space back to the original input space using the decoder. Accordingly, deep autoencoders have a "bottleneck" architecture designed for extraction of representative features [**Figure 4**]. The autoencoder algorithm has been attracting attention in fluid mechanics community for efficient development of reduced-order models.

2.3 Semi-Supervised Learning

Semi-supervised learning models operate based on limited labeled data with a large amount of unlabeled data. Hence, they can be regarded as combination results of supervised learning and unsupervised learning algorithms. The generative adversarial network (GAN) is a well-known semi-supervised learning algorithm for estimating generative models via an adversarial process. One important feature of semi-supervised learning algorithms is their labelled-data efficiency. To this end, it may be reasonable to consider the physics-informed deep learning (PIDL) as a semi-supervised model that leverages physics-based equations in the augmented loss function to significantly reduce the data demand during training process.

2.3.1 Generative Adversarial Network

The GAN model consists of two competing neural networks, namely the generator and the discriminator (Goodfellow et al., 2014). It generates new data based on a probability distribution that approximately represents the training data (true or labelled data). Specifically, the generator produces fake samples to imitate the distribution of a real dataset, then the discriminator tries to distinguish (through a classification process) between the real samples and fake ones (from the generator). The GAN model is trained such that the new generated samples accurately represent the underlying mechanisms of the studied system. The architecture of a typical GAN model is illustrated in **Figure 5**.

2.3.2 Physics-Informed Deep Learning

The concept of PIDL models was originally proposed several decades ago (Psichogios and Ungar 1992; Dissanayake and Phan-Thien 1994) in which prior knowledge (in terms of the physics-based governing equations) is integrated within the neural networks to reduce the high-volume of required training data. Typically, a small amount of labelled data along with a large number of unlabeled data that satisfy the underlying physics of the system of interest (also denoted as collocations points) are used to train these models. Hence, self-supervision plays a significant role in PIDL models. Recently, Raissi et al. (2017a,

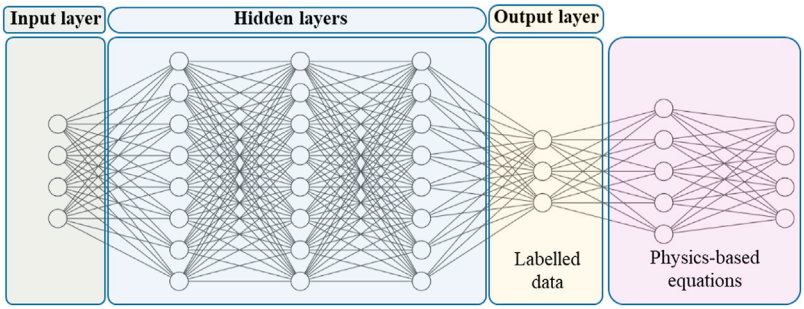

FIGURE 6 | Architecture of a typical PIDL model.

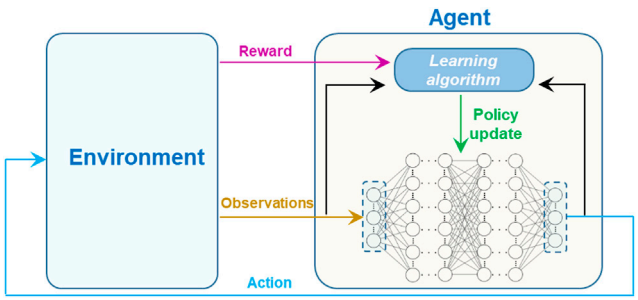

FIGURE 7 | Architecture of a typical RL.

b) advanced the PIDL models by leveraging the automatic differentiation technique to solve partial differential equations. The architecture of a typical PIDL model is presented in **Figure 6**.

2.4 Reinforcement Learning

RL algorithm is usually formulated based on Markov decision process (Sutton and Barto, 2018). The core part of RL is its agent that interacts with its environment. Accordingly, the agent learns a policy that maps the states to the actions by maximizing the expected cumulative reward using an automated trial-and-error process (e.g., Mnih et al., 2015; Silver et al., 2017). Typical reinforcement learning models include value-based models (e.g., Q-learning or deep Q-learning) (Watkins and Dayan 1992), policy-based models (e.g., deep deterministic policy gradient) (Lillicrap et al., 2015) and hybrid models (e.g., actor-critic) (Williams 1992). Recently, the deep RL (with DNN-based policy) has been gaining attention in wind engineering community as an efficient way for dynamic control and shape optimization (Li et al., 2021a; 2021b). The architecture of a typical deep RL is depicted in **Figure 7**.

3 APPLICATIONS OF MACHINE LEARNING TO WIND ENGINEERING

This section provides a comprehensive review of the state of research and practice of ML for its applications to wind engineering. In addition to ML applications to wind climate, terrain/topography, aerodynamics/aeroelasticity and structural dynamics (following traditional Alan G. Davenport Wind Loading Chain), the review also extends to cover wind damage assessment and wind-related hazard mitigation and response (considering emerging performance-based and resilience-based wind design methodologies). Considering the overwhelming number of existing research publications, this review is by no means exhaustive. Rather, it attempts to provide a state-of-the-art perspective on ML applications to wind engineering-related fields.

3.1 Wind Climate

The review of ML applications to wind climate is organized by classifying it into classical boundary-layer winds, tropical cyclones and non-synoptic events. By leveraging the increasingly available datasets (e.g., satellite data), ML has become a supporting tool or even a reliable competitor of classical approaches for wind climate modeling (e.g., CFD). Most reviewed articles employed ML algorithms as a regression (e.g., long-term prediction of surface wind speed) or a classification (e.g., downburst occurrence prediction) tool. The selected metrics to evaluate the performance of ML algorithms included the root mean square (RMS), coefficient of correlation, mean squared error (MSE), mean absolute error (MAE), mean absolute percentage error (MAPE), coefficient of determination (R2), among others.

3.1.1 Classical Boundary-Layer Winds

Air movement in the planetary boundary layer plays a fundamental role in current wind design of structures and infrastructure. Although a detailed universal description of flow characteristics in the boundary-layer region has not been possible, the classical boundary-layer winds in gales from large depressions or in monsoons can be well represented by a number of empirical or semi-empirical models [e.g., power-law profile for distribution of mean wind speed (Davenport 1960) and power spectrum for turbulent fluctuations (Panofsky and McCormick 1960)]. The major research efforts have been focused on the accurate estimate of design wind speed in a statistical analysis framework (Simiu and Scanlan 1978). Specifically, long-term wind data from meteorological observations are analyzed based on extreme value theory to obtain the design wind speed at each location. However, the accurate forecast of

classical boundary-layer winds is very challenging since it involves a large range of various temporal and spatial scales (e.g., from fractions of a meter to several thousand kilometers for spatial scale and from fractions of seconds to several years for time scales). Usually, the temporal and spatial resolutions from the state-of-the-art weather forecast models [e.g., global forecast system from National Oceanic and Atmospheric Administration (NOAA)] are not sufficient for wind engineering purpose. On the other hand, the unprecedented volumes of data from field measurements (e.g., weather station and satellite) provide a solid foundation to advance ML applications for classical boundary-layer winds.

Table 1 presents the reviewed applications of ML for classical boundary-layer winds, where the ML model, training scheme, input data, output data, data source and performance metric are summarized for each application. The training/testing data were essentially retrieved from field measurements. From **Table 1**, it can be concluded that most applications used ML as a regression model for prediction of mean wind speed (averaging time ranged from minutes to months), while the short-term prediction of turbulent fluctuations that are very important to structural dynamics is very limited. In many applications, the selection of ML models is simply based on gut feeling or past experience. Although several researchers conducted comparison studies to select good ML models for their specific applications, it might be very challenging to generalize the obtained results to other applications due to a lack of a systematic comparison framework.

3.1.2 Tropical Cyclones

Tropical cyclones (TCs), also commonly known as hurricanes in North Atlantic, typhoons in western North Pacific and cyclones in Australia, are low-pressure storms that form over a warm ocean surface (Holton and Hakim 2013). With an average of 90 events reported annually (Zhao et al., 2012), TCs and their cascading hazards (e.g., wind, rain, storm surge and wave) pose a serious threat to public safety, livelihoods and local economies in many coastal regions around the globe. Hence, significant efforts have been made in modeling and predicting TCs and relatively well-established mesoscale numerical weather prediction frameworks [e.g., Weather Research and Forecasting (WRF) model] are available for high-fidelity simulations. However, the high-fidelity computationally expensive models might not be always appropriate for planning activities in an uncertain environment where Monte Carlo simulations are needed or emergency managements where real-time or near-real-time predictions are required. The high demand for a rapid and reliable technique used to assist decision-makers and planers results in many ML models for efficient simulations of key stages in the life cycle of a TC. These ML applications to TCs are fueled by increasingly available remotely-sensed and high-fidelity numerical data. The review in this section is organized following the four important components of full track of a TC, namely genesis, translation, intensity and wind field.

3.1.2.1 Tropical Cyclone Genesis

TC genesis requires several necessary environmental conditions (e.g., existence of low-pressure area and sea surface temperature of at least 26°C), however, the exact mechanisms of TC formation are still not well understood (Gray 1968, 1979; Emanuel 2003; Holton and Hakim 2013). To predict the TC genesis, both numerical and statistical models were developed. The numerical models (e.g., global forecast system) are essentially based on the physical principles and their performance heavily depends on improved understanding of TC genesis mechanism. The statistical models (e.g., Michael 2017; Chen and Duan 2018; Cui and Caracoglia 2019) linearly relate the TC genesis to a few selected environmental factors, and hence show poor interpolation and limited predictability. The lack of a deep understanding of underlying mechanisms stimulated data-driven techniques for TC genesis simulations. As a result, increasing ML applications are available to accurately predict TC genesis. **Table 2i** presents the reviewed applications of ML for TC genesis, where the ML model, training scheme, input data, output data, data source and performance metric are summarized for each application. The training/testing data were essentially retrieved from satellite measurements along with reanalysis results. It is expected the improved spatial resolution of currently available datasets will further enhance simulation results of ML models. From **Table 2i**, it can be concluded that most applications used ML as a classification model for either short-term or long-term forecasting of TC genesis. Although more dynamic and thermodynamic environmental factors can be retrieved using advanced remote sensing technologies in recent years, the identification of the most appropriate set of inputs to ML models (predictors) is still very challenging.

3.1.2.2 Tropical Cyclone Translation

Numerical forecast models have been successfully applied in forecasting normal TC trajectories, but they are computationally expensive. Although several statistical models were also developed based on a large amount of historical TC path records (e.g., Vickery et al., 2000,2009; Emanuel et al., 2006; Hall and Jewson 2007; Chen and Duan 2018; Snaiki and Wu 2020a; Snaiki and Wu 2020b), their linear nature makes them incapable of capturing the inherent nonlinearities in such a complex dynamic system (Zhang and Nishijima 2012). Both numerical and statistical models or their combinations (statistical-dynamics models) show poor performance in forecasting sudden speed change, recurvature and stagnation in TC movement (Chen et al., 2020). To satisfy both simulation accuracy and efficiency, increasing ML applications emerged for TC path prediction. **Table 2ii** presents the reviewed applications of ML for TC translation, where the ML model, training scheme, input data, output data, data source and performance metric are summarized for each application. The training/testing data were essentially retrieved from meteorological databases (e.g., satellite data) and reanalysis results. Typically, the TC track information is available only at each 6-h interval. From **Table 2ii**, it can be concluded that most applications used ML as a regression model for TC path prediction. Since the forecast of TC track can be regarded as a

TABLE 1 | Summary of ML applications for classical boundary-layer winds.

Application	ML model	Training scheme	Input data	Output data	Data source	Performance metric	Remarks
Forecasting mean hourly wind speed time series Sfetsos (2000)	LNN-ANN-NLN-RBF-ANFIS-ERNN	Gradient descent, Levenberg Marquardt	Past mean hourly data (six past measurements)	Next mean hourly wind speed	Field measurements at the Odigitria of the Greek island of Crete on March 1996 (total of 744 h)	RMS	NLN with logic rule outperformed all other models
Forecasting daily, weekly and monthly mean wind speeds More and Deo (2003)	ANN-JRNN	Back-propagation, cascade correlation	Past daily-, weekly- and monthly averaged mean wind speed	Next daily, weekly and monthly averaged mean wind speeds	Field measurements from 1989 to 2000 in two locations in Mumbai, India	Coefficient of correlation	Best performance by RNN trained with the cascade correlation
Prediction of the next daily mean wind speed Mohandes et al. (2004)	ANN-SVM	Levenberg-Marquardt	mean daily wind speed of previous days (ranging between 1 and 11)	Next daily mean wind speed	12 years of mean daily wind speed in Medina city, Saudi Arabia	MSE	SVM model outperformed the ANN model
Long-term wind speed and power forecasting Barbounis et al. (2006)	IIRANN, DRNN, LAFMN	Global recursive prediction error	3-days forecast of wind speed and direction provided by meteorological models at four nearby sites	Hourly mean wind speed and power for up to 72-h	Atmospheric modeling system SKIRON and wind turbines data from April 1st, 2000 until 31 December 2000 in Rokas' wind park on the Greek island of Crete	MAE-RMS	Similar performance results for the three models
Short-term mean wind speed forecasting Potter and Negnevitsky (2006)	ANFIS	least-squares estimator and the gradient descent	4 to 6 past mean wind speeds and direction with a 2.5 min time step	Next mean wind speed and direction at 2.5 min	21-month time series of 2.5 min mean wind from Hydro Tasmania at Tasmania, Australia	Mean absolute percentage error	ANFIS model outperformed a locally developed persistence model
Prediction of the next hourly mean wind speed Li and Shi (2010)	ANN, RBF, ALEN	Levenberg–Marquardt	Past hourly mean wind speed observations (up to 8 observations)	Next hourly mean wind speed	Anemometers data for 1 year (2002) in two sites in North Dakota	Mean absolute error and RMSE	ANN outperformed other models
Prediction of the hourly mean wind speed and direction Lahouar and Slama (2014)	SVM (radial basis kernel)	-	Past hourly mean wind speed and direction in the site (up to 10 past samples)	Next hourly mean wind speed and direction for a lead time up to 10 h	Sidi Daoud wind farm in Tunisia from 2010 to 2011	RMSE and MAE	Satisfactory results
Short-term wind direction forecasting Tagliaferri et al. (2015)	ANN, SVM (RBF kernel)	Gradient descent	Wind direction at past minutes	Next 1–2 min wind direction	34 days data from the 34th America's Cup in 2013, San Francisco	Mean absolute error and mean effectiveness index	SVM model outperformed the ANN model
Prediction of the monthly averaged mean wind speed Kumar and Malik (2016)	ANN, GRNN	Missing	10 variables (e.g., latitude, longitude, earth temperature, atmospheric pressure)	Monthly averaged mean wind speed	Data retrieved from NASA corresponding to various cities in India	MSE and RMSE	GRNN outperformed the ANN model
Predict of short-term	Hybrid model (wavelet packet	-	Past values of the wind speeds	Mean wind speed for up to 1 day	Data from several sites in the Sichuan	MAE and RMSE	WPD-DBSCAN-ENN

(Continued on following page)

TABLE 1 | (*Continued*) Summary of ML applications for classical boundary-layer winds.

Application	ML model	Training scheme	Input data	Output data	Data source	Performance metric	Remarks
mean wind speed Yu et al. (2018)	decomposition [WPD] + density-based spatial clustering of applications with noise [DBSCAN] + ENN), WPD-ENN, ENN		determined based on the gradient boosted regression trees	with a 10-min time step	Province, China over 16 days with an average wind speed of 10 min		outperformed all other models
Time-series prediction of mean wind speed Khosravi et al. (2018a)	ANN, SVR, FIS, ANFIS, GMDH	Bayesian Regularization, Scaled Conjugate Gradient, BFGS Quasi-Newton, Levenberg Marquardt and Resilient backpropagation	Past values of wind speed (number not mentioned)	Mean wind speed for approximately 361-time steps ahead with several time intervals (e.g., 5-min and 30-min)	Osorio wind farm in the south of Brazil	RMSE, MSE	SVR, GMDH and ANFIS models preformed the best. The prediction accuracy of ANFIS was increased when coupled with particle swarm optimization (PSO) and genetic algorithm (GA). The Levenberg Marquardt performed the best
Prediction of the mean wind speed, direction and power Khosravi et al. (2018b)	ANN, SVR (with radial basis function), ANFIS	Levenberg Marquardt, Conjugate Gradient and Bayesian Regularization	Pressure, local time, temperature and relative humidity	Mean wind speed, direction and power (in 5-min, 10-min, 30-min and 1-h intervals) for up to 24 h	Wind farm in Bushehr, Iran	RMSE	Levenberg Marquardt and Bayesian Regularization algorithms gave the best performance for ANN. SVR was the best to simulate the wind speed. Low prediction results were obtained by the 3 models for the wind direction
Short-term prediction of wind speed and direction Chitsazan et al. (2019)	ESN, ANFIS, NESN-P with polynomial functions and NESN-MP with multivariable polynomials	-	Past values of wind speed and direction at time interval of 10 min (the exact number was not specified)	Mean wind speed and direction at 10 min intervals for up to 1 day and 6 days, respectively	Several Nevada weather information stations in Reno, Nevada	RMSE	The best prediction results given by the NESN-MP
Probabilistic prediction of the wind gusts Wang et al. (2020)	Ensemble of 3 machines models (RF, LSTM and GPR), RF, LSTM and GBRT	Adaptive momentum estimation	Past values of wind speed (the number was determined based on the partial autocorrelation function)	Wind gusts for up to 72 h	Sutong Cable-Stayed Bridge in Jiangsu province of China (sampling frequency of 1 Hz with a total of a total of 720 h)	RMSE, MAE and the mean absolute percent error (MAPE)	The ensemble model achieves the highest accuracy
Prediction of mean wind speed Sharma et al. (2020)	MFQL, SVR, KNN	-	7 intrinsic mode functions obtained from past wind speed values using empirical model decomposition technique	1-min ahead mean wind speed	National Institute of Wind Energy and Wind Resource Assessment data portal (in ten Indian cities)	Mean Absolute Percentage Error (MAPE)	MFQL outperformed the other models
		-					

(Continued on following page)

TABLE 1 | (*Continued*) Summary of ML applications for classical boundary-layer winds.

Application	ML model	Training scheme	Input data	Output data	Data source	Performance metric	Remarks
Prediction of mean wind speed Zhongda Tian et al. (2020)	LSSVM optimized with four algorithms Backtracking search, genetic algorithm, particle swarm, and improved feature selection		Past values of mean (hourly) wind speed (50 values)	1-h mean wind speed (next 1-48 h)	The training data were sampled every 1-h from a wind farm in Jinzhou, China	RMSE, MAE, mean absolute percentile error (MAPE), R-square and reliability	LSSVM optimized with the backtracking search optimization algorithm outperformed all other models

time series prediction problem, the feedback neural networks such as RNNs and LSTMs are preferred and lead to good performance. However, their performance within each 6-h interval is unknown due to the sampling limitation in the training data.

3.1.2.3 Tropical Cyclone Intensity

The TC intensity (over ocean or land) can be measured in terms of central pressure or maximum sustained wind speed. It is impacted by several complicated physical phenomena (e.g., atmosphere-ocean interaction and vertical wind shear), and hence remains one of the most challenging issues in TC forecasting especially for rapid intensification prediction. To avoid the high computational cost of numerical forecast models, both statistics-based (e.g., Vickey et al., 2000; DeMaria et al., 2005; Hall and Jewson 2007; Vickey et al., 2009) and physics-based (e.g., Snaiki and Wu 2020a) tools were developed for fast prediction of TC intensity. However, neither statistical nor physical models guarantee prediction accuracy of TC intensity due essentially to the over-simplification of such a complicated dynamic system. To improve simulation accuracy while keeping a high efficiency, increasing ML applications are available for TC intensity prediction. **Table 2iii** presents the reviewed applications of ML for TC intensity, where the ML model, training scheme, input data, output data, data source and performance metric are summarized for each application. The training/testing data were essentially retrieved from meteorological databased (e.g., satellite data) and reanalysis results. From **Table 2iii**, it can be concluded that most applications used ML as a regression (or a classification) model for estimation of intensity time series (or levels). Although encouraging simulation results indicate a good performance of ML models in predicting TC intensity for their specific applications, the selection of the most appropriate set of inputs (including the number of predictors and previous time steps) is still very challenging. In addition, it is not easy to conduct a systematic comparison among reviewed ML models since the used performance metrics differ substantially from one application to another.

3.1.2.4 Tropical Cyclone Wind Field

TC wind hazard is of great significance since it (directly) induces significant damage to life and property and (indirectly) triggers other TC-induced hazards (e.g., storm surge and waves). Substantial research efforts have been made for development of numerical models (e.g., WRF) or analytical models (e.g., Snaiki and Wu 2017a; Snaiki and Wu 2017b; Snaiki and Wu 2018; Snaiki and Wu 2020c; Fang et al., 2018; He et al., 2019) to simulate the boundary-layer wind field. However, none of these models can simultaneously achieve simulation accuracy and efficiency. To address this issue, increasing ML applications emerged for TC boundary-layer wind field simulation. **Table 2iv** presents the reviewed applications of ML for TC wind field, where the ML model, training scheme, input data, output data, data source and performance metric are summarized for each application. The training/testing data were essentially retrieved from meteorological databases (e.g., satellite data) and high-fidelity simulations. It is expected the improved spatial resolution of currently available datasets will further enhance simulation results of ML models. From **Table 2iv**, it can be concluded that most applications use ML as a regression model for prediction of surface wind speed. Since these ML models were often trained and fine-tuned to predict the TC wind field at a specific region, it might be very challenging to generalize the obtained results to other locations. It is noted that only wind field at a certain altitude is available in most ML applications due essentially to training data sparsity issue in vertical dimension. The widely-used logarithmic or power-law profiles are typically employed to obtain the TC boundary-layer winds. Accordingly, the supergradient winds that may have significant implications to the wind design of tall buildings is not captured (Snaiki and Wu 2020c).

3.1.3 Non-synoptic Winds

Unlike synoptic winds that are associated with large-scale meteorological systems characterized by horizontal scales of thousands of kilometers and time scales of days, the non-synoptic wind systems are local phenomena (e.g., a horizontal scale of several hundreds of meters) and short lived (e.g., a time scale of a few minutes) (Chowdhury and Wu 2021). Furthermore, the transient nature of non-synoptic winds makes them exhibit time-varying mean wind speeds and nonstationary/non-Gaussian fluctuations. Accordingly, the detection, measurement, and modeling of non-synoptic wind systems lag behind those of synoptic winds. However, numerous studies have demonstrated the importance of the non-synoptic wind events on the structural design (e.g., Holmes 1999; Letchford et al., 2002; Hao and Wu 2017). For example, the design wind speeds with relatively high return periods are usually dominated by the thunderstorm downbursts (Twisdale and Vickery 1992; Solari

et al., 2015) and the ASCE 7–22 includes the first-ever criteria for tornado-resistant design (ASCE, 2021). Recently, there is a rapid development of field-measurement networks (e.g., THUNDERR project at University of Genova) and laboratory facilities (e.g., WindEEE at Western University) for improved understanding of non-synoptic wind systems. These advances offer an unprecedented volume of data, and hence provide an opportunity to facilitate ML applications to non-synoptic winds. Although the non-synoptic wind systems can be originated from various mechanisms (e.g., convective storm, gravity wave or negative buoyancy) (Bluestein 2021), the review only focuses on those associated with convective storms. Specifically, ML applications to thunderstorms (subsynoptic-scale weather system) are first presented, followed by detailed reviews of its applications to two important types of non-synoptic wind events associated with thunderstorms, namely downbursts and tornadoes.

3.1.3.1 Thunderstorms

A thunderstorm is short-lived atmospheric weather system accompanied by lightning and thunder, gusty winds, heavy rain, and sometimes hail (Solari 2020). The life cycle of a thunderstorm usually consists of cumulus stage, mature stage and dissipative stage, and it typically lasts around 30 min. Both mesoscale and microscale numerical models have been developed for simulation of thunderstorms (Hawbecker 2021). Mesoscale modeling covers a large-scale computational domain (and hence fully considers physics involved), however, it is limited to a low spatiotemporal resolution. Microscale modeling utilizes a high spatiotemporal resolution (and hence obtains important small-scale features in the simulation of winds), however, it is limited to a relatively small-scale computational domain resulting in insufficiently reliable boundary conditions. To avoid shortcomings of currently available numerical models, ML models may provide a promising approach for efficient and accurate simulation of key stages in the life cycle of a thunderstorm. **Table 3i** presents the reviewed applications of ML thunderstorms, where the ML model, training scheme, input data, output data, data source and performance metric are summarized for each application. The training/testing data were essentially retrieved from meteorological databases and reanalysis results. From **Table 3i**, it can be concluded that most applications used ML as either a classification or a regression model for prediction of thunderstorm occurrence. Obviously, there is still room for more comprehensive applications of ML in terms of modeling and forecasting each aspect of the thunderstorm from formation to dissipation. In addition, most ML applications to thunderstorm were limited to simple models with standard algorithms (e.g., ANN with backpropagation).

3.1.3.2 Downbursts

Downbursts are one of the most spectacular and dangerous events resulting from thunderstorms (Solari 2020). Their radial outflows and ring vortices after touchdown produce strong wind gusts very close to the ground and therefore lead to substantial structural damages (e.g., Yang et al., 2018). Downbursts are typically simulated numerically using CFD (e.g., Mason et al., 2009; Aboshosha et al., 2015; Haines and Taylor 2018; Hao and Wu 2018; Oreskovic et al., 2018; Oreskovic and Savory 2018; Iida and Uematsu 2019) or experimentally using wind tunnels (e.g., Jesson et al., 2015; Jubayer et al., 2016; Hoshino et al., 2018; Aboutabikh et al., 2019; Asano et al., 2019; Junayed et al., 2019; Romanic et al., 2019). Both numerical and experimental approaches to obtain wind fields associated with downbursts are very time consuming (either computational expensive or labor intensive). This shortcoming motivated increasing use of ML tools for efficient and accurate simulations of downbursts. **Table 3ii** presents the reviewed applications of ML for downbursts, where the ML model, training scheme, input data, output data, data source and performance metric are summarized for each application. The training/testing data were essentially retrieved from field measurement. From **Table 3ii**, it can be concluded that most applications used ML as a classification model for prediction of the occurrence of downburst or probability of damaging wind. There are a very limited number of ML applications for modeling and forecasting the downburst wind field, hence more research efforts are needed in this aspect. It is noted that the reviewed ML applications usually involved a high number of predictors. The employment of relatively high number of input variables may be necessary due to the complexity of downburst prediction. However, it makes the ML models not easy to use since these input variables might not be always available.

3.1.3.3 Tornadoes

Tornadoes are characterized by a rotating column of air descending from supercell thunderstorms lasting from several minutes to few hours. They are the most intense of all non-synoptic wind events, and hence result in significant damage and collapse of structures (Hao and Wu 2016, 2020). Several analytical and empirical models have been developed to simulate the vertical and radial wind profiles of tornado-like vortices (e.g., Wen and Chu 1973; Baker and Sterling 2017). These models are clearly over-simplified. The tornado wind fields are also modeled using CFD simulations (e.g., Kuai et al., 2008; Ishihara et al., 2011; Liu and Ishihara 2015; Eguchi et al., 2018; Gairola and Bitsuamlak 2019; Kawaguchi et al., 2019; Huo et al., 2020; Liu et al., 2021) or laboratory tests (e.g., Sarkar et al., 2006; Refan and Hangan 2016; Razavi and Sarkar 2018; Tang et al., 2018; Ashton et al., 2019; Gillmeier et al., 2019; Hou and Sarkar 2020; Razavi and Sarkar 2021). However, CFD simulations of tornadoes are computational expensive while the laboratory tests are labor intensive. These shortcomings motivated increasing use of ML tools for efficient and accurate modeling of tornadoes. **Table 3iii** presents the reviewed applications of ML for tornadoes, where the ML model, training scheme, input data, output data, data source and performance metric are summarized for each application. The training/testing data were essentially retrieved from meteorological datasets (e.g., Radio-based data). From **Table 3iii**, it can be concluded that most applications use ML as a classification or a regression model for prediction of tornado occurrence. Obviously, there is still room for more comprehensive applications of ML in terms of simulation of the full track of a tornado (including its intensity and associated

TABLE 2 | Summary of ML applications for tropical cyclones.

	Application	ML model	Training scheme	Input data	Output data	Data source	Performance metric	Remarks
i) Genesis	Prediction of the number of TCs in the northwest of Australia Richman and Leslie (2012)	SVR with radial basis function coupled with sequential minimal optimization algorithm, MLR	-	Nine predictors (e.g., El Niño Southern Oscillation)	Number of TCs in the northwest of Australia	Australian Government, Bureau of Meteorology website	RMSE, MAE, R^2	SVR outperformed the MLR model – The prediction accuracy was further improved by coupling the SVR model with Quasi-Biennial Oscillation
	Prediction of TC genesis in the South Pacific Ocean and Australian region Wijnands et al. (2014)	SVM with polynomial kernel, LDA	-	El Niño—Southern Oscillation indices, Multivariate ENSO Index, El Niño Modoki Index, Dipole Mode Index and the Southern Oscillation Index	TC genesis (number of TCs) in the South Pacific Ocean and Australian region	Bureau of Meteorology's National Climate Center - Australia	MAE	SVM outperformed LDA model. Overall prediction performance for both models is low
	Prediction of TCs genesis in the western North Pacific region Zhang et al. (2015)	DT (C4.5 algorithm)	-	Sea surface temperature, rainfall intensity, divergence averaged between 1000- and 500-hPa levels, maximum 800-hPa relative vorticity and the 300-hPa air temperature anomaly	TCs genesis in the western North Pacific region	Navy Operational Global Atmospheric Prediction System and the Tropical Rainfall Measuring Mission (TRMM) Microwave Imager (TMI) from 2004 to 2013	Prediction accuracy = (correctly classified samples/number of samples in the whole dataset)	Satisfactory results were obtained based on the C4.5 algorithm
	Variable selection and prediction of TC genesis Wijnands et al. (2016)	LR and Peter-Clark algorithm	-	Selected variables: relative vorticity (925 hPa), potential vorticity (600 hPa) and vertical wind shear (200–700 hPa)	TCs genesis in region between 30°N and 30°S	IBTrACS, tropical cloud cluster (TCC) and ERA-Interim (1979–2014)	*p*-value and area under the receiver operating characteristic (ROC) curve	Top ranked variables include the relative vorticity (925 hPa), potential vorticity (600 hPa) and vertical wind shear (200–700 hPa)
	Development a TC genesis detection model over the western North Pacific Park et al. (2016)	DT (C5.0 algorithm)	-	8 WindSat-derived indices tested and 2 were selected as the most dominant predictors: circulation symmetry and intensity	TC genesis	WindSat satellite data (wind and rainfall) were used to extract the training/testing data from 2005 to 2009 over the western North Pacific	Prediction accuracy = (correctly classified samples/number of samples in the whole dataset)	Good simulation results were obtained
	Prediction of the number of seasonal TCs in the North Atlantic region Richman et al. (2017)	SVR (with 2 kernels: polynomial and radial basis function)	-	SST and El Niño 3.4 were the best attributes	Number of seasonal TCs in the North Atlantic region	Hurricane database in the North Atlantic basin and Hadley Centre Sea Ice and Sea Surface Temperature dataset	RMSE	The SVR model gave enhanced prediction compared to an operational statistical model that was developed by Colorado State University. The polynomial kernel gave a slightly improved simulation results compared to the RBF kernel
	Prediction of TC formation from mesoscale convective system Zhang et al. (2019)	LR, NB, DT, KNN, ANN, QDA, SVM (with a radial basis function kernel), AdaBoostRF.	-	Several thermodynamic and dynamic predictors were employed in this study (e.g., genesis potential index, 850-hPa vorticity and vertical wind shear)	Genesis prediction at different lead times (e.g., 6 h)	Mesoscale convective system (MCS) dataset, IBTrACS, and ERA-Interim (1985–2008)	F1-score accuracy	AdaBoost algorithm was the best classifier. Both the genesis potential index and the low-level vorticity were the most dominant predictors for the tropical cyclone genesis
	Detection of TC genesis over the western North Pacific Kim M et al. (2019)	DT, RF, SVM (with three different kernels: linear, polynomial, and radial basis functions), LDA	-	8 dynamic and hydrological predictors (e.g., rain rate, circular variance of wind speed)	Genesis detection for a lead time up to 30 h	WindSat satellite measurements from 2005 to 2009 over the western North Pacific basin	F1-score accuracy and PSS score	Best performance from the SVM model with a radial basis function kernel
ii) Translation	Prediction of cyclone track over	ANN	Pseudo invert learning	12 h of past track observations (in terms	24 h of cyclone track over the	Joint Typhoon Warning Center	MAE	Acceptable accuracy

(Continued on following page)

TABLE 2 | (*Continued*) Summary of ML applications for tropical cyclones.

	Application	ML model	Training scheme	Input data	Output data	Data source	Performance metric	Remarks
	the Indian Ocean Ali et al. (2007)			of latitude and longitude)	Indian Ocean at 6 h intervals	(JTWC) from 1971 to 2002		
	Prediction of TCs track of over the western North Pacific basin Wang et al. (2011)	ANN	Levenberg Marquardt	2 previous 6-h positions and the current one (in terms of latitude and longitude)	24 h of cyclone track over the western North Pacific basin at 6 hourly intervals	20 years of historical tack data from the JTWC	Correlation coefficient	Good simulation results
	Trajectory Prediction of Atlantic Hurricanes Moradi Kordmahalleh et al. (2016)	RNN	Genetic algorithm	Past hurricane track locations which are selected by the RNN model (6-hourly hurricane center's latitude and longitude)	hurricane track for up to 12 h in advance	National Oceanic and Atmospheric Administration (NOAA) from 1900 to 2013	MAE	Acceptable accuracy
	Cyclone track prediction over the South Indian ocean Zhang et al. (2018)	MNN, RNN, LSTM, GRU	Backpropagation	Past hurricane trajectories -automatically selected by the algorithm-	1-step of 6-h ahead TC trajectory (in terms of latitude and longitude)	JTWC between 1985 and 2013 in the South Indian ocean	RMSE	MNN-based model outperformed the three recurrent neural networks
	Prediction of hurricane trajectories over the Atlantic basin Alemany et al. (2019)	Grid-based RNN, sparse RNN	Backpropagation	Past hurricane locations (6-hourly distributed)	Hurricane tracks over the Atlantic basin up to 120 h	NOAA database	MSE, RMSE	The grid-based algorithm outperformed the sparse RNN
	Prediction of a typhoon track in the Korean Peninsula Rüttgers et al. (2019)	GAN	Backpropagation	Satellite images	Typhoon tracks in the Korean Peninsula at 6 h lead time	Korean Meteorological Administration and the ERA-interim databases with a total of 76 typhoons that hit the Korean peninsula from 1993 till 2017	Average absolute error	Acceptable accuracy
	Prediction of the spatial-temporal hurricane trajectory Kim S et al. (2019)	ConvLSTM	AdaGrad	Last 5 consecutive hurricane density-maps	Spatial-temporal hurricane trajectory (up to 15-h) with a 3-h time steps	Community Atmospheric Model v5 from 1995 to 2015	RMSE	The error increased with the increasing leading time
	Tropical cyclone track forecasting Giffard-Roisin et al. (2020)	CNN	Adam	Atmospheric fields (image-like data) corresponding to the current and past data (with a 6-h time step) including the latitude, longitude and geospatial height fields at three pressure levels: 700, 500, and 225 hPa (e.g., wind speed components)	TC trajectory (in terms of latitude and longitude) for up to 24-h leading time	TCs data in both hemispheres from NOAA, IBTrACS and ERA-Interim since 1979 (more than 3,000 storms with 6-h time steps)	RMSE, MAE	The proposed model outperformed the statistical CLP5 model
iii) Intensity	Prediction of typhoon intensity changes in the western North Pacific basin Baik and Paek (2000)	ANN, MLR	Backpropagation	11 predictors (e.g., initial storm intensity, initial storm latitude, vertical wind shear and 850-mb horizontal moisture flux)	Typhoon intensity changes in the western North Pacific basin from 12-h and up to 72-h (1 output)	National Centers for Environmental Prediction/National Center for Atmospheric Research (NCEP/NCAR) reanalysis from 1983 to 1996	Average error	The ANN-based model outperformed THE MLR model
	Prediction of the cyclone intensity over the Arabian Sea and Bay of Bengal Chaudhuri et al. (2013)	ANN, RBF, MLR, OLR	Backpropagation	5 predictors: sea surface temperature, central pressure, pressure drop, maximum sustained surface wind speed and total ozone column	Cyclone intensity over the Arabian Sea and Bay of Bengal for approximately 72 h lead time (1 output)	Indian Meteorological Department from 2005 to 2010	RMSE, MAE	ANN model provided the best prediction results
	Prediction of the cyclone intensity levels Chen et al. (2018)	ANN, MLR, SVM	Backpropagation	Multispectral Imagery	Cyclone intensity level (class labels)	Tropical cyclone Nalgae data from 04/08/2017 till 06/08/2017 retrieved from No. 4 meteorological satellite (FY-4) of China	Kappa coefficient and overall accuracy (%)	The three models provided comparable classification results
	Prediction of time series of typhoon	RNN	Backpropagation	3 previous time steps along with the current	Time series prediction of	Western North Pacific typhoon database	Average forecast error	Performance comparable to the

(Continued on following page)

TABLE 2 | (*Continued*) Summary of ML applications for tropical cyclones.

	Application	ML model	Training scheme	Input data	Output data	Data source	Performance metric	Remarks
	intensity Pan et al. (2019)			time of typhoon location and intensity	intensity up to 48 h with a 6 h time step	from the Chinese Meteorological Administration and the Shanghai Typhoon Institute from 1949 till 2016		Japanese Meteorological Agency-Global Spectral model
	Cyclone intensify forecasting over the Western Pacific, Eastern Pacific and North Atlantic basins Chen et al. (2019)	Hybrid CNN-LSTM model (2D-CNN, 3D-CNN and LSTM)	Gradient descent and Adam	3-D atmospheric variables (wind components, temperature, relative humidity and geopotential height) and 2-D sea surface variables (sea surface temperature)	Intensity (24-h lead time) with a 6 h time step	International Best Track Archive for Climate Stewardship (IBTrACS) and ERA-Interim reanalysis	MAE	Good simulation results comparable to other operational forecast models (e.g., Hurricane Weather and Research Forecasting Model)
	TC intensity prediction over the Pacific Northwest and Atlantic Ocean Wei Tian et al. (2020)	CNN	Adam	Satellite images of TCs in real time	TC intensity in near real time	Satellite outputs from 2003 till 2016 from the Meteorological Satellite Research Cooperation Institute and JWTC	RMSE	Good simulation results
	Hurricane intensity prediction Maskey et al. (2020)	CNN	Adam	Satellite images of TCs in real time	TC intensity in near real time	U.S. Naval research laboratory and the NOAA Geostationary Operational Environmental Satellite from 2000 through 2019	RMSE	Acceptable simulation results
iv) Wind field hazard	Estimation of surface wind field based on satellite data Stiles et al. (2014)	ANN (a total of 3 were used)	Levenberg-Marquardt	ANN 1: SeaWinds scatterometer measurements ANN 2: Outputs of ANN 1 ANN 3: 6 predictors (outputs of the first two ANNs, QuikSCAT radiometer rain rate and rain impact quantity, maximum likelihood estimation direction interval wind speed and cross-track distance)	ANN 1: wind speed from 0 to 20 m/s ANN 2: corrected wind speed over 20 m/s (retrieved from H*Wind) ANN 3: final optimized wind speed with a 12.5 km resolution	QuikSCAT mission and H*Wind between 1999 and 2009 for all basins (globally)	MAE	Good simulation results for the surface wind speed were obtained
	Forecasting surface wind speeds during tropical cyclones Wei (2015)	SVM with 4 kernels: linear, polynomial, radial basis function and Pearson VII	-	13 features are considered (e.g., central pressure, latitude, longitude, sea surface pressure) based on stepwise regression method	Surface wind speed (1-h average) for up to 6 h over two offshore islands near Taiwan	Central Weather Bureau of Taiwan from 2000 till 2012 (84 typhoon events)	RMSE	-Pearson VII SVR model is the most accurate technique among all other tested kernel-based SVM models -Resolution not discussed
	Estimation of TCs inner-core surface wind structure based on infrared satellite images Zhang et al. (2017)	LSSVM, RBFNN, linear regression	-	TC age, center latitude and maximum surface wind speed	Critical wind radii of 34- and 50-kt winds in real time	National Satellite Meteorological Centre of China and the Shanghai Typhoon Institute from 2005 to 2008	MAE	LSSVM outperformed all other models
	Simulation of TC boundary-layer winds Snaiki and Wu (2019)	KEDL	L-BFGS-B	Storm parameters (e.g., spatial coordinates, storm size and intensity)	Hurricane boundary-layer winds	H*Wind snapshots	RMSE	Good simulation results were obtained
	Surface wind simulation in near real time Wei (2019)	DNN	Back-propagation algorithm	16 inputs for Taipei and 14 for Keelung corresponding to the typhoon characteristics (e.g., central pressure) and surface meteorological data (e.g., relative humidity)	Hourly surface wind field with 1-degree by 1-degree resolution in 2 locations in Taiwan (Taipei and Keelung)	Central Weather Bureau of Taiwan and Weather Research and Forecasting (47 typhoons from 2000 till 2017)	RMSE	Good consistency between the simulated and WRF results

TABLE 3 | Summary of ML applications for non-synoptic winds.

	Application	ML model	Training scheme	Input data	Output data	Data source	Performance metric	Remarks
i) Thunderstorm	Prediction of severe thunderstorms McCann (1992)	ANN	Backpropagation	Lifted index and surface moisture convergence	Value between 0 and 1 representing the likelihood of the thunderstorm occurrence for a 3-7 h lead time	Centralized Storm Information System of the National Severe Storms Forecast Center (NSSFC) from April to August 1990 over the eastern two-thirds of the United States	critical success index	Acceptable results
	Prediction of the surface peak gust wind speed during thunderstorm events Chaudhuri and Middey (2011)	ANFIS, ANN, RBFNN, MLR	Gradient descent and the least squares estimate	Lift index, Convective Inhibition Energy, Convective Available Potential Energy and bulk Richardson number	Surface peak gust wind speed in Kolkata, India with a lead time up to 12 h	Radiosonde and rawinsonde from the Department of Atmospheric Sciences, University of Wyoming for the location of Kolkata, India from 1997 till 2009	RMSE, MAE	ANFIS model outperformed the other machine learning models
	Prediction of thunderstorms occurrences Litta et al. (2012)	ANN	Levenberg Marquardt, Momentum, Conjugate Gradient, Delta Bar Delta, Quick Propagation and Step	Wind speed, humidity and mean sea level pressure	Hourly temperature during thunderstorm, proxy for thunderstorm occurrence, over the northeastern region of India	Indian meteorological department from 2007 to 2009 (hourly data)	RMSE, MAE, correlation coefficient	Best results with Levenberg–Marquardt learning algorithm
	Prediction of severe thunderstorms occurrences Chakrabarty et al. (2013)	ANN, KNN	Gradient descent	2 predictors at 5 geopotential heights: dry adiabatic lapse rate and moisture difference (a total of 10 inputs)	Likelihood of occurrence of severe thunderstorms with a lead time between 10 and 14 h over the northeastern region of India	Indian Meteorological Department from 1969 to 2008	Correlation coefficient	KNN model was the best classifier
	Prediction of thunderstorm occurrence Yasen et al. (2017)	ANN, Bayes Network, C4.5 decision Tree, KNN	Artificial Bee Colony (ABC), gradient descent	31 thermodynamic and dynamic predictors	Thunderstorm occurrence	METeorological Aerodrome Reports and Surface Synoptic observation from December 2015 to November 2016 at lake Charles airport in Louisiana	Accuracy, AUC, and F-measure	ANN model optimized with ABC algorithm outperformed the other classifiers in detecting thunderstorms
	Prediction of thunderstorm occurrence Ukkonen et al. (2017)	ANN	Scaled conjugate gradient	15 inputs (e.g., most unstable lifted index and relative humidity near 700 hPa) identified based on skill scores	Thunderstorm occurrence in the next 6-h period	ERA-Interim database from 2002 to 2015 over Finland	Heidke skill score	Acceptable results
	Forecasting thunderstorms occurrence Kamangir et al. (2020)	SD-AE	Stochastic gradient descent	38 features (e.g., total predictable water and convective precipitation)	Thunderstorm occurrence through cloud-to-ground lightning parameter for a maximum lead time of 15 h and within 400 km^2 of a selected site in South Texas	North American Mesoscale Forecast System and the National Lightning Data Network from the 2004–2012	Peirce skill score	The SD-AE model outperformed an ANN model developed by Collins and Tissot (2015, 2016) for the same region and with similar lead time
	Forecasting the occurrence of thunderstorms events (Chen and Lombardo 2020)	CNN	Backpropagation	91-min time series of wind speed and direction	Event type (thunderstorm or non-thunderstorm event)	Automated Surface Observing System (ASOS) (1-min averaged data) from 2000 to 2018 with a total of 76,480 time series of 91 min of wind speed and direction	F1 score and average success rate	Reliable classifier for thunderstorms occurrences

(Continued on following page)

TABLE 3 | (*Continued*) Summary of ML applications for non-synoptic winds.

	Application	ML model	Training scheme	Input data	Output data	Data source	Performance metric	Remarks
ii) Downburst	Prediction of damaging wind from tornadic and straight-line events (including downbursts) (Marzban and Stumpf 1998)	ANN	Conjugate gradient	23 radar-derived predictors characterizing the circulations (e.g., depth of circulation, maximum rotational velocity and low altitude shear)	Probability of damaging wind (with a damaging wind excessing 25 m/s) with a lead time of 20-min	National Severe Storms Laboratory (NSSL) Mesocyclone Detection Algorithm (MDA)	Fraction Correct and Heidke's Skill Score	Acceptable results
	Classification of damaging downburst winds (Smith et al. (2004)	LDA	-	26 reflectivity and radial velocity-based attributes (e.g., cell volume, max reflectivity and height of the max reflectivity)	Severity of downburst winds (severe or non-severe events) with a maximum lead time of 15 min	WSR-88D radars (in several locations within the U.S.) from the National Climatic Data Center's Storm. It contains 91 events that produced severe downbursts and 1247 events that did not produce severe downbursts	median Heidke skill	Acceptable results for the prediction of severe downburst events
	Prediction of the probability of occurrence of damaging straight-line winds (including downbursts) from storm cells Lagerquist et al. (2017)	LR, LR with an elastic network, ANN, RF, GBTE	Gradient descent	431 predictors. They can be divided into 4 main categories, namely radar statistics, storm shape parameters, storm motion and sounding indices	Probability of occurrence of damaging winds with a lead time up to 90 min	Near-surface wind observations (from the Meteorological Assimilation Data Ingest System, the Oklahoma Mesonet, and the National Weather Service), radar scans (from the Multiyear Reanalysis of Remotely Sensed Storms) and soundings (from the Rapid Update Cycle and the North American Regional Reanalysis) [from 2001 to 2011]	AUC	- The simulation results indicated that storm motion and sounding indices are the dominant predictors - Both random forest and gradient-boosted tree ensembles gave the best simulation results
	Downburst wind speed forecasting Li and Li (2018)	LSSVM (coupled with variational mode decomposition and particle swarm) – with several kernels (linear, polynomial, Mexican Hat, radial basis function, and Morlet wavelet)	-	Time series of downburst wind (up to 1600 s)	Time series of downburst wind from 1600 s through 1800 s	Time series of downburst wind from two measurements data consisting of 450 sample points with a sampling frequency of 0.25 Hz for a total of 1800 s (the data source was not mentioned)	MAE, RMSE, 2-norms relative error and Pearson correlation coefficient	The combined Morlet wavelet and radial basis kernel functions (RBF) gave the best simulation results
	Identification of the downburst occurrence Medina et al. (2019)	RF	-	8 dual-polarization radar signatures (e.g., maximum vertically integrated liquid and temperature colder than 0°C)	Downburst related events or null events around the Cape Canaveral Air Force Station and Kennedy Space Center	Weather observation towers around the Cape Canaveral Air Force Station and Kennedy Space Center from 2015 to 2016	Mean Decrease Accuracy (MDA) and Mean Decrease Gini (MDG)	Although the model provided good simulation results, strong events were better classified compared to weaker ones
iii) Tornado	Prediction of the tornado's occurrences Marzban and Stumpf (1996); Marzban et al. (1997); Marzban (2000)	ANN	Conjugate Gradient	23 input variables (e.g., maximum shear, low- and mid-altitude convergence)	occurrence/non-occurrence of tornados for a given mesoscale circulation in the next 20 min	National Severe Storms Laboratory's (NSSL) Mesocyclone Detection Algorithm (MDA) with a total of 3258 circulation events	Critical Success Index	The ANN model outperformed other statistical models such as the discriminant analysis bur still the performance is low
	Detection of the tornado's occurrences Lakshmanan et al. (2005)	ANN	Resilient backpropagation	13 features (e.g., rotational velocity)	Tornado occurrence from given circulations in the next 20 min	National Severe Storms Laboratory based on the Mesocyclone Detection Algorithm (MDA) and the near-storm environment (NSE) with 110 storm days	Heidke Skill Score	Simulation results acceptable

(Continued on following page)

TABLE 3 | (*Continued*) Summary of ML applications for non-synoptic winds.

Application	ML model	Training scheme	Input data	Output data	Data source	Performance metric	Remarks
Prediction of the tornado occurrence Santosa (2007)	SVM, LDA, BNN	Backpropagation	34 input features (e.g., meso core depth and meso low-level shear)	Tornado occurrence in the next 20 min	Weather Surveillance Radar 1998 Doppler	Heidke Skill Score	- linear programming support vector machine was used for feature selection - BNN model gave the best performance in detecting tornados from given circulations
Prediction of the tornado occurrence Adrianto et al. (2009)	SVM with 3 kernels (linear, polynomial and RBF), ANN, LDA	Backpropagation	53 input features (e.g., azimuthal shear low level average, gradient direction maximum and reflectivity aloft average)	Tornado occurrence in the next 30 min	Radar measurements from the National Climatic Data center with a total of 33 storm days sampled at 30 min	Heidke Skill Score	-The best classifier was the SVM model with the RBF kernel -SVM model outperformed the other algorithms
Prediction of the tornado occurrence Trafalis et al. (2014)	SVM (radial basis function kernel), LR, RF, rotation forest	-	22 attributes (e.g., wind shear and humidity)	Tornado occurrence from mesocyclones events (no leading time indicated)	MDA and NSE databases with 111 storm days	Heidke Skill Score	-Feature selection was performed using the SVM-Recursive Feature Elimination algorithm with a radial basis function kernel - SVM with threshold adjustment outperformed all other classifiers
Prediction of the probability of occurrence of a tornado Lagerquist et al. (2018), (2020)	CNN	Adam	Storm-centered radar image and a proximity sounding	Probability of occurrence of a tornado in the next-hour	Multiyear Reanalysis of Remotely Sensed Storms (MRRSS) in the [period from 2000 to 2011] and Gridded NEXRAD WSR-88D Radar (GNWR) [period from 2011 to 2018]	Area under the receiver-operating-characteristic curve (AUC) score	Excellent simulation results
Predicting property damage from tornadoes Diaz and Joseph (2019)	ANN (2)	AdaGrad	Storm, land cover, socioeconomic and demographic features	ANN1: occurrence or non-occurrence of damage due to a tornado event ANN2: level of damage when it occurs	NOAA's tornado database, the National Land Cover database and the American Community Survey	AUC, MSE, R^2	-Only the initial tornado coordinates are accounted for rather than the tornado path -Acceptable results
Prediction of the occurrence of tornadic events Coffer et al. (2020)	RF, CNN	Stochastic gradient descent	222 input features at various geopotential heights were initially selected (e.g., temperature, pressure) –Exact final parameters not mentioned-	Tornadic and non-tornadic events	Rapid Update Cycle sounding data from the National Climatic Data Center from 2003 to 2017	Overall accuracy score (in %)	-The input feature selection was carried out using RF which indicated that the pressure terms are not as important as the other environmental parameters (e.g., v-wind component) - RF outperformed CNN

TABLE 4 | Summary of ML applications for terrain and topography.

Application	ML model	Training scheme	Input data	Output data	Data source	Performance metric	Remarks
Modeling the effects of topography on the wind profile Bitsuamlak (2004); Bitsuamlak et al. (2002), (2006), (2007)	ANN	Cascade correlation	6 inputs including simple geometric properties (i.e., "Windward slope of the hill", "Distance between hills", "Height from the crest of the hill" and "Longitudinal location"), roughness element and hill count	Fractional speed-up ratio	CFD simulations corresponding to different topographic configurations: single and multiple hills and escarpments	R^2 coefficient	-Comparison with experimental data from wind tunnel -Good performance
Wind field simulation considering terrain effects Martínez-Vázquez and Rodríguez-Cuevas (2007)	ANN combined with conditional simulation technique	Backpropagation	Terrain roughness, mean wind profile and spectral density	Wind velocity time series (3 min of time series with a time step of 0.1 s) at different points	The time series of wind speed were generated using the procedure of Simiu and Scanlan (1978) at two heights (i.e., 10 and 200 m) with 11 local velocities (from 0.5 to 100 m/s) and surface roughness between 0.001 and 0.050 m	MSE	-The conditional simulation technique significantly decreased the number of required layers in the ANN -Good simulation results
Estimation of the effect of wind direction on wind speed prediction in complex terrain Lopez et al. (2008)	ANN	Bayesian regularization	4 inputs: 10-min mean wind speed from 3 stations nearby and wind direction from another nearby station	Annual average wind speed at a given site with complex terrain configuration	Meteo-Galicia during 2003 at the Galicia region in the northwest Spain corresponding to 5 stations and representing various terrain conditions (e.g., inland and offshore conditions) and elevations	RMS	-Wind direction is important to be considered to improve the simulation results for a site with complex terrain
Prediction of typhoon wind speed and profile over complex terrain Huang and Xu (2013)	ANN	Backpropagation	Upstream wind speed and direction at height z	Wind speed and direction at height z on a bridge site	Reynolds-averaged Navier-Stokes simulations which provides the wind profiles at the bridge site given an inlet upstream wind field (which does not account for topographic effects)	MAE	Good simulation results for both wind speed and direction
Prediction of the wind flow over complex topographies Mayo et al. (2018)	DNN	Proximal adagrad	3 cartesian coordinates (x,y,z) of the selected point and the incoming uniform mean wind speed	Mean wind speed over a given site with complex topography	4 CFD simulations of the wind field in a given coastal dune system with complex terrain	MAE	Acceptable simulation results
Selection of the experimental hardware within a wind tunnel Abdi et al. (2009)	ANN (2)	cascade correlation	ANN1: height from floor, the bottom-spire width, the surface roughness and the top spire width	ANN1: mean longitudinal wind velocity and turbulence intensity	RWDI USA LLC wind tunnel in Miramar, Florida	No error scores were provided	- Visual inspection of the predicted wind profile and turbulence intensity of the first neural network

(Continued on following page)

TABLE 4 | (*Continued*) Summary of ML applications for terrain and topography.

Application	ML model	Training scheme	Input data	Output data	Data source	Performance metric	Remarks
							indicated good simulation results - Results from ANN2 were not satisfactory
			ANN2: target mean longitudinal wind speed, target turbulence intensity and height from floor	ANN2: difference between top and bottom spire width and the surface roughness			
Prediction of wind properties in urban environments based on wind tunnel tests Varshney and Poddar (2012)	ANN (2)	Lavenberg–Marquardt	ANN1: number of roughness elements, number of barriers, height from floor and slot width ANN2: number of roughness elements, number of barriers and slot width	ANN1: mean wind speed, turbulence intensity and length scale factor ANN2: instantaneous velocity	Boundary-layer wind tunnel tests of the National Wind Tunnel Facility in Kanpur, India (18 configurations)	No error scores were provided	- Visual inspection of the predicted results indicated satisfactory simulations
Designing laboratory wind simulations Križan et al. (2015)	ANN (2)	RPROP Riedmiller and Braun (1993)	ANN1: basis barrier height, barrier castellation height, surface roughness elements' spacing density, surface roughness elements' height and height of measurement points	ANN1: mean wind speed, turbulent intensities (in the three directions), length scales (in the three directions) and turbulent Reynolds stress	Boundary-layer wind tunnel at the Technische Universität München with a total of 23 configurations of hardware setups	R^2	-ANN1: except the turbulent length scale in the *x*-direction (not that accurate) all other results were good
			ANN2: basis barrier height, surface roughness elements' spacing density, surface roughness elements' height, frequency and height of measurement points	ANN2: power spectral densities of the velocity fluctuations in the three directions			- ANN2: good simulation results were obtained

wind field). Just like ML applications to downbursts, a high number of input variables (predictors) were utilized for the reviewed ML models. The identification of the most appropriate set of predictors is still very challenging, and a trail-and error approach was typically employed. In addition, it is not easy to conduct a systematic comparison among reviewed ML models since the used performance metrics differ substantially from one application to another.

3.2 Terrain and Topography

Wind characteristics including mean wind speeds and turbulent fluctuations are much affected by the surrounding terrain and topography. As a consequence, careful consideration of local terrain roughness and topographic features as well as surrounding obstacles is vital to the accurate determination of wind pressures on structures and pedestrian level winds. Wind codes and standards consider the terrain effects corresponding to limited (and simplified) terrain geometries (e.g., escarpment and single hill) through correction factors. To examine the effects of complex terrain condition on wind fields, wind tunnel tests are usually employed with a very small geometric scale (e.g., 1:500). Alternatively, numerical schemes such as the mass-conservation or momentum-conservation model can be used to capture the terrain effects on oncoming wind fields. Although the topographic effects can be well simulated based on momentum-conservation models (e.g., using Reynolds-averaged Navier-Stokes equations), the needed computational time makes it impractical for use as a real-time decision support tool. The mass-conservation model computes wind fields over complex terrain in seconds to a few minutes (Forthofer et al., 2014a; 2014b), but the accuracy of simulation may be poor because nonlinear momentum effects are not considered (Jackson and Hunt 1975). Considering the complex terrain-wind data from high-fidelity CFD simulations, wind tunnel tests and field measurements are increasingly available, ML tools can be utilized (as computationally efficient reduced-

order models that possess high simulation accuracy of complex nonlinear systems) to provide rapid estimation of wind flows over various terrain conditions. However, ML development for terrain and topographic considerations is still at an early stage with a limited number of studies reported in the literature. **Table 4** presents the reviewed applications of ML for terrain and topography, where the ML model, training scheme, input data, output data, data source and performance metric are summarized for each application. The training/testing data were essentially retrieved from either CFD simulations or wind tunnel tests. From **Table 4**, it can be concluded that most applications used ML as a regression model for prediction of wind fields over various terrain conditions and topographic configurations. There are a few studies that applied ML techniques to assist in efficient search for a correct layout of passive flow altering devices (e.g., spires and roughness elements) in the boundary-layer wind tunnel. It is noted that the current ML applications to consider topographic effects on wind fields are usually limited to terrain configurations that can be characterized by several parameters, hence, the employed ML models and training schemes are simple and standard (e.g., ANN with backpropagation). However, several advanced ML models such as autoencoder (e.g., Fukami et al., 2019) and GAN (Kim and Lee 2020) have been utilized to assist in the generation of turbulent inflow (as a realistic inlet boundary condition of CFD simulations).

3.3 Aerodynamics and Aeroelasticity

The bluff-body aerodynamics and aeroelasticity play a critical role in the safe and cost-effective design of wind-sensitive structures, and their considerations rely heavily on boundary-layer wind tunnels. In addition to the Reynolds number effects (due to very small model scales), wind tunnel tests are very time consuming and labor intensive. To this end, CFD techniques have been rapidly developed for simulations of structural aerodynamics (gust-induced effects) and aeroelasticity (motion-induced effects). The purpose is to make CFD simulations serve as a complementary or even alternative approach to wind tunnel tests. Despite significant advances of hardware and algorithms, the reliable CFD simulations of wind-structure interactions are still computationally very expensive due to three-dimensional nature of wakes and intensive flow separations from structures. Hence, a number of reduced-order models have been developed to efficiently model structural aerodynamics and aeroelasticity (Wu and Kareem 2013). Unfortunately, these reduced-order models do not always have a satisfactory representation of the full nonlinear equations that govern the wind-structure interactions. Specifically, modern bridge decks and super tall buildings with unusually geometries all exhibit nonlinear unsteady aerodynamics and aeroelasticity that limit the applicability of the state-of-the-art reduced-order modeling methodologies. On the other hand, the Kolmogorov Neural Network existence theorem offers mathematical foundation for applying multilayer neural networks to approximate arbitrary nonlinear systems with any precision (Huang and Lippmann 1988; Hornik, 1991). With high-fidelity data and advanced algorithms, ML models can simultaneously achieve great simulation efficiency and accuracy. It is noted that there are numerous ML applications to aerodynamics and aeroelasticity of both bluff bodies (e.g., circular cylinder) and streamlined bodies (e.g., airfoil) in fluid mechanics community (e.g., Kutz 2017; Brunton et al., 2020), however, they are not discussed here. The review in this section only covers wind-sensitive structures in civil engineering. The ML applications for bridge aerodynamics and aeroelasticity are first reviewed in **Table 5i** and then followed by buildings and other structures in **Table 5ii**, where the ML model, training scheme, input data, output data, data source and performance metric are summarized for each application. The training/testing data were essentially retrieved from either CFD simulations or wind tunnel tests. From **Table 5**, it can be concluded that most applications used ML as a regression model for prediction of steady-state force coefficients, flutter derivatives and vortex-induced vibrations (VIV) of various bridges and for modeling of wind pressure coefficients of various buildings (as well as estimation of the interference factors for adjacent buildings). The different aerodynamic representations in bridges (mainly using global quantities such as force coefficients) and buildings (mainly using local quantities such as pressure coefficients) are partially due to available data types from wind tunnel tests. Although satisfactory ML simulation results have been obtained (in terms of interpolations), most reviewed applications do not necessarily have good performance in terms of extrapolations outside the training datasets. It is noted that the currently available ML models of aerodynamics and aeroelasticity are developed for the main purpose of being used as preliminary design tools to avoid the high-cost wind tunnel tests in the early design stage. There is a lack of systematic comparison among various ML models, hence, their selection for specific applications is rather rudimentary.

3.4 Structural Dynamics and Damage Assessment

Due to the computational complexity of numerical techniques (e.g., finite element method) for solving wind-induced nonlinear structural response, reduced-order models (e.g., ANN) have been developed to alleviate the computational cost of the high-fidelity models. The ML models have been used for structural dynamics and damage assessment for several decades mainly in the field of earthquake engineering (e.g., Wu et al., 1992; Masri et al., 1993; Jiang and Adeli 2005; Pei et al., 2005; Gholizadeh et al., 2009; Facchini et al., 2014; Derkevorkian et al., 2015; Liang 2019; Wu and Jahanshahi 2019; Yu et al., 2020). However, similar applications have not emerged in wind engineering community until recently due essentially to the linear consideration of the wind-induced structural response [ASCE 7-16 (ASCE, 2017)]. Recent advances of performance-based wind design methodology have placed increasing importance on effective simulations of nonlinear, inelastic structural dynamics response under strong winds. The numerical estimation of wind-induced nonlinear structural response using a high-fidelity finite element model is computationally very expensive due to its small time-step size and long simulation duration. Accordingly, several ML applications to wind-induced structural dynamics have been

TABLE 5 | Summary of ML applications for aerodynamics and aeroelasticity.

	Application	ML model	Training scheme	Input data	Output data	Data source	Performance metric	Remarks
i) Bridges	Estimation of aeroelastic parameters of bridge decks Jung et al. (2004)	ANN	Resilient backpropagation Riedmiller and Braun (1993)	100 inputs:90 inputs representing the section geometry and 10 inputs for the nondimensional velocity	Flutter derivatives (6) of a rectangular section	Wind tunnel test (total of 17 experiments)	MSE	Acceptable performance
	Prediction of flutter derivatives of a rectangular section model Chen et al. (2008)	ANN (total of 8)	Gradient descent	Width-to-depth ratio and a set of reduced frequency	8 flutter derivatives (each given by 1 ANN separately) of rectangular section model	Experimental data from wind tunnel tests	No error metrics	From the graphical results, the simulation results were in good agreement with the experimental ones
	Prediction of flutter derivatives of a cable stayed bridge Lute et al. (2009)	SVM (RBF kernel)	-	Non-dimensional velocity and width to depth ratio of bridge deck	8 flutter derivatives of a cable stayed bridge	Wind tunnel tests were retrieved form Matsumoto et al. (1996)	MSE	Good simulation results
	Estimation of flutter derivatives of a rectangular section Chung et al. (2012)	ANN (total of 8)	Backpropagation	Width-to-depth ratio, reduced frequency and reduced velocities	8 flutter derivatives (each given by 1 ANN separately) of rectangular section model	CFD simulations and forced-vibration test in a wind tunnel	No error metrics	Good performance
	Modeling vortex-induced vibration of a long-span suspension bridge Li et al. (2018)	DT, SVR (with Gaussian radial basis kernel)	-	DT: incoming wind speed and direction at three locations on the bridge deck SVR: same inputs as DT model at the current step along with the response of the previous step	DT: VIV modes (a total of 6) SVR: VIV amplitudes	Field measurements of a full-scale suspension bridge over a period of 6-years (2010–2015) located in the eastern ocean of China	RMSE, accuracy (%), squared correlation coefficient	Good simulation results
	Prediction of nonlinear unsteady bridge aerodynamics Li et al. (2020)	LSTM	Back-pass algorithm	Bridge deck motions	Motion-induced aerodynamic forces	CFD simulations (total of 14,880 input-output data corresponding to a 2-D bridge deck cross-section)	No error metrics	Excellent agreement (through visual inspection) between the LSTM model and CFD was obtained
	Prediction of aeroelastic response of bridge decks Abbas et al. (2020)	ANN	Levenberg-Marquardt	18 inputs corresponding to the response for heave and pitch (in terms of displacement, velocity and acceleration) at previous time steps with three lag terms	Normalized lift force and torsional moment coefficients at current time step	2 dimensional CFD simulations for the two bridge cross-sections	MSE	Good simulation results were obtained
	Prediction of the flutter velocity of suspension bridges Rizzo and Caracoglia (2020)	ANN (different topologies)	Levenberg-Marquardt	1st ANN category: deck chord, deck weight or the ratio between the 1st torsional and the 1st vertical circular frequencies of the bridge, structural damping, air density and the flutter derivatives 2nd ANN category: deck chord, the ratio between the first torsional and the first vertical circular frequencies of the bridge, and the flutter derivatives	Critical flutter velocity of suspension bridge with closed box deck sections	Wind tunnel experiments along with finite element-based simulation corresponding to various geometrical and mechanical parameters of the bridge deck cross-section	R^2	While the performance of the ANN models varied according to the topology, their performance was good

(Continued on following page)

TABLE 5 | (*Continued*) Summary of ML applications for aerodynamics and aeroelasticity.

	Application	ML model	Training scheme	Input data	Output data	Data source	Performance metric	Remarks
ii) Building & other structures	Prediction of wind load distribution for air-supported structures Turkkan and Srivastava (1995)	ANN	Gradient descent	Hemispherical membrane: internal pressure ratio and two spatial orientations Cylindrical membrane: Similar inputs as the first case + membrane aspect ratio	Steady-state wind pressure coefficient for air-supported structures (e.g., cylindrical and hemispherical membranes)	Wind tunnel tests	R^2	Acceptable results
	Modelling wind-induced interference effects on high-rise buildings Khanduri et al. (1997)	ANN	Generalized delta rule	Spacing between two adjacent buildings in the along- and across-wind directions	Mean and dynamic along- and across-wind directions interference factors	Wind-tunnel tests from two references Saunders and Melbourne (1980); Taniike and Inaoka (1988)	No error metrics	-
	Modelling wind-induced interference effects on high-rise buildings English and Fricke (1999)	ANN	Backpropagation	Building aspect ratio, normalized separation distance and power law index	Interference index	Wind tunnel tests from several sources e.g., Zambrano and Peterka (1978); Blessmann and Riera (1985)	No error metrics	-
	Interpolation of wind-induced pressure time series on a scaled model Chen et al. (2002)	ANN	Levenberg–Marquardt	4 adjacent experimental pressure taps at the next time step (t+1) and values of the pressure taps at current & two previous time steps in the target tap (central one)	Wind pressure coefficient at the next time step	Wind tunnel tests of a 1:50 scale model	R^2	Good simulation results
	Prediction of pressure coefficients on roofs of low buildings Chen et al. (2003)	ANN (2 models)	Levenberg–Marquardt	Roof height, wind direction and two normalized roof coordinates (for the two models)	ANN1: mean pressure coefficients on a gable roof of low-rise building ANN2: root-mean-square pressure coefficients on a gable roof of low-rise building	Wind tunnels experimental data	MSE	Good simulation results
	Prediction of building interference effects Zhang and Zhang (2004)	ANN, RBFNN (with Gaussian kernel)	Backpropagation	Ground roughness, relative orientation of two buildings	Inference factor	Experimental data from literature e.g., Bailey and Kwok (1985)	MSE	RBF outperformed the ANN model
	Prediction of wind loads on a large flat roof Fu et al., (2006), (2007)	FNN (2 models)	Backpropagation	FNN1: wind direction and the positions of the available pressure taps FNN2: wind direction and the frequency for the few selected tap locations	FNN1: Mean pressure coefficients on a large flat roof FNN2: Power spectral density (at given input frequencies) at few locations in the roof corners and leading edge	Boundary-layer wind tunnels tests	MSE	- Acceptable results for the 1st FNN model - No error metrics were reported for the 2nd FNN model
	Wind load evaluation for the design of roof cladding of spherical domes Uematsu and Tsuruishi (2008)	ANN (4 models)	Quickprop algorithm Fahlman (1988)	'2 geometric parameters of the dome', '2 coordinates parameters x and y', 'turbulence intensity of the incoming wind at the mean roof height'	Statistics of wind pressure coefficient on the roof of a spherical dome: mean, standard deviation, skewness and kurtosis	Experimental wind tunnel tests	Predefined error index (normalized by the standard deviation of the target data)	- Acceptable results
	Estimation of the wind force coefficients on a rectangular building Wang et al. (2013),	ANN, RBFNN, GRNN	Backpropagation	Aspect & side ratio and ground roughness	Along-wind mean coefficient of base shear of a rectangular building	Wind tunnel tests	RMSE	RBFNN outperformed all other models

(Continued on following page)

TABLE 5 | (*Continued*) Summary of ML applications for aerodynamics and aeroelasticity.

Application	ML model	Training scheme	Input data	Output data	Data source	Performance metric	Remarks
Wang and Cheng (2015), (2017)							
Wind load prediction of large-span dry coal sheds Sun et al. (2017)	GRNN	-	rise-span ratio, depth-span ratio, wind angle, and local coordinates	Statistics of the pressure coefficients: mean, RMS. Skewness, kurtosis of pressure coefficients, three auto-correlation coefficients and coherence exponent	Wind tunnel tests	R^2	While the mean pressure coefficient was predicted accurately, the kurtosis of the pressure coefficient was poorly predicted
Prediction of wind loads on high-rise building Huang et al. (2017)	ANN (2 models)	Levenberg–Marquardt	ANN1: coordinates (x, y, z) of the pressure taps	ANN1: mean or root-mean-square pressure coefficients on a high-rise building	Wind tunnel tests	RMSE	- No error metric was reported for the 1st ANN model
			ANN2: coordinates (x, y, z) of the pressure taps and time	ANN2: time series of wind-induced pressures on a high-rise building			- Good simulation results for the 2nd ANN model based on RMSE.
Prediction of wind pressure coefficients on building surfaces Bre et al. (2018)	ANN (3 models for flat-, gable, and hip-roofed low-rise buildings)	Levenberg–Marquardt	Wind direction and building characteristics (1 parameter for the flat-roofed building, and 2 parameters for the gable roofed and hip-roofed buildings)	Mean pressure coefficients over few locations on the roofs and walls (5 outputs for the flat-roofed, 6 for the gable-roofed and 8 for the hip-roofed)	Tokyo Polytechnique University experimental database	MSE, R^2	Good simulation accuracies
Prediction of roof pressures on a low-rise structure Fernández-Cabán et al. (2018)	ANN	Levenberg–Marquardt	Turbulence intensity (at eave height) and 2 normalized roof coordinates	Mean, root-mean-square, and peak pressure coefficients on the roof (at 152 roof taps) of 3 scaled low-rise buildings (1: 50, 1:30, and 1:20)	Wind tunnel tests	RMSE, MAE, R^2	The accuracy of simulation results depends on the pressure taps location
Modeling for unsteady flows around bluff bodies of various shapes Hasegawa et al. (2019), (2020)	CNN-AE + LSTM	Adam	Temporal variation of the flow field around different 2-D cross-sections shapes: 2 velocity components and pressure	Temporal variation (next time step) of the flow field around different 2-D cross-sections shapes: 2 velocity components and pressure	Direct numerical simulation (DNS): 100 different bluff-bodies shapes (in 2-D space) with 500 instantaneous time-series flow fields each	MSE	-The use of CNN-AE allows the mapping between the high-dimensional space and a low-dimensional latent space which facilitates the training of the LSTM model - Excellent performance
Prediction of wind pressures on a tall building under interference effects Hu et al. (2020)	DT, RF, XGBoost, GAN	-	GAN: wind direction and location of the interfering building DT, RF, XGBoost: wind direction, the coordinates of the pressure tap and the location of the interfering building	GAN: mean and fluctuating pressure coefficients over all faces of the building DT, RF, XGBoost: mean and fluctuating pressure coefficient at one point on the building surface	Aerodynamic database of Tokyo Polytechnic University	R^2	The GANs-based model outperformed the other three machine learning algorithms and provided accurate mean and fluctuating pressure coefficients on the principle building
Prediction of low-rise gable roof building pressures Jianqiao Tian et al. (2020)	DNN	Levenberg–Marquardt	Prediction's location (x, y, z) and the incoming wind direction	Mean and peak wind pressure coefficients on the surface of a scale model corresponding to a low-rise, gable roof building	Wind tunnel tests	R^2	Excellent performance results
Predicting wind pressures around circular cylinders Hu and Kwok (2020)	RF, DT, GBRT	Gradient descent	Turbulence intensity, incoming wind, Reynolds number and circumferential angle of the cylinder	Mean and fluctuating wind pressures around a circular cylinder for high Reynolds numbers	From published papers e.g., Cheng et al. (2016), Gao et al. (2017)	R^2	GBRT outperformed all other models

TABLE 6 | Summary of ML applications for structural dynamics and damage assessment.

	Application	ML model	Training scheme	Input data	Output data	Data source	Performance metric	Remarks
i) Structural dynamics	Modeling hysteretic nonlinear behavior of bridge aerodynamics Wu and Kareem (2011)	ANN	Gradient descent	12 inputs: mean wind velocity in the current and next time steps, fluctuating components in the longitudinal and vertical direction in the current and next time steps, and the vertical and torsional displacement with their first and second derivatives in the current time step	Vertical (torsional) acceleration of the bridge deck section in the next time step	Tongji-1 wind tunnel at State Key Lab in Tongji University	No error metrics	- Cellular automata-based system was employed to optimize the ANN configuration - The visual inspection of the results indicated the good agreement between the simulated and measured - ANN model showed good promise in simulating the hysteretic nonlinear behavior of the bridge deck which interacts with the incoming fluctuating wind
	Analysis of tall building for across wind response Vyavahare et al. (2012)	ANN	Backpropagation	Building shape (height, breadth and depth), the terrain category and incoming wind speed	Shear force and bending moments of tall buildings	Data generated from numerical examples	No error metrics	From visual inspection, it can be concluded that a good agreement between the simulated and numerical results has been obtained
	Identification of the dynamic properties high-rise buildings subjected to wind Oh et al. (2017)	ERBFN	Genetic algorithm	Wind speed and direction	Column stress of a tall building subjected to wind loads	Wind tunnel tests	RMSE, maximum error between the measured and estimated values	Good simulation results were obtained
	Identification of the dynamic properties high-rise buildings subjected to wind Nikose and Sonparote (2019a); (2019b), (2020)	ANN	Backpropagation	Building geometry (height, breadth and depth), incoming wind velocity and terrain category	Dynamic response in the along-wind and across-wind in terms of base shear and base bending moment	Dataset were generated based on the Indian Wind Code (IWC) for various building configurations	RMSE	Good simulation results were obtained
	Wind-induced response estimation for tall buildings Oh et al. (2019)	CNN	Backpropagation	Top-level (top floor of a tall building) wind induced displacement in both time and frequency domain and measured wind speed in the	Maximum and minimum strains of the building columns	Wind tunnel tests	RMSE	Good simulation results were obtained

(Continued on following page)

TABLE 6 | (*Continued*) Summary of ML applications for structural dynamics and damage assessment.

	Application	ML model	Training scheme	Input data	Output data	Data source	Performance metric	Remarks
				frequency domain				
	Wind-induced nonlinear structural dynamic analysis Wang and Wu (2020)	KE-LSTM	AdaMax	Wavelet coefficients of the normalized wind excitation (external wind force)	Normalized structural displacement at different nodes	Numerically for the case of SDOF and MDOF	MAE	- The governing equation of motion was embedded within the loss function - Excellent simulation results
	Prediction of structural response of wind-excited tall buildings Micheli et al. (2020)	AWN	Backpropagation	Wind load and high-performance control systems (HPCS) characteristics	Maximum absolute acceleration of the structure	Dataset generated numerically corresponding to a 39-stoery steel-frame system building subjected to wind load and equipped with several equipment (e.g., damping devices, sensors and global controller)	RMSE	- AWN parameters were updated sequentially each time data arrives (online training) - Good simulation results
ii) Damage assessment	Constructing and validating geographically refined HAZUS-MH4 hurricane wind risk models Subramanian et al. (2013)	Ensemble models composed of 50 bagged DT	-	10 predictors were identified (e.g., number of floors, terrain roughness, wind speed and direction)	Classification: Structures that were correctly or not well predicted by HAZUS-MH4 (in terms of hurricane induced wind damage) in 1-km square blocks	The data contains the damage states and corresponds to approximately 700,000 residences in the Harris County following hurricane Ike (2008)	Accuracy (%) and customized error metric	- The results of this study suggest that HAZUS-MH4 fragility curves for certain home types, need to be refined to improve the prediction results
	Probabilistic damage estimation for asphalt shingle roofing Huang et al. (2015)	ANN	Backpropagation	8 predictors: wind speed, angle of attack, shingle resistance, building length, building width, building height, roof slope and surface roughness	Mean damage ratio of an asphalt shingle roof	Boundary-layer wind tunnel tests from the University of Western Ontario	Accuracy (%)	Good performance
	Estimatin of the fatigue damage of coastal bridges under coupled loads Zhu and Zhang (2018)	SVR (with Gaussian kernel)	-	Gross vehicle weight; 10-min wind speed; significant wave height; and peak wave period	Daily equivalent fatigue damage accumulation	Traffic data from a cable-stayed bridge located in southern China coastal regions & the wind/wave data from Meteorological Observatory near the bridge location from 1980 to 2012	RMSE, MAE, MAPE	Good simulation results were obtained
	Performance assessment of a vertical structure subjected to non-stationary, tornadic wind	ANN	Levenberg-Marquadt	Maximum mean tangential velocity of the tornado and its radial length scale	Fragility values associated with each intensity measures combination	Numerically generated in which the Monte Carlo simulation was employed	Absolute differences	Various architectures were tested and the best ANN model has one

(Continued on following page)

TABLE 6 | (*Continued*) Summary of ML applications for structural dynamics and damage assessment.

Application	ML model	Training scheme	Input data	Output data	Data source	Performance metric	Remarks
loads Le and Caracoglia (2020)							hidden layer with 4 neurons
Object detection in aerial imagery for disaster response and recovery after the occurrence of hurricanes Pi et al. (2020)	Series of CNN trained using transfer learning	Backpropagation	Digital images and videos	Bounding boxes of the ground objects of interest (i.e., flooded area, building roofs damage, debris, vegetation and cars) and their corresponding class labels (e.g., damaged or undamaged)	-The models were pretrained on the common objects in context/visual object classes (COCO/VOC) databases Everingham et al. (2010); Lin et al. (2017) - Then they were retrained on new aerial video dataset Volan 2018 (corresponding to hurricanes that occurred in 2017–2018) obtained using web mining algorithms	Mean average precision	Acceptable results

developed in recent years for simultaneously achieving high simulation accuracy and efficiency. The performance-based (and further resilience-ba sed) wind design philosophies also require accurate damage assessment of structures and infrastructure under extreme storms. The structural damages under winds depend on numerous factors including wind features (e.g., wind speed/direction and topography) and built environment characteristics (e.g., building opening and roof slope), hence its assessment and quantification are extremely challenging. On the other hand, increasingly available field-measurement data characterizing structural damages under strong wind events [e.g., resulting from post-disaster reconnaissance activities such NHERI Natural Hazards Reconnaissance (RAPID) Facility and NSF Structural Extreme Events Reconnaissance (StEER) Network] provide a great opportunity to learn from data by using various ML models. The ML applications for structural dynamics are first reviewed in **Table 6i** and then followed by damage assessment in **Table 6ii**, where the ML model, training scheme, input data, output data, data source and performance metric are summarized for each application. The training/testing data were essentially retrieved from numerical simulations, wind tunnel tests and field measurements. From **Table 6**, it can be concluded that most applications used ML as a regression model for modeling structural dynamics and as a regression or a classification model for structural damage assessment. While many applications employed simple ML models and standard training schemes (e.g., ANN with backpropagation), some advanced schemes such as knowledge-enhanced LSTM have been successfully applied to predict time series of wind-induced nonlinear structural response. It is noted that the selection of the most appropriate set of inputs to ML models for damage assessment (predictors or features) is still very challenging.

3.5 Mitigation and Response

Both long-term and short-term strategies are needed to enhance resilience of individual structures or communities to withstand wind-related hazards. One important long-term consideration is to mitigate structural response/vibration subjected to winds through structural optimization and/or control. For structural optimization under winds, the shape optimization is probably the most effective approach to reduce aerodynamic loading. For wind-induced vibration control, both aerodynamic and mechanical measures are well recognized in wind engineering community. Although the structural performance evaluation under winds is typically a very complicated task, the corresponding simulations during optimization or (active) control process is required to be efficient and accurate because they need to be conducted either repeatedly for numerous scenarios or in a (near) real-time sense. As noted earlier, the ML models are very promising to simultaneously achieve the high simulation efficiency and accuracy goal. In addition, the RL models that have gained increasing popularity in recent years can be used as very effective optimization or control algorithms compared to conventional approaches (Silver et al., 2017). In the consideration of short-term actions, efficient management strategies are critically important. Although the ML models used in the disaster (including wind-related hazard) management framework (i.e., covering preparedness, response and recovery) have recently been systematically reviewed (e.g., Sun et al., 2020), its applications to social media-informed response are still discussed here since the unprecedentedly

TABLE 7 | Summary of ML applications for mitigation and response.

	Application	ML model	Training scheme	Input data	Output data	Data source	Performance metric	Remarks
i) Structural optimization & control under winds	Vibration control of wind-induced response of tall buildings with active tuned mass damper Bani-Hani (2007)	ANN (2 models)	Backpropagation	ANN1&2: 20 inputs-absolute wind-induced acceleration of 3 selected floors at the current and previous 4-time steps, and the active tuned mass damper control forces at the current and previous 4-time steps	ANN1: 4-time steps ahead the absolute acceleration of three floors (i.e., 50th, 60th and 70th) ANN2: future control force at the next time step of the active tuned mass damper	Numerically generated using a SIMULINK model with a total of 50 s of data and a sampling time of 0.001s for a tall building with 76-stoery (data generated with and without random white noise control force of up to 5 Hz frequency)	RMS and defined dimensionless performance indexes	The coupled ANN models were able to reduce substantially the peak displacement and the absolute acceleration response of the building storeys
	Aerodynamic shape optimization of tall buildings Elshaer et al. (2016), (2017)	ANN with a genetic algorithm	-	Geometric variables of the cross section and the wind angle of attacks	Objective function = the mean drag coefficient or the standard deviation of the lift coefficient	LES simulations of a two-dimensional flow corresponding to different geometric properties of the cross section	R^2	- Good simulation results - Significant optimization of the mean drag coefficient and standard deviation of the lift coefficient
	Aerodynamic shape optimization of tall buildings Li et al. (2021a)	KE-DRL	Gradient descent	State: external shape of the structure	Action: design adjustment of the cross section to maximize the aerodynamic mitigation (by minimizing the drag of a high-rise building)	RANS and LES simulation of a 2-D cross section example	-	- Both specific direct-domain and cross-domain knowledge are leveraged through transfer-learning and meta-learning - The deep deterministic policy gradient algorithm (DDPG) was used for the RL algorithm - RL-based shape optimizer outperformed the basic gradient descent, particle swarm optimization (PSO) and typical RL without knowledge
	Bluff body active flow control in experiments and simulations Fan et al. (2020)	DRL	Adam	States: drag and lift coefficients	Action: ratio of the rotation rate for each rotating cylinder and the maximum rotation rate to minimize the drag in both simulations and experiments	Entropy-viscosity-based large eddy simulation (LES) (for the numerical simulation) and an experimental setup	-	-The Twin Delayed Deep Deterministic policy gradient algorithm was selected as the RL-algorithm to update the agent - The RL-agent was capable to efficiently learn a control strategy, for both experiment and simulation, that will allow the reattachment of flow behind the cylinder and reduce the drag coefficient
ii) Disaster response informed by social media	Information classification from disaster-related messages in twitter Imran et al. (2013)	NB (2 classifiers)	-	NB1: tweets	NB1: classification of tweets as personal, direct informative, indirect informative direct-indirect informative and other following the tornado event in Joplin, Missouri (2011)	206,764 tweets collected during the Joplin tornado of 2011 in Joplin, Missouri	F1 score	Acceptable performance

(Continued on following page)

TABLE 7 | (*Continued*) Summary of ML applications for mitigation and response.

Application	ML model	Training scheme	Input data	Output data	Data source	Performance metric	Remarks
			NB2: informative tweets	NB2: classification of informative tweets as caution, donation, advice, or information source			
Classification of tweets to inform disaster response Ashktorab et al. (2014)	SLDA, LR, KNN, NB, DT	-	Tweets	Classification of tweets to identify those that reported human casualties or structural damage (requiring intervention)	17 million tweets collected during 12 different natural disasters in the U.S since 2006 (e.g., tornado and hurricane)	AUC	The LR was the best classifier
Information classification from disaster-related messages in twitter Imran et al. (2016)	RF, SVM, NB	-	Tweets	9 classes (e.g., injured or dead people, infrastructure and utilities damage, displaced people and evacuations, caution and advice)	52 million tweets for events related to 19 natural hazards and crisis (e.g., typhoon, floods and earthquake) occurring between 2013 and 2015 in different parts of the world was used	Area under ROC curve	- Good results were obtained for all classes (for the three classifiers) except for the "*missing trapped or found people*" - poor classification-
Information classification from disaster-related events O'Neal et al. (2018)	SVM, KNN, GNB, MNB, BNB, DT, SGD	-	Images	Image classes in terms of human roles: rescuees or rescuers	The images were collected from August 17th to 3 September 2017 based on private social media platforms (e.g., twitter) during Hurricane Harvey (2017)	Average precision	SVM-based model gave the best prediction accuracy
Real-time disaster communication Robertson et al. (2019)	VGG-16 CNN, ANN	Adam	Tweeter-based images	VGG-16 CNN: informative features (pre-storm, landfall and the period after landfall) ANN: urgency level (highly urgent, moderately urgent, somewhat urgent, not urgent, and unrelated to the hurricane event)	A total of 17,483 images were extracted from Twitter between 17th August and 17 September 2017 from Hurricane Harvey (2017)	Accuracy	Acceptable simulation results
Information classification from disaster-related events Manna and Nakai (2019)	ANN, SVM, NB, LR	-	Tweets	2 classes: crisis-related tweets and non-crisis-related tweets	6 crisis related datasets were used (e.g., hurricane Harvey 2017 and the 2011 Joplin Tornado) with approximately 10,000 tweets for each event	Accuracy	ANN classifier outperformed all other classifiers
Real-time information classification from hurricane-related events Yu et al., (2019)	CNN, SVM, LR	RMSprop	Tweets	5 classes: Information Sources, Caution and Advice, Infrastructure and Resources, Casualties and Damage, and Donation and Aid	3 manually labeled datasets were used corresponding to hurricane Sandy (2012), Irma (2017) and Harvey (2017), respectively with approximatively 2000–3000 tweets per each event	Accuracy	CNN outperformed other classifiers
Identification of social media-based requests for urgent help during hurricanes Devaraj et al., (2020)	DT, SVM, ANN, LR, NB, AdaBoost, RR	-	Tweets	Tweets from people requiring or not urgent rescue by first responders	2,072,715 tweets related to Hurricane Harvey (2017) event	F1-score	CNN, SVM and ANN achieve the best simulation results

abundant data from various powerful communication tools (e.g., Twitter) greatly facilitate the rapid ML model developments in this field. **Table 7i,ii** respectively present the reviewed applications of ML for mitigation and response, where the ML model, training scheme, input data, output data, data source and performance metric are summarized for each application. The training/testing data were essentially retrieved from CFD simulations and experimental tests for structural mitigation or

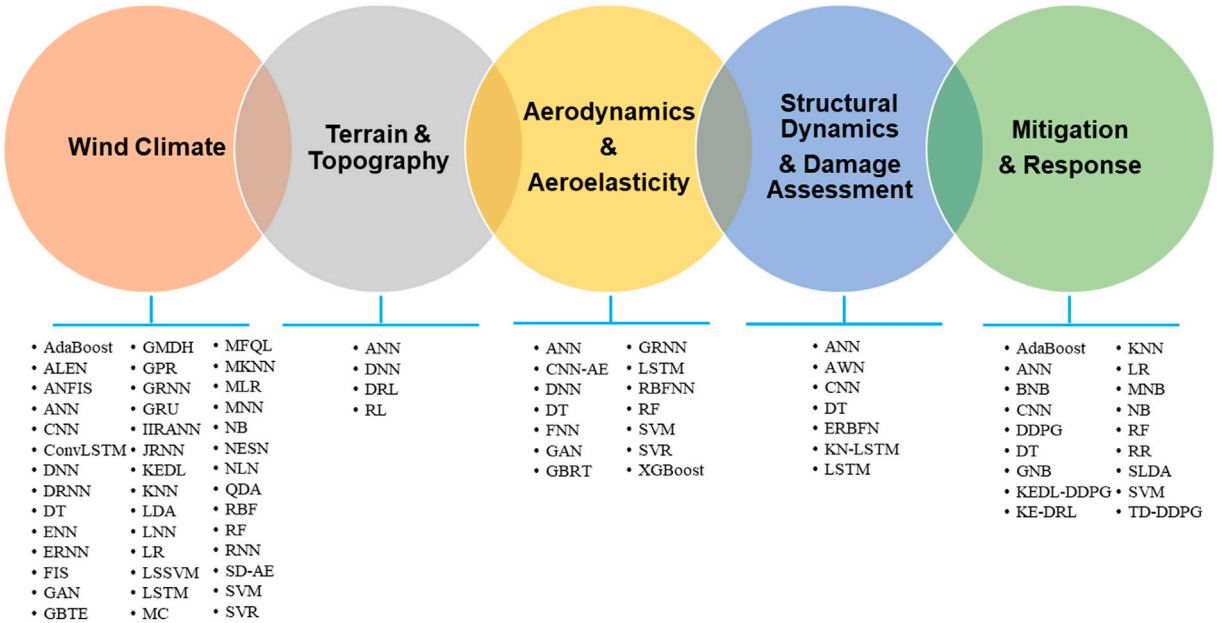

FIGURE 8 | Overview of reviewed ML applications in wind engineering (following Alan G. Davenport Wind Loading Chain).

from social media platforms for disaster response. From **Table 7i**, it can be concluded that the structural performance evaluations in mitigation applications usually used ML as a regression model while RL was typically utilized as an effective optimization or control algorithm. It is noted that relatively few ML applications for structural optimization and control under winds have been generated compared to those in earthquake engineering community (e.g., Ghaboussi and Joghataie 1995; Adam and Smith 2008; Jiang and Adeli 2008; Yakut and Alli 2011; Subasri et al., 2014; Khodabandehlou et al., 2018; Khalatbarisoltani et al., 2019; Hayashi and Ohsaki 2020). From **Table 7ii**, it can be concluded that most social media-informed response applications used ML as a classification model for disaster rescue and relief information dissemination. Although these ML applications present promising results in terms of effectively supporting timely decision-making, there is a concern of using information from social media platforms due to a lack of data quality control.

3.6 Summary

The ML applications in each topical area of wind engineering are summarized in **Figure 8**. As shown in the figure, ML models are unevenly distributed among these areas. The wind climate area has the most ML applications followed by the aerodynamics and aeroelasticity area, and they are respectively contributed by wind engineering-related fields of meteorology and fluid mechanics. On the other hand, the wind engineering-exclusive field of terrain and topography has the least applications of ML. Although ML models have been instrumental in modern structural design for winds, their developments are in a very preliminary stage and there is still a long way to go before they can complement or even replace existing approaches of wind tunnel tests and CFD simulations. In general, the supervised learning dominates the ML applications in wind engineering with the podium position attributed to simple models with standard algorithms (e.g., ANN with backpropagation). Actually, the selection of various ML models is rather rudimentary since there is a lack of systematic comparison among them (e.g., in terms of model complexity and performance). It is noted that the great potential of semi-supervised learning and unsupervised learning (as well as RL) with little or no labelled data is not leveraged yet. Accordingly, the current ML developments in wind engineering heavily rely on available labelled data. For example, the ML applications to non-synoptic winds are much less than those of synoptic winds due essentially to the difficulty in obtaining the data of local and short-lived storms. On the other hand, the recent emergence of numerous ML applications to social media-informed disaster response is due mainly to the unprecedentedly abundant data from various powerful communication tools. For the reviewed ML applications, the training/testing data are retrieved from several major sources (e.g., field measurements, wind tunnel tests, numerical simulations and social media platforms). In the determination of ML model inputs and outputs, a good understanding of underlying physics of each application is critical to effectively select an appropriate set of predictors (ML inputs) while the output types heavily depend on the needs of traditional analysis procedure in each application (e.g., local wind pressures for building design and global wind forces for bridge design).

4 CHALLENGES AND PROSPECTS

The rapidly increasing ML applications to wind engineering have generated a large volume of datasets associated with a large set of

domain-specific algorithms. It is strongly believed that the platforms encouraging open sharing of these datasets and algorithms would greatly benefit the ML research progress in wind engineering. The openly available wind engineering datasets will greatly reduce efforts for their creation/collection and pre-processing, and open-source ML algorithms will save significant time for their re-implementation. The reduced need of time and effort to use the state-of-the-art or latest developed ML tools under such a culture of openness would spur interests among researchers in wind engineering, and hence result in more related ML applications. Moreover, the developed cyberinfrastructure to store and share data usually has a systematic curation procedure to ensure the high quality of its standardized benchmark datasets. Also, the open-source software allows the hidden bugs/tricks of ML algorithms to be easily uncovered and accordingly makes them more robust. In addition to availability, the reproducibility and testability of wind engineering data and domain-specific algorithms due to a culture of openness would also facilitate the adoption of the obtained transparent and trustworthy ML tools in real-world problems. Although the wind engineering community has started to embrace the prevalent openness of ML community (e.g., NHERI DesignSafe platform), the culture of openness is still in its early stage. It is expected that more incentives based on the existing reward system (e.g., a digital object identifier for each dataset or algorithm published by the platform) are needed to motivate the ML wind engineering community towards open science. Given a potential open-science environment with openly available datasets and open-source algorithms (supported by open-access scientific publications), some remaining challenges and future prospects are discussed in terms of data in wind engineering and algorithms in ML. It is noted that both challenge and prospect lists are not exhaustive.

4.1 Challenges and Research Gaps

The reviewed various ML models for a wide range of topics in wind engineering suggests that their cross field has recently attracted much interest. However, there are still numerous challenges to advance ML applications to wind engineering from conception and research into practice. These remaining challenges of data in wind engineering and algorithms in ML are discussed in this sub-section.

4.1.1 Wind Engineering Data Challenges

Wind engineering data could be rich in some dimensions but may be poor in others. For example, a large volume of flow data or pressure data could be obtained by one wind tunnel test (using advanced measurement systems with high resolution in space and high sampling rate in time), however, all these data would be located at a point in the Reynolds number dimension. For structural response under winds, most of the data are located in the linear elastic domain, while very limited nonlinear inelastic data needed to advance implementation of performance-based wind design are available. Another example is that the anemometric monitoring network typically generates abundant data in time dimension but sparse data in space. More importantly, it is usually very challenging or expensive to create extra points in currently data-scarce dimensions. Wind engineering data could be short in time span of their collection. For example, the climate changing impacts are not easy to be considered based on the currently available wind data since their record period is much shorter than the time scale of climate changing. Also, few structural performance data under winds are long enough to take the life-span deterioration behaviors into account. Essentially, the learning machine based on current wind-structure interaction data cannot be used for accurately predicting future long-term behaviors of the same wind-structure system. Wind engineering data could be highly heterogeneous for collaborative or large-scale ML applications. Many complex tasks (e.g., life-cycle performance evaluation of structures under winds) and/or real-world problems (e.g., hurricane resilience assessment of coastal communities) in wind engineering need collaborative efforts and/or large-scale implementations. The datasets generated from these activities may result from various CFD simulation tools or field measurement devices, and they are typically interpreted by different entities before sent to a central processing platform. Accordingly, significant processing efforts (e.g., data cleaning, data aggregation, dimension reduction and data standardization) are needed for these heterogeneous datasets with high variability of data types and formats (e.g., mixtures of structured, semi-structured and unstructured data). In addition, advanced powerful learning machines are necessary to generate new knowledge from large, heterogeneous sets of wind engineering data.

4.1.2 Machine Learning Algorithm Challenges

ML algorithms commonly-used in wind engineering are standard ones designed for solving problems in other fields (e.g., handwriting recognition or computer vision). While these classical algorithms (e.g., ANN with backpropagation) achieved great success for simple wind engineering applications, they are not necessarily concise and efficient. More importantly, the immediate applications of these popular algorithms to modern wind engineering (involving nonstationary and non-Gaussian wind flow, transient and nonlinear aerodynamics, nonlinear and inelastic structural dynamics, or time-variant wind-structure system under a changing climate) may be very challenging. On the other hand, the newly developed ML algorithms (e.g., advanced LSTM and GAN) need to be carefully scrutinized for their applicability to these complex problems. ML algorithms commonly-used in wind engineering are supervised ones that need a significant amount of labelled data. Although the cost of obtaining/collecting the data from various sources (e.g., numerical simulations, wind tunnel tests, or field measurements) is greatly reduced and accordingly unprecedented volume of data are increasingly available, these datasets may be limited to unlabeled due to a lack of sufficient human resources (with expert knowledge) for data labeling. ML algorithms commonly-used in wind engineering are purely data-driven ones that are usually consider as black boxes. Furthermore, currently available ML models usually present a conflict between their advances (and hence performance) and explainability. One important feature of human intelligence is the ability to explain the rationale behind its decisions to others, hence, the explainability of

learning machines is often an essential prerequisite for establishing a trust relationship between human intelligence and artificial intelligence. The highly non-transparent nature of ML algorithms may be acceptable for some applications in wind engineering (e.g., a CNN mapping the oncoming winds to pressure fields on or velocity fields around various bridge decks), however, it may be a clear drawback for many high-stake applications (e.g., evacuation planning or transportation infrastructure management under a landfalling hurricane) since any error in prediction may have catastrophic consequences. It is noted that the high-stake applications also place a high demand for quantification of uncertainties involved in ML algorithm selection, training and performance evaluation (along with data collection), whereas the formalization of uncertainty quantification for purely data-driven approaches is very challenging and not well established yet. ML algorithms commonly-used in wind engineering are typically selected based on past experience (or simply by "gut feeling") and the associated model hyperparameters (e.g., layer and neuron numbers, activation function and learning rate) are usually obtained by extensive trial and error. While the selected ML algorithms present good performance for the particular applications of interest, they are not necessarily an optimal choice. A systematic approach to identify the most appropriate ML model and associated best hyperparameters essentially needs a global optimization within a high dimensional space, and is currently very challenging for wind engineering applications.

4.2 Prospects and Future Directions

The remaining challenges, while not trivial, provide new research opportunities for the development of more effective ML tools. The identified prospects of data in wind engineering and algorithms in ML are discussed in this sub-section.

4.2.1 Wind Engineering Data Prospects

To generate/collect wind engineering data that are scarce in certain dimensions, advanced full-scale/laboratory/numerical tools and technologies need to be utilized or developed. In addition to large-scale facilities (e.g., WindEEE), various high-fidelity and efficient modern CFD techniques (e.g., hybrid large eddy simulation/Reynolds-averaged Navier-Stokes schemes) should be exploited to generate data of high-Reynolds number scenarios. The rational loading protocols for extreme wind performance cyclic testing of deformation-controlled MWFRS (Main Wind Force Resisting System) members need to be designed to generate the wind-induced nonlinear inelastic structural response data. Also, data reconstructions using linear/nonlinear dimensionality reduction techniques (e.g., singular value decomposition/autoencoder) should be employed to enhance spatial resolution of full-scale measurements. To generate/collect wind engineering data that cover sufficiently-long time span of structural behaviors, more reliable long-term structural health monitoring systems should be established in addition to high-fidelity modeling of aging and deterioration of wind-sensitive structures. For the consideration of wind engineering data under a changing climate, synthesized wind fields (resulting from tropical cyclones, extratropical cyclones or local non-synoptic storms) need to be generated by global climate models coupled with accurate and efficient downscaling exercises under projected climate conditions [e.g., various RCP (Representative Concentration Pathway) scenarios]. To effectively learn from heterogeneous data that need to be first unified, they can be efficiently processed by advanced big data analytics. For example, unsupervised or semi-supervised clustering techniques could be used for data cleaning, data fusion techniques of Kalman filters could be used for data aggregation, and linear principal component analysis or nonlinear self-organizing map could be used for dimensional reduction.

4.2.2 ML Algorithm Prospects

To facilitate ML applications to complex wind engineering problems, the state-of-the-art or latest algorithms emerging in ML community could be leveraged. For example, the GAN could be used for effectively generating nonstationary and non-Gaussian wind flow through its two competing sub-networks, the CNN could be employed for efficiently mapping oncoming winds to pressure fields (characterizing transient and nonlinear aerodynamics) on structures with an arbitrary shape because it is particularly good at handling input-output data with a known grid-like topology, the LSTM could be utilized for accurately simulating nonlinear and inelastic structural dynamics since its forget gates ensure a reliable consideration of long-term dependencies (where the structural response at the current time depends on not only the current wind load but also the load history), and the lifelong learning networks should be explored for adaptively modeling time-variant wind-structure system assuming their underlying parameters can be continuously modified to accommodate new data inputs. The direct or immediate applications of the advanced ML algorithms to complex wind engineering problems may not necessarily result in parsimonious models that may need specialized customization for each application. To reduce the demand for labelled data in ML applications to wind engineering, both unsupervised learning and semi-supervised learning (including physics-informed machine learning) are promising alternatives to popularly used supervised learning. In addition, advanced ML algorithms have been emerging (e.g., reservoir computing) for processing information generated by complicated dynamical systems using very small training datasets. To open the ML black box, model explainability and interpretability in wind engineering applications needs to be enhanced. Various general techniques have been developed to improve understanding of the ML model predictions, such as sensitivity analysis and layer-wise relevance propagation. On the other hand, the definitions of explainability and interpretability are typically domain dependent, hence, the domain knowledge in wind engineering should be leveraged for enhanced explainability/interpretability of each ML application. It is expected that the explainability/interpretability analysis (along with uncertain quantification) will likely become a fundamental building block for bounding the overall confidence in ML applications in wind engineering (parallel to verification and validation in CFD simulations). To enable an

automatic search of ML model hyperparameters in wind engineering applications, increasingly available optimization schemes with improved efficiency and accuracy (e.g., grid search, random search, Bayesian optimization and population-based training) can be utilized to find the best configuration for each task. On the other hand, it is believed that a practical guide to selection of ML models in wind engineering applications will greatly facilitate their appropriate use. The best practices for model selection in each application are essentially consistent with the principle of Ockham's razo by first testing simple linear ML models (due to their easy to implement and high model explainability), and then followed by more complex nonlinear models (without data overfitting). Among ML models with similar complexity, a predetermined performance metric is typically used for further model selection. Since iteration is generally needed in a purely performance-driven ML model selection, the domain knowledge is suggested to be utilized for a more effective search process.

4.3 Knowledge-Enhanced Machine Learning

As discussed in preceding sections, domain knowledge could be leveraged for improved selection of ML model and its inputs and outputs in wind engineering applications. Hence, a good understanding of fundamental physics and other types of domain knowledge underlying each subfield of wind engineering would enable more effective use of ML tools. It is noted that the fundamental physics in terms of governing equations is a special type of domain knowledge, and recent studies have demonstrated that the required labelled datasets could be significantly reduced by incorporating the underlying physics into training process (and hence enhancing the regularization mechanism) (e.g., Raissi et al., 2017a; 2017b). Other equation-based domain knowledge such as empirical/semi-empirical formulas were also employed as part of the loss function in deep learning to provide machine-readable prior knowledge that facilitates the effective regularization of the neural networks for simulations of tropical cyclone winds (Snaiki and Wu 2019) and nonlinear structural dynamics (Wang and Wu 2020). In addition, the equation-free domain knowledge has been integrated into a deep RL-based aerodynamic shape optimizer (via the transfer-learning and meta-learning techniques) to remarkably enhance the training efficiency for wind engineering applications (Li et al., 2021a). These emerging successful applications indicate that this novel scheme of knowledge-enhanced machine learning (KEML) could significantly enhance ML applications to wind engineering. To fully embrace the promising potential of KEML, systematic research efforts are needed to efficiently identify knowledge representations (invariances, physics equations, empirical formulas, probabilistic relations, logic rules, simulation results, field observations, human feedback, and others) in various subfields of wind engineering and then to effectively integrate them into each module of machine learning pipeline (data preparation, model selection, model training, and others). While domain knowledge could be employed to enhance purely data-driven ML tools, it is expected that learning machines could be utilized for harnessing data to discover new knowledge in wind engineering (e.g., governing laws characterizing transport of turbulence quantities or optimization of wind-structure system).

5 CONCLUDING REMARKS

A total of 65 machine learning (ML) algorithms were reviewed in terms of their applications to each topical area of wind engineering, namely wind climate, terrain/topography, aerodynamics/aeroelasticity, structural dynamics, wind damage assessment and wind-related hazard mitigation and response. The most ML applications were found in wind climate area, while the terrain/topography area had the least applications of ML. Although the ML-based wind engineering is fueled by the unprecedented volume of analytical, numerical, experimental and field-measurement data together with rapidly evolving learning algorithms and high-performance computational hardware, it is still at an early stage of development. Most of wind engineering applications employed supervised learning with standard ML models designed for solving problems in other fields, and the promising unsupervised and semi-supervised learning tools were rarely used to reduce the high demand of labelled data. For the selection of ML models and associated hyperparameters in wind engineering applications, it was typically based on expertise and extensive trial and error. In this review, the culture of openness, explainability/interpretability and uncertainty quantification were identified as important research gaps that need to be addressed in ML-based wind engineering community. Furthermore, the knowledge-enhanced machine learning was considered as a very promising scheme to enhance ML applications to wind engineering.

AUTHOR CONTRIBUTIONS

All authors contributed to the study conception and design, data collection, analysis and interpretation of results, drafted manuscript preparation, reviewed the results, and approved the final version of the manuscript.

REFERENCES

Abbas, T., Kavrakov, I., Morgenthal, G., and Lahmer, T. (2020). Prediction of Aeroelastic Response of Bridge Decks Using Artificial Neural Networks. *Comput. Structures* 231, 106198. doi:10.1016/j.compstruc.2020.106198

Abdi, D., Levine, S., and Bitsuamlak, G. "Application of an Artificial Neural Network Model for Boundary Layer Wind Tunnel Profile Development," in Proceedingsof the 11th Americas Conference on Wind Engineering, San Juan, Puerto Rico, June 2009.

Abdullah, S. A., Aswegan, K., Jaberansari, S., Klemencic, R., and Wallace, J. W. (2020). Performance of Reinforced Concrete Coupling Beams Subjected to

Simulated Wind Loading. *ACI Struct. J.* 117 (3), 283–295. doi:10.14359/51724555

Aboshosha, H., Bitsuamlak, G., and El Damatty, A. (2015). Turbulence Characterization of Downbursts Using LES. *J. Wind Eng. Ind. Aerodynamics* 136, 44–61. doi:10.1016/j.jweia.2014.10.020

Aboutabikh, M., Ghazal, T., Chen, J., Elgamal, S., and Aboshosha, H. (2019). Designing a Blade-System to Generate Downburst Outflows at Boundary Layer Wind Tunnel. *J. Wind Eng. Ind. Aerodynamics* 186, 169–191. doi:10.1016/j.jweia.2019.01.005

Adam, B., and Smith, I. F. (2008). Reinforcement Learning for Structural Control. *J. Comput. Civ. Eng.* 22 (2), 133–139. doi:10.1061/(asce)0887-3801(2008)22:2(133)

Adeli, H., and Yeh, C. (1989). Perceptron Learning in Engineering Design. *Computer-Aided Civil Infrastructure Eng.* 4 (4), 247–256.

Adrianto, I., Trafalis, T. B., and Lakshmanan, V. (2009). Support Vector Machines for Spatiotemporal Tornado Prediction. *Int. J. Gen. Syst.* 38, 759–776. doi:10.1080/03081070601068629

Alemany, S., Beltran, J., Perez, A., and Ganzfried, S. (2019). Predicting Hurricane Trajectories Using a Recurrent Neural Network. *Aaai* 33 (01), 468–475. doi:10.1609/aaai.v33i01.3301468

Ali, M. M., Kishtawal, C. M., and Jain, S. (2007). Predicting Cyclone Tracks in the north Indian Ocean: An Artificial Neural Network Approach. *Geophys. Res. Lett.* 34 (4), L04603. doi:10.1029/2006gl028353

American Society of Civil Engineers (2017). *Minimum Design Loads and Associated Criteria for Buildings and Other Structures*. Reston, VA: Structural Engineering Institute of American Society of Civil Engineers.

American Society of Civil Engineers (2021). *Minimum Design Loads for Buildings and Other Structures*. Reston, VA: Structural Engineering Institute of American Society of Civil Engineers.

Asano, K., Iida, Y., and Uematsu, Y. (2019). Laboratory Study of Wind Loads on a Low-Rise Building in a Downburst Using a Moving Pulsed Jet Simulator and Their Comparison with Other Types of Simulators. *J. Wind Eng. Ind. Aerodynamics* 184, 313–320. doi:10.1016/j.jweia.2018.11.034

Ashktorab, Z., Brown, C., Nandi, M., and Culotta, A. "Tweedr: Mining Twitter to Inform Disaster Response," in Proceedings of the 11th International ISCRAM Conference, Pennsylvania, USA, May 2014, 269–272.

Ashton, R., Refan, M., Iungo, G. V., and Hangan, H. (2019). Wandering Corrections from PIV Measurements of Tornado-like Vortices. *J. Wind Eng. Ind. Aerodynamics* 189, 163–172. doi:10.1016/j.jweia.2019.02.010

Baik, J.-J., and Paek, J.-S. (2000). A Neural Network Model for Predicting Typhoon Intensity. *J. Meteorol. Soc. Jpn.* 78 (6), 857–869. doi:10.2151/jmsj1965.78.6_857

Bailey, P. A., and Kwok, K. C. S. (1985). Interference Excitation of Twin Tall Buildings. *J. Wind Eng. Ind. Aerodynamics* 21 (3), 323–338. doi:10.1016/0167-6105(85)90043-1

Baker, C. J., and Sterling, M. (2017). Modelling Wind fields and Debris Flight in Tornadoes. *J. Wind Eng. Ind. Aerodynamics* 168, 312–321. doi:10.1016/j.jweia.2017.06.017

Bani-Hani, K. A. (2007). Vibration Control of Wind-induced Response of Tall Buildings with an Active Tuned Mass Damper Using Neural Networks. *Struct. Control. Health Monit.* 14 (1), 83–108. doi:10.1002/stc.85

Barbounis, T. G., Theocharis, J. B., Alexiadis, M. C., and Dokopoulos, P. S. (2006). Long-term Wind Speed and Power Forecasting Using Local Recurrent Neural Network Models. *IEEE Trans. Energ. Convers.* 21 (1), 273–284. doi:10.1109/tec.2005.847954

Bengio, Y., Simard, P., and Frasconi, P. (1994). Learning Long-Term Dependencies with Gradient Descent Is Difficult. *IEEE Trans. Neural Netw.* 5 (2), 157–166. doi:10.1109/72.279181

Berg, J., Mann, J., and Patton, E. G. (2013). Lidar-observed Stress Vectors and Veer in the Atmospheric Boundary Layer. *J. Atmos. oceanic Technol.* 30 (9), 1961–1969. doi:10.1175/jtech-d-12-00266.1

Berggren, K., Xia, Q., Likharev, K. K., Strukov, D. B., Jiang, H., Mikolajick, T., et al. (2020). Roadmap on Emerging Hardware and Technology for Machine Learning. *Nanotechnology* 32 (1), 012002. doi:10.1088/1361-6528/aba70f

Bitsuamlak, G., Stathopoulos, T., and Bedard, C. (2006). Effects of Upstream Two-Dimensional hills on Design Wind Loads: a Computational Approach. *Wind and Structures* 9 (1), 37–58. doi:10.12989/was.2006.9.1.037

Bitsuamlak, G. T., Bédard, C., and Stathopoulos, T. (2007). Modeling the Effect of Topography on Wind Flow Using a Combined Numerical-Neural Network Approach. *J. Comput. Civ. Eng.* 21 (6), 384–392. doi:10.1061/(asce)0887-3801(2007)21:6(384)

Bitsuamlak, G. T. (2004). "Evaluating the Effect of Topographic Elements on Wind Flow: a Combined Numerical Simulation-Neutral Network Approach," (Montreal, Quebec, Canada: Concordia University). Doctoral dissertation.

Bitsuamlak, G. T., Stathopoulos, T., and Bédard, C. "Neural Network Predictions of Wind Flow over Complex Terrain," in 4th Structural Specialty Conf. of the Canadian Society for Civil Engineering, Whistler, BC Canada, May 2002.

Blessmann, J., and Riera, J. D. (1985). Wind Excitation of Neighbouring Tall Buildings. *J. wind Eng. Ind. aerodynamics* 18 (1), 91–103. doi:10.1016/0167-6105(85)90076-5

Blocken, B. (2014). 50 Years of Computational Wind Engineering: Past, Present and Future. *J. Wind Eng. Ind. Aerodynamics* 129, 69–102. doi:10.1016/j.jweia.2014.03.008

Bluestein, H. B. (2021). "The Types of Non-synoptic Wind Systems," in *The Oxford Handbook of Non-synoptic Wind Storms*. Editors H. Hangan and A. Kareem (Oxford, United Kingdom: Oxford University Press). doi:10.1093/oxfordhb/9780190670252.013.1

Bre, F., Gimenez, J. M., and Fachinotti, V. D. (2018). Prediction of Wind Pressure Coefficients on Building Surfaces Using Artificial Neural Networks. *Energy and Buildings* 158, 1429–1441. doi:10.1016/j.enbuild.2017.11.045

Breiman, L. (2001). Random Forests. *Mach Learn.* 45, 5–32. doi:10.1023/a:1010933404324

Brunton, S. L., Noack, B. R., and Koumoutsakos, P. (2020). Machine Learning for Fluid Mechanics. *Annu. Rev. Fluid Mech.* 52, 477–508. doi:10.1146/annurev-fluid-010719-060214

Cermak, J. E. (1975). Applications of Fluid Mechanics to Wind Engineering—A Freeman Scholar Lecture. *J. Fluids Eng.* 97 (1), 9–38. doi:10.1115/1.3447225

Chakrabarty, H., Murthy, C. A., and Gupta, A. D. (2013). Application of Pattern Recognition Techniques to Predict Severe Thunderstorms. *Ijcte* 5 (6), 850–855. doi:10.7763/ijcte.2013.v5.810

Chaudhuri, S., Dutta, D., Goswami, S., and Middey, A. (2013). Intensity Forecast of Tropical Cyclones over North Indian Ocean Using Multilayer Perceptron Model: Skill and Performance Verification. *Nat. Hazards* 65 (1), 97–113. doi:10.1007/s11069-012-0346-7

Chaudhuri, S., and Middey, A. (2011). Adaptive Neuro-Fuzzy Inference System to Forecast Peak Gust Speed during Thunderstorms. *Meteorology Atmos. Phys.* 114 (3-4), 139. doi:10.1007/s00703-011-0158-4

Chen, C. H., Wu, J. C., and Chen, J. H. (2008). Prediction of Flutter Derivatives by Artificial Neural Networks. *J. wind Eng. Ind. aerodynamics* 96 (10-11), 1925–1937. doi:10.1016/j.jweia.2008.02.044

Chen, G., and Lombardo, F. T. (2020). An Automated Classification Method of Thunderstorm and Non-thunderstorm Wind Data Based on a Convolutional Neural Network. *J. Wind Eng. Ind. Aerodynamics* 207, 104407. doi:10.1016/j.jweia.2020.104407

Chen, R., Wang, X., Zhang, W., Zhu, X., Li, A., and Yang, C. (2019). A Hybrid CNN-LSTM Model for Typhoon Formation Forecasting. *Geoinformatica* 23 (3), 375–396. doi:10.1007/s10707-019-00355-0

Chen, R., Zhang, W., and Wang, X. (2020). Machine Learning in Tropical Cyclone Forecast Modeling: A Review. *Atmosphere* 11 (7), 676. doi:10.3390/atmos11070676

Chen, Y., and Duan, Z. (2018). A Statistical Dynamics Track Model of Tropical Cyclones for Assessing Typhoon Wind hazard in the Coast of Southeast China. *J. Wind Eng. Ind. Aerodynamics* 172, 325–340. doi:10.1016/j.jweia.2017.11.014

Chen, Y., Kopp, G. A., and Surry, D. (2002). Interpolation of Wind-Induced Pressure Time Series with an Artificial Neural Network. *J. Wind Eng. Ind. Aerodynamics* 90 (6), 589–615. doi:10.1016/s0167-6105(02)00155-1

Chen, Y., Kopp, G. A., and Surry, D. (2003). Prediction of Pressure Coefficients on Roofs of Low Buildings Using Artificial Neural Networks. *J. wind Eng. Ind. aerodynamics* 91 (3), 423–441. doi:10.1016/s0167-6105(02)00381-1

Chen, Z., Yu, X., Chen, G., and Zhou, J. "Cyclone Intensity Estimation Using Multispectral Imagery from the FY-4 Satellite," in Proceedings of the 2018 International Conference on Audio, Language and Image Processing (ICALIP), Shanghai, China, July 2018 (Piscataway, New Jersey, United States: IEEE), 46–51.

Cheng, X. X., Zhao, L., and Ge, Y.-J. (2016). Field Measurements on Flow Past a Circular cylinder in Transcritical Reynolds Number Regime. *Acta Phys. Sin.* 65 (21), 214701. doi:10.7498/aps.65.214701

Cherkassky, V., and Mulier, F. M. (2007). *Learning from Data: Concepts, Theory, and Methods*. Hoboken, New Jersey, United States: John Wiley & Sons.

Chitsazan, M. A., Sami Fadali, M., and Trzynadlowski, A. M. (2019). Wind Speed and Wind Direction Forecasting Using echo State Network with Nonlinear Functions. *Renew. Energ.* 131, 879–889. doi:10.1016/j.renene.2018.07.060

Chowdhury, J., and Wu, T. (2021). "Aerodynamic Loading Due to Non-synoptic Wind Systems," in *The Oxford Handbook of Non-synoptic Wind Storms*. Editors H. Hangan and A. Kareem (Oxford, United Kingdom: Oxford University Press), 337.

Chung, J., Lee, S. W., Chang, S., and Kim, Y. S. "Estimation of Flutter Derivatives of Various Sections Using Numerical Simulation and Neural Network," in The 2012 World Congress on Advances in Civil, Environmental, and Materials Research (ACEM' 12), Seoul, Korea, August 26-30, 2012.

Coffer, B., Kubacki, M., Wen, Y., Zhang, T., Barajas, C. A., and Gobbert, M. K. (2020). "Using Machine Learning Techniques for Supercell Tornado Prediction with Environmental Sounding Data," in *Tech. Rep. HPCF–2020–18, UMBC High Performance Computing Facility* (Baltimore County: University of Maryland).

Collins, W. G., and Tissot, P. (2016). *Thunderstorm Predictions Using Artificial Neural networksArtificial Neural Networks-Models and Applications*. London: IntechOpen.

Collins, W., and Tissot, P. (2015). An Artificial Neural Network Model to Predict Thunderstorms within 400 Km2 South Texas Domains. *Met. Apps* 22 (3), 650–665. doi:10.1002/met.1499

Cortes, C., and Vapnik, V. (1995). Support-vector Networks. *Mach Learn.* 20 (3), 273–297. doi:10.1007/bf00994018

Cui, W., and Caracoglia, L. (2019). A New Stochastic Formulation for Synthetic hurricane Simulation over the north Atlantic Ocean. *Eng. Structures* 199, 109597. doi:10.1016/j.engstruct.2019.109597

Davenport, A. G. (1960). Rationale for Determining Design Wind Velocities. *J. Struct. Div.* 86 (5), 39–68. doi:10.1061/jsdeag.0000521

Deierlein, G. G., and Zsarnóczay, A. (2021). *State of the Art in Computational Simulation for Natural Hazards Engineering*. Second Edition. Plano, Texas: Center Comput. Modeling Simulation. SimCenter.

DeMaria, M., Mainelli, M., Shay, L. K., Knaff, J. A., and Kaplan, J. (2005). Further Improvements to the Statistical hurricane Intensity Prediction Scheme (SHIPS). *Weather Forecast.* 20 (4), 531–543. doi:10.1175/waf862.1

Deng, L., and Yu, D. (2014). Deep Learning: Methods and Applications. *Foundations Trends. Signal. Processing* 7 (3–4), 197–387. doi:10.1561/2000000039

Derkevorkian, A., Hernandez-Garcia, M., Yun, H.-B., Masri, S. F., and Li, P. (2015). Nonlinear Data-Driven Computational Models for Response Prediction and Change Detection. *Struct. Control. Health Monit.* 22 (2), 273–288. doi:10.1002/stc.1673

Devaraj, A., Murthy, D., and Dontula, A. (2020). Machine-learning Methods for Identifying Social media-based Requests for Urgent Help during Hurricanes. *Int. J. Disaster Risk Reduction* 51, 101757. doi:10.1016/j.ijdrr.2020.101757

Diaz, J., and Joseph, M. B. (2019). Predicting Property Damage from Tornadoes with Zero-Inflated Neural Networks. *Weather Clim. Extremes* 25, 100216. doi:10.1016/j.wace.2019.100216

Dissanayake, M. W. M. G., and Phan-Thien, N. (1994). Neural-network-based Approximations for Solving Partial Differential Equations. *Commun. Numer. Meth. Engng.* 10 (3), 195–201. doi:10.1002/cnm.1640100303

Duraisamy, K., Iaccarino, G., and Xiao, H. (2019). Turbulence Modeling in the Age of Data. *Annu. Rev. Fluid Mech.* 51, 357–377. doi:10.1146/annurev-fluid-010518-040547

Eguchi, Y., Hattori, Y., Nakao, K., James, D., and Zuo, D. (2018). Numerical Pressure Retrieval from Velocity Measurement of a Turbulent Tornado-like Vortex. *J. Wind Eng. Ind. Aerodynamics* 174, 61–68. doi:10.1016/j.jweia.2017.12.021

Elshaer, A., Bitsuamlak, G., and El Damatty, A. (2017). Enhancing Wind Performance of Tall Buildings Using Corner Aerodynamic Optimization. *Eng. Structures* 136, 133–148. doi:10.1016/j.engstruct.2017.01.019

Elshaer, A., Bitsuamlak, G., and El Damatty, A. "June. Aerodynamic Shape Optimization of Tall Buildings Using Twisting and Corner Modifications," in Proceedings of the 8th International Colloquium on Bluff Body Aerodynamics and Applications, June 2016Northeastern University. Boston, Massachusetts.

Emanuel, K., Ravela, S., Vivant, E., and Risi, C. (2006). A Statistical Deterministic Approach to hurricane Risk Assessment. *Bull. Amer. Meteorol. Soc.* 87 (3), 299–314. doi:10.1175/bams-87-3-299

Emanuel, K. (2003). Tropical Cyclones. *Annu. Rev. Earth Planet. Sci.* 31 (1), 75–104. doi:10.1146/annurev.earth.31.100901.141259

English, E. C., and Fricke, F. R. (1999). The Interference index and its Prediction Using a Neural Network Analysis of Wind-Tunnel Data. *J. Wind Eng. Ind. Aerodynamics* 83 (1-3), 567–575. doi:10.1016/s0167-6105(99)00102-6

Everingham, M., Van Gool, L., Williams, C. K. I., Winn, J., and Zisserman, A. (2010). The Pascal Visual Object Classes (Voc) challenge. *Int. J. Comput. Vis.* 88 (2), 303–338. doi:10.1007/s11263-009-0275-4

Facchini, L., Betti, M., and Biagini, P. (2014). Neural Network Based Modal Identification of Structural Systems through Output-Only Measurement. *Comput. Structures* 138, 183–194. doi:10.1016/j.compstruc.2014.01.013

Fahlman, S. E. (1988). "Faster-learning Variations of Back-Propagation: An Empirical Study," in *Proc. 1988 Connectionist Models Summer School*. Editors D. Touretzky, G. Hinton, and T. Sejnowski (San Mateo, CA: Morgan Kaufmann), 38–51.

Fang, G., Zhao, L., Cao, S., Ge, Y., and Pang, W. (2018). A Novel Analytical Model for Wind Field Simulation Under Typhoon Boundary Layer Considering Multi-Field Correlation and Height-Dependency. *J. Wind. Eng. Ind. Aerodyn.* 175, 77–89.

Fan, D., Yang, L., Wang, Z., Triantafyllou, M. S., and Karniadakis, G. E. (2020). Reinforcement Learning for bluff Body Active Flow Control in Experiments and Simulations. *Proc. Natl. Acad. Sci. USA* 117 (42), 26091–26098. doi:10.1073/pnas.2004939117

Fernández-Cabán, P. L., Masters, F. J., and Phillips, B. M. (2018). Predicting Roof Pressures on a Low-Rise Structure from Freestream Turbulence Using Artificial Neural Networks. *Front. Built Environ.* 4, 68. doi:10.3389/fbuil.2018.00068

Forthofer, J. M., Butler, B. W., McHugh, C. W., Finney, M. A., Bradshaw, L. S., Stratton, R. D., et al. (2014b). A Comparison of Three Approaches for Simulating fine-scale Surface Winds in Support of Wildland Fire Management. Part II. An Exploratory Study of the Effect of Simulated Winds on Fire Growth Simulations. *Int. J. Wildland Fire* 23 (7), 982–994. doi:10.1071/wf12090

Forthofer, J. M., Butler, B. W., and Wagenbrenner, N. S. (2014a). A Comparison of Three Approaches for Simulating fine-scale Surface Winds in Support of Wildland Fire Management. Part I. Model Formulation and Comparison against Measurements. *Int. J. Wildland Fire* 23 (7), 969–981. doi:10.1071/wf12089

Fu, J. Y., Li, Q. S., and Xie, Z. N. (2006). Prediction of Wind Loads on a Large Flat Roof Using Fuzzy Neural Networks. *Eng. Structures* 28 (1), 153–161. doi:10.1016/j.engstruct.2005.08.006

Fu, J. Y., Liang, S. G., and Li, Q. S. (2007). Prediction of Wind-Induced Pressures on a Large Gymnasium Roof Using Artificial Neural Networks. *Comput. structures* 85 (3-4), 179–192. doi:10.1016/j.compstruc.2006.08.070

Fukami, K., Nabae, Y., Kawai, K., and Fukagata, K. (2019). Synthetic Turbulent Inflow Generator Using Machine Learning. *Phys. Rev. Fluids* 4 (6), 064603. doi:10.1103/physrevfluids.4.064603

Gairola, A., and Bitsuamlak, G. (2019). Numerical Tornado Modeling for Common Interpretation of Experimental Simulators. *J. Wind Eng. Ind. Aerodynamics* 186, 32–48. doi:10.1016/j.jweia.2018.12.013

Gao, D.-L., Chen, W.-L., Li, H., and Hu, H. (2017). Flow Around a Circular cylinder with Slit. *Exp. Therm. Fluid Sci.* 82, 287–301. doi:10.1016/j.expthermflusci.2016.11.025

Ghaboussi, J., and Joghataie, A. (1995). Active Control of Structures Using Neural Networks. *J. Eng. Mech.* 121 (4), 555–567. doi:10.1061/(asce)0733-9399(1995)121:4(555)

Gholizadeh, S., Salajegheh, J., and Salajegheh, E. (2009). An Intelligent Neural System for Predicting Structural Response Subject to Earthquakes. *Adv. Eng. Softw.* 40 (8), 630–639. doi:10.1016/j.advengsoft.2008.11.008

Giffard-Roisin, S., Yang, M., Charpiat, G., Kumler Bonfanti, C., Kégl, B., and Monteleoni, C. (2020). Tropical Cyclone Track Forecasting Using Fused Deep Learning from Aligned Reanalysis Data. *Front. Big Data* 3, 1–13. doi:10.3389/fdata.2020.00001

Gillmeier, S., Sterling, M., and Hemida, H. (2019). Simulating Tornado-like Flows: the Effect of the Simulator's Geometry. *Meccanica* 54 (15), 2385–2398. doi:10.1007/s11012-019-01082-4

Goodfellow, I., Bengio, Y., and Courville, A. (2016). *Deep Learning*, 1. Cambridge: MIT press, 2.

Goodfellow, I., Pouget-Abadie, J., Mirza, M., Xu, B., Warde-Farley, D., Ozair, S., et al. (2014). "Generative Adversarial Nets," in *Advances in Neural Information Processing Systems*. Editors M. I. Jordan, Y. LeCun, and S. A. Solla (Cambridge, Massachusetts, United States: MIT Press), 2672–2680.

Gray, W. M. (1968). Global View of the Origin of Tropical Disturbances and Storms. *Mon. Wea. Rev.* 96 (10), 669–700. doi:10.1175/1520-0493(1968)096<0669:gvotoo>2.0.co;2

Gray, W. M. (1979). "Hurricanes: Their Formation, Structure and Likely Role in the Tropical Circulation. Meteorology over the Tropical Oceans," in *Meteorology over the Tropical Oceans*. Editor D. B. Shaw (James Glaisher House, Grenville, Bracknell: Royal Meteorological Society), 155–218.

Haines, M., and Taylor, I. (2018). Numerical Investigation of the Flow Field Around Low Rise Buildings Due to a Downburst Event Using Large Eddy Simulation. *J. Wind Eng. Ind. Aerodynamics* 172, 12–30. doi:10.1016/j.jweia.2017.10.028

Hall, T. M., and Jewson, S. (2007). Statistical Modelling of North Atlantic Tropical Cyclone Tracks. *Tellus A: Dynamic Meteorology and Oceanography* 59 (4), 486–498. doi:10.1111/j.1600-0870.2007.00240.x

Hangan, H., Refan, M., Jubayer, C., Romanic, D., Parvu, D., LoTufo, J., et al. (2017). Novel Techniques in Wind Engineering. *J. Wind Eng. Ind. Aerodynamics* 171, 12–33. doi:10.1016/j.jweia.2017.09.010

Hao, J., and Wu, T. (2018). Downburst-induced Transient Response of a Long-Span Bridge: A CFD-CSD-Based Hybrid Approach. *J. Wind Eng. Ind. Aerodynamics* 179, 273–286. doi:10.1016/j.jweia.2018.06.006

Hao, J., and Wu, T. (2017). Nonsynoptic Wind-Induced Transient Effects on Linear Bridge Aerodynamics. *J. Eng. Mech.* 143 (9), 04017092. doi:10.1061/(asce)em.1943-7889.0001313

Hao, J., and Wu, T. (2020). Numerical Analysis of a Long-Span Bridge Response to Tornado-like Winds. *Wind and Structures* 31 (5), 459–472.

Hao, J., and Wu, T. "Tornado-induced Effects on Aerostatic and Aeroelastic Behaviors of Long-Span Bridge," in Proceeding of the 2016 World Congress on Advances in Civil Environmental & Materials Research, Jeju, Korea, September 2016.

Hasegawa, K., Fukami, K., Murata, T., and Fukagata, K. "Data-driven Reduced Order Modeling of Flows Around Two-Dimensional bluff Bodies of Various Shapes," in Fluids Engineering Division Summer Meeting, American Society of Mechanical Engineers, San Francisco, CA, July 28–August 1, 2019, V002T02A075.

Hasegawa, K., Fukami, K., Murata, T., and Fukagata, K. (2020). Machine-learning-based Reduced-Order Modeling for Unsteady Flows Around bluff Bodies of Various Shapes. *Theor. Comput. Fluid Dyn.* 34, 367–383. doi:10.1007/s00162-020-00528-w

Hawbecker, P. (2021). "Mesoscale, Microscale, and Numerical Models," in *The Oxford Handbook of Non-synoptic Wind Storms*. Editors H. Hangan and A. Kareem (Oxford, United Kingdom: Oxford University Press), 239.

Hayashi, K., and Ohsaki, M. (2020). Reinforcement Learning for Optimum Design of a Plane Frame under Static Loads. *Eng. Comput.* 37, 1999–2011. doi:10.1007/s00366-019-00926-7

He, Y. C., Li, Y. Z., Chan, P. W., Fu, J. Y., Wu, J. R., and Li, Q. S. (2019). A Height-Resolving Model of Tropical Cyclone Pressure Field. *J. Wind. Eng. Ind. Aerodyn.* 186, 84–93.

Hinton, G. E., Osindero, S., and Teh, Y.-W. (2006). A Fast Learning Algorithm for Deep Belief Nets. *Neural Comput.* 18 (7), 1527–1554. doi:10.1162/neco.2006.18.7.1527

Hochreiter, S., and Schmidhuber, J. (1997). Long Short-Term Memory. *Neural Comput.* 9 (8), 1735–1780. doi:10.1162/neco.1997.9.8.1735

Holmes, J. D. (1999). "Modeling of Extreme Thunderstorm Winds for Wind Loading of Structures and Risk Assessment," in *Wind Engineering into the 21st Century, Proceedings of the Tenth International Conference on Wind Engineering, Copenhagen, Denmark, 21-24 June 1999*. Editor A. Larsen (Boca Raton, Florida, United States: CRC Press), 1409–1415.

Holton, J. R., and Hakim, G. J. (2013). *An Introduction to Dynamic Meteorology*. Fifth edition. Amsterdam: Academic Press.

Hopfield, J. J. (1982). Neural Networks and Physical Systems with Emergent Collective Computational Abilities. *Proc. Natl. Acad. Sci.* 79 (8), 2554–2558. doi:10.1073/pnas.79.8.2554

Hornik, K. (1991). Approximation Capabilities of Multilayer Feedforward Networks. *Neural networks* 4 (2), 251–257. doi:10.1016/0893-6080(91)90009-t

Hoshino, N., Iida, Y., and Uematsu, Y. (2018). Effects of Non-stationarity of Downburst on the Wind Loading of Buildings. *J. Wind Eng.* 43 (1), 1–13. doi:10.5359/jwe.43.1

Hou, F., and Sarkar, P. P. (2020). Aeroelastic Model Tests to Study Tall Building Vibration in Boundary-Layer and Tornado Winds. *Eng. Structures* 207, 110259. doi:10.1016/j.engstruct.2020.110259

Hu, G., and Kwok, K. C. S. (2020). Predicting Wind Pressures Around Circular Cylinders Using Machine Learning Techniques. *J. Wind Eng. Ind. Aerodynamics* 198, 104099. doi:10.1016/j.jweia.2020.104099

Hu, G., Liu, L., Tao, D., Song, J., Tse, K. T., and Kwok, K. C. S. (2020). Deep Learning-Based Investigation of Wind Pressures on Tall Building under Interference Effects. *J. Wind Eng. Ind. Aerodynamics* 201, 104138. doi:10.1016/j.jweia.2020.104138

Huang, D., Shiqing, H., Xuhui, H., and Xue, Z. (2017). Prediction of Wind Loads on High-Rise Building Using a BP Neural Network Combined with POD. *J. Wind Eng. Ind. Aerodynamics* 170, 1–17. doi:10.1016/j.jweia.2017.07.021

Huang, G., He, H., Mehta, K. C., and Liu, X. (2015). Data-based Probabilistic Damage Estimation for Asphalt Shingle Roofing. *J. Struct. Eng.* 141 (12), 04015065. doi:10.1061/(asce)st.1943-541x.0001300

Huang, W. F., and Xu, Y. L. (2013). Prediction of Typhoon Design Wind Speed and Profile over Complex Terrain. *Struct. Eng. Mech.* 45 (1), 1–18. doi:10.12989/sem.2013.45.1.001

Huang, W. Y., and Lippmann, R. P. (1988). "Neural Net and Traditional Classifiers," in *Neural Information Processing Systems*. Editor D. Z. Anderson (Berlin/Heidelberg, Germany: Springer Science & Business Media), 387–396.

Huo, S., Hemida, H., and Sterling, M. (2020). Numerical Study of Debris Flight in a Tornado-like Vortex. *J. Fluids Structures* 99, 103134. doi:10.1016/j.jfluidstructs.2020.103134

Iida, Y., and Uematsu, Y. (2019). Numerical Study of Wind Loads on Buildings Induced by Downbursts. *J. Wind Eng. Ind. Aerodynamics* 191, 103–116. doi:10.1016/j.jweia.2019.05.018

Imran, M., Elbassuoni, S., Castillo, C., Diaz, F., and Meier, P. "Extracting Information Nuggets from Disaster-Related Messages in Social media," in Proceedings of the 10th International Conference on Information Systems for Crisis Response and Management, Information Systems for Crisis Response and Management, Baden-Baden, Germany, May 2013, 791–801.

Imran, M., Mitra, P., and Castillo, C. "Twitter as a Lifeline: Human-Annotated Twitter Corpora for NLP of Crisis-Related Messages," in Proceedings of the Tenth International Conference on Language Resources and Evaluation (LREC 2016), European Language Resources Association (ELRA), Portorož, Slovenia, May 2016.

Ishihara, T., Oh, S., and Tokuyama, Y. (2011). Numerical Study on Flow fields of Tornado-like Vortices Using the LES Turbulence Model. *J. Wind Eng. Ind. Aerodynamics* 99 (4), 239–248. doi:10.1016/j.jweia.2011.01.014

Jackson, P. S., and Hunt, J. C. R. (1975). Turbulent Wind Flow over a Low hill. *Q.J R. Met. Soc.* 101 (430), 929–955. doi:10.1002/qj.49710143015

Jesson, M., Sterling, M., Letchford, C., and Haines, M. (2015). Aerodynamic Forces on Generic Buildings Subject to Transient, Downburst-type Winds. *J. wind Eng. Ind. aerodynamics* 137, 58–68. doi:10.1016/j.jweia.2014.12.003

Jiang, X., and Adeli, H. (2008). Dynamic Fuzzy Wavelet Neuroemulator for Non-linear Control of Irregular Building Structures. *Int. J. Numer. Meth. Engng* 74 (7), 1045–1066. doi:10.1002/nme.2195

Jiang, X., and Adeli, H. (2005). Dynamic Wavelet Neural Network for Nonlinear Identification of Highrise Buildings. *Comp-aided Civil Eng.* 20 (5), 316–330. doi:10.1111/j.1467-8667.2005.00399.x

Jubayer, C., Elatar, A., and Hangan, H., "Pressure Distributions on a Low-Rise Building in a Laboratory Simulated Downburst." in Proceedings of the 8th

International Colloquium on Bluff Body Aerodynamics and Applications, Boston, Massachusetts, USA. June 2016

Junayed, C., Jubayer, C., Parvu, D., Romanic, D., and Hangan, H. (2019). Flow Field Dynamics of Large-Scale Experimentally Produced Downburst Flows. *J. Wind Eng. Ind. Aerodynamics* 188, 61–79. doi:10.1016/j.jweia.2019.02.008

Jung, S., Ghaboussi, J., and Kwon, S.-D. (2004). Estimation of Aeroelastic Parameters of Bridge Decks Using Neural Networks. *J. Eng. Mech.* 130 (11), 1356–1364. doi:10.1061/(asce)0733-9399(2004)130:11(1356)

Kamangir, H., Collins, W., Tissot, P., and King, S. A. (2020). Deep-learning Model Used to Predict Thunderstorms within 400 Km2 of South Texas Domains. *Meteorol. Appl.* 27 (2), e1905. doi:10.1002/met.1905

Kareem, A. (2020). Emerging Frontiers in Wind Engineering: Computing, Stochastics, Machine Learning and beyond. *J. Wind Eng. Ind. Aerodynamics* 206, 104320. doi:10.1016/j.jweia.2020.104320

Kareem, A., and Wu, T. (2013). Wind-induced Effects on bluff Bodies in Turbulent Flows: Nonstationary, Non-gaussian and Nonlinear Features. *J. Wind Eng. Ind. Aerodynamics* 122, 21–37. doi:10.1016/j.jweia.2013.06.002

Kawaguchi, M., Tamura, T., and Kawai, H. (2019). Analysis of Tornado and Near-Ground Turbulence Using a Hybrid Meteorological Model/engineering LES Method. *Int. J. Heat Fluid Flow* 80, 108464. doi:10.1016/j.ijheatfluidflow.2019.108464

Kelley, H. J. (1960). Gradient Theory of Optimal Flight Paths. *Ars J.* 30 (10), 947–954. doi:10.2514/8.5282

Khalatbarisoltani, A., Soleymani, M., and Khodadadi, M. (2019). Online Control of an Active Seismic System via Reinforcement Learning. *Struct. Control. Health Monit.* 26 (3), e2298. doi:10.1002/stc.2298

Khanduri, A. C., Bédard, C., and Stathopoulos, T. (1997). Modelling Wind-Induced Interference Effects Using Backpropagation Neural Networks. *J. wind Eng. Ind. aerodynamics* 72, 71–79. doi:10.1016/s0167-6105(97)00259-6

Khodabandehlou, H., Pekcan, G., Fadali, M. S., and Salem, M. M. A. (2018). Active Neural Predictive Control of Seismically Isolated Structures. *Struct. Control. Health Monit.* 25 (1), e2061. doi:10.1002/stc.2061

Khosravi, A., Koury, R. N. N., Machado, L., and Pabon, J. J. G. (2018b). Prediction of Wind Speed and Wind Direction Using Artificial Neural Network, Support Vector Regression and Adaptive Neuro-Fuzzy Inference System. *Sustainable Energ. Tech. Assessments* 25, 146–160. doi:10.1016/j.seta.2018.01.001

Khosravi, A., Machado, L., and Nunes, R. O. (2018a). Time-series Prediction of Wind Speed Using Machine Learning Algorithms: A Case Study Osorio Wind Farm, Brazil. *Appl. Energ.* 224, 550–566. doi:10.1016/j.apenergy.2018.05.043

Kim, J., and Lee, C. (2020). Deep Unsupervised Learning of Turbulence for Inflow Generation at Various Reynolds Numbers. *J. Comput. Phys.* 406, 109216. doi:10.1016/j.jcp.2019.109216

Kim, M., Park, M.-S., Im, J., Park, S., and Lee, M.-I. (2019). Machine Learning Approaches for Detecting Tropical Cyclone Formation Using Satellite Data. *Remote Sensing* 11 (10), 1195. doi:10.3390/rs11101195

Kim, S., Kim, H., Lee, J., Yoon, S., Kahou, S. E., Kashinath, K., et al. "Deep-hurricane-tracker: Tracking and Forecasting Extreme Climate Events," in Proceedings of the 2019 IEEE Winter Conference on Applications of Computer Vision (WACV), Waikoloa, HI, USA, January 2019 (Piscataway, New Jersey, United States: IEEE), 1761–1769.

Kolmogorov, A. N. (1941). The Local Structure of Turbulence in Incompressible Viscous Fluid for Very Large Reynolds Numbers. *Cr Acad. Sci. URSS* 30, 301–305.

Križan, J., Gašparac, G., Kozmar, H., Antonić, O., and Grisogono, B. (2015). Designing Laboratory Wind Simulations Using Artificial Neural Networks. *Theor. Appl. climatology* 120 (3-4), 723–736. doi:10.1007/s00704-014-1201-4

Krizhevsky, A., Sutskever, I., and Hinton, G. E. (2012). Imagenet Classification with Deep Convolutional Neural Networks. *Adv. Neural Inf. Process. Syst.* 60, 84–90. doi:10.1145/3065386

Kuai, L., Haan, F. L. J., Jr., Gallus, W. A. J., Jr., and Sarkar, P. P. (2008). CFD Simulations of the Flow Field of a Laboratory-Simulated Tornado for Parameter Sensitivity Studies and Comparison with Field Measurements. *Wind and Structures* 11 (2), 75–96. doi:10.12989/was.2008.11.2.075

Kumar, G., and Malik, H. (2016). Generalized Regression Neural Network Based Wind Speed Prediction Model for Western Region of India. *Proced. Comput. Sci.* 93, 26–32. doi:10.1016/j.procs.2016.07.177

Kutz, J. N. (2017). Deep Learning in Fluid Dynamics. *J. Fluid Mech.* 814, 1–4. doi:10.1017/jfm.2016.803

Lagerquist, R. A., Homeyer, C. R., McGovern, A., Potvin, C. K., Sandmael, T., and Smith, T. M. "Deep Learning for Real-Time Storm-Based Tornado Prediction," in Proceedings of the 29th Conference on Severe Local Storms, Stowe, VT, October 2018 (Boston, Massachusetts, United States: AMS).

Lagerquist, R., McGovern, A., Homeyer, C. R., Gagne, D. J., and Smith, T. (2020). Deep Learning on Three-Dimensional Multiscale Data for Next-Hour Tornado Prediction. *Monthly Weather Rev.* 148, 2837–2861. doi:10.1175/mwr-d-19-0372.1

Lagerquist, R., McGovern, A., and Smith, T. (2017). Machine Learning for Real-Time Prediction of Damaging Straight-Line Convective Wind. *Weather Forecast.* 32 (6), 2175–2193. doi:10.1175/waf-d-17-0038.1

Lahouar, A., and Slama, J. B. H. "Wind Speed and Direction Prediction for Wind Farms Using Support Vector Regression." in Proceedings of the 2014 5th International Renewable Energy Congress (IREC). Hammamet, Tunisia. March 2014 (Piscataway, New Jersey, United States: IEEE), 1–6.

Lakshmanan, V., Stumpf, G., and Witt, A. "A Neural Network for Detecting and Diagnosing Tornadic Circulations Using the Mesocyclone Detection and Near Storm Environment Algorithms," in Proceedings of the AI Applications with a Nowcasting Flavor (Joint between the Fourth Conference on Artificial Intelligence and the 21st International Conference on Interactive Information and Processing Systems (IIPS) for Meteorology, Oceanography, and Hydrology), San Diego, CA, USA, January 2005 (Boston, Massachusetts, United States: AMS).

Le, V., and Caracoglia, L. (2020). A Neural Network Surrogate Model for the Performance Assessment of a Vertical Structure Subjected to Non-stationary, Tornadic Wind Loads. *Comput. Structures* 231, 106208. doi:10.1016/j.compstruc.2020.106208

LeCun, Y., Boser, B., Denker, J. S., Henderson, D., Howard, R. E., Hubbard, W., et al. (1989). Backpropagation Applied to Handwritten Zip Code Recognition. *Neural Comput.* 1 (4), 541–551. doi:10.1162/neco.1989.1.4.541

Letchford, C. W., Mans, C., and Chay, M. T. (2002). Thunderstorms—their Importance in Wind Engineering (A Case for the Next Generation Wind Tunnel). *J. Wind Eng. Ind. Aerodynamics* 90 (12-15), 1415–1433. doi:10.1016/s0167-6105(02)00262-3

Li, G., and Shi, J. (2010). On Comparing Three Artificial Neural Networks for Wind Speed Forecasting. *Appl. Energ.* 87 (7), 2313–2320. doi:10.1016/j.apenergy.2009.12.013

Li, S., Laima, S., and Li, H. (2018). Data-driven Modeling of Vortex-Induced Vibration of a Long-Span Suspension Bridge Using Decision Tree Learning and Support Vector Regression. *J. Wind Eng. Ind. Aerodynamics* 172, 196–211. doi:10.1016/j.jweia.2017.10.022

Li, S., Snaiki, R., and Wu, T. (2021a). A Knowledge-enhanced Deep Reinforcement Learning-based Shape Optimizer for Aerodynamic Mitigation of Wind-sensitive Structures. *Computer-Aided Civil Infrastructure Eng.* 36 (6), 733–746. doi:10.1111/mice.12655

Li, S., Snaiki, R., and Wu, T. (2021b). Active Simulation of Transient Wind Field in a Multiple-Fan Wind Tunnel via Deep Reinforcement Learning. *J. Eng. Mech.* 147 (9), 04021056. doi:10.1061/(asce)em.1943-7889.0001967

Li, T., Wu, T., and Liu, Z. (2020). Nonlinear Unsteady Bridge Aerodynamics: Reduced-Order Modeling Based on Deep LSTM Networks. *J. Wind Eng. Ind. Aerodynamics* 198, 104116. doi:10.1016/j.jweia.2020.104116

Li, Z., and Li, C. (2018). "Selection of Kernel Function for Least Squares Support Vector Machines in Downburst Wind Speed Forecasting," in Proceedings of the 2018 11th International Symposium on Computational Intelligence and Design (ISCID), Hangzhou, China (Piscataway, New Jersey, United States: IEEE), 337–341. doi:10.1109/iscid.2018.10178

Liang, X. (2019). Image-based post-disaster Inspection of Reinforced concrete Bridge Systems Using Deep Learning with Bayesian Optimization. *Computer-Aided Civil Infrastructure Eng.* 34 (5), 415–430. doi:10.1111/mice.12425

Lillicrap, T. P., Hunt, J. J., Pritzel, A., Heess, N., Erez, T., Tassa, Y., et al. (2015). Continuous Control with Deep Reinforcement Learning. *arXiv*. arXiv: 1509.02971.

Lin, T. Y., Goyal, P., Girshick, R., He, K., and Dollár, P. "Focal Loss for Dense Object Detection," in Proceedings of the IEEE international conference on computer vision, Venice, Italy, October 2017, 2980–2988. doi:10.1109/iccv.2017.324

Litta, A. J., Idicula, S. M., and Francis, C. N. (2012). Artificial Neural Network Model for the Prediction of Thunderstorms over kolkata. *Int. J. Comput. Appl.* 50 (11), 50–55. doi:10.5120/7819-1135

Liu, Z., Cao, Y., Cao, J., Wang, Y., and Cao, S. (2021). Numerical Study of Tornado-Borne Debris on a Low-Rise Building through Large Eddy Simulation. *J. Fluids Structures* 106, 103379. doi:10.1016/j.jfluidstructs.2021.103379

Liu, Z., and Ishihara, T. (2015). Numerical Study of Turbulent Flow fields and the Similarity of Tornado Vortices Using Large-Eddy Simulations. *J. Wind Eng. Ind. Aerodynamics* 145, 42–60. doi:10.1016/j.jweia.2015.05.008

López, P., Velo, R., and Maseda, F. (2008). Effect of Direction on Wind Speed Estimation in Complex Terrain Using Neural Networks. *Renew. Energ.* 33 (10), 2266–2272. doi:10.1016/j.renene.2007.12.020

Lute, V., Upadhyay, A., and Singh, K. K. (2009). Support Vector Machine Based Aerodynamic Analysis of cable Stayed Bridges. *Adv. Eng. Softw.* 40 (9), 830–835. doi:10.1016/j.advengsoft.2009.01.008

Mandic, D., and Chambers, J. (2001). *Recurrent Neural Networks for Prediction: Learning Algorithms, Architectures and Stability*. Hoboken, New Jersey, United States: John Wiley & Sons.

Manna, S., and Nakai, H. "Effectiveness of Word Embeddings on Classifiers: A Case Study with Tweets," in Proceedings of the 2019 IEEE 13th International Conference on Semantic Computing (ICSC), Newport Beach, CA, USA, January 2019 (Piscataway, New Jersey, United States: IEEE), 158–161.

Manohar, K., Brunton, B. W., Kutz, J. N., and Brunton, S. L. (2018). Data-driven Sparse Sensor Placement for Reconstruction: Demonstrating the Benefits of Exploiting Known Patterns. *IEEE Control. Syst. Mag.* 38 (3), 63–86. doi:10.1109/MCS.2018.2810460

Martínez-Vázquez, P., and Rodríguez-Cuevas, N. (2007). Wind Field Reproduction Using Neural Networks and Conditional Simulation. *Eng. structures* 29 (7), 1442–1449. doi:10.1016/j.engstruct.2006.08.024

Marzban, C. (2000). A Neural Network for Tornado Diagnosis: Managing Local Minima. *Neural Comput. Appl.* 9, 133–141. doi:10.1007/s005210070024

Marzban, C., Paik, H., and Stumpf, G. J. (1997). Neural Networks vs. Gaussian Discriminant Analysis. *AI Appl.* 11 (1), 49–58.

Marzban, C., and Stumpf, G. J. (1998). A Neural Network for Damaging Wind Prediction. *Wea. Forecast.* 13, 151–163. doi:10.1175/1520-0434(1998)013<0151:annfdw>2.0.co;2

Marzban, C., and Stumpf, G. J. (1996). A Neural Network for Tornado Prediction Based on Doppler Radar-Derived Attributes. *J. Appl. Meteorol.* 35, 617–626. doi:10.1175/1520-0450(1996)035<0617:annftp>2.0.co;2

Maskey, M., Ramachandran, R., Ramasubramanian, M., Gurung, I., Freitag, B., Kaulfus, A., et al. (2020). Deepti: Deep-Learning-Based Tropical Cyclone Intensity Estimation System. *IEEE J. Sel. Top. Appl. Earth Observations Remote Sensing* 13, 4271–4281. doi:10.1109/jstars.2020.3011907

Mason, M. S., Wood, G. S., and Fletcher, D. F. (2009). Numerical Simulation of Downburst Winds. *J. Wind Eng. Ind. Aerodynamics* 97 (11-12), 523–539. doi:10.1016/j.jweia.2009.07.010

Masri, S. F., Chassiakos, A. G., and Caughey, T. K. (1993). Identification of Nonlinear Dynamic Systems Using Neural Networks. *J. Appl. Mech.* 60 (1), 123–133. doi:10.1115/1.2900734

Matsumoto, M., Kobayashi, Y., and Shirato, H. (1996). The Influence of Aerodynamic Derivatives on Flutter. *J. Wind Eng. Ind. Aerodynamics* 60, 227–239. doi:10.1016/0167-6105(96)00036-0

Maulik, U., and Bandyopadhyay, S. (2002). Performance Evaluation of Some Clustering Algorithms and Validity Indices. *IEEE Trans. Pattern Anal. Machine Intell.* 24 (12), 1650–1654. doi:10.1109/tpami.2002.1114856

Mayo, M., Wakes, S., and Anderson, C. "Neural Networks for Predicting the Output of Wind Flow Simulations over Complex Topographies," in Proceedings of the 2018 IEEE International Conference on Big Knowledge (ICBK), Singapore, November 2018 (Piscataway, New Jersey, United States: IEEE), 184–191.

McCann, D. W. (1992). A Neural Network Short-Term Forecast of Significant Thunderstorms. *Wea. Forecast.* 7 (3), 525–534. doi:10.1175/1520-0434(1992)007<0525:annstf>2.0.co;2

McCarthy, J. (2007). From Here to Human-Level AI. *Artif. Intelligence* 171 (18), 1174–1182. doi:10.1016/j.artint.2007.10.009

McCulloch, W. S., and Pitts, W. (1943). A Logical Calculus of the Ideas Immanent in Nervous Activity. *Bull. Math. Biophys.* 5 (4), 115–133. doi:10.1007/bf02478259

Medina, B., Carey, L., Amiot, C., Mecikalski, R., Roeder, W., McNamara, T., et al. (2019). A Random forest Method to Forecast Downbursts Based on Dual-Polarization Radar Signatures. *Remote Sensing* 11 (7), 826. doi:10.3390/rs11070826

Medsker, L., and Jain, L. C. (1999). *Recurrent Neural Networks: Design and Applications*. Boca Raton, Florida, United States: CRC Press.

Michael, B. (20172017). *Tropical Cyclone Genesis Forecasting and Pre-genesis Forecasts Report*. Miami, FL, USA: National Hurricane Center.

Micheli, L., Hong, J., Laflamme, S., and Alipour, A. (2020). Surrogate Models for High Performance Control Systems in Wind-Excited Tall Buildings. *Appl. Soft Comput.* 90, 106133. doi:10.1016/j.asoc.2020.106133

Mnih, V., Kavukcuoglu, K., Silver, D., Rusu, A. A., Veness, J., Bellemare, M. G., et al. (2015). Human-level Control through Deep Reinforcement Learning. *nature* 518 (7540), 529–533. doi:10.1038/nature14236

Mohandes, M. A., Halawani, T. O., Rehman, S., and Hussain, A. A. (2004). Support Vector Machines for Wind Speed Prediction. *Renew. Energ.* 29 (6), 939–947. doi:10.1016/j.renene.2003.11.009

Mohri, M., Rostamizadeh, A., and Talwalkar, A. (2018). *Foundations of Machine Learning*. Cambridge, Massachusetts, United States: MIT press.

Moradi Kordmahalleh, M., Gorji Sefidmazgi, M., and Homaifar, A. (2016). "A Sparse Recurrent Neural Network for Trajectory Prediction of atlantic Hurricanes," in *Proceedings of the Genetic and Evolutionary Computation Conference 2016*. Editor F. Neumann (New York, United States: Association for Computing Machinery), 957–964.

More, A., and Deo, M. C. (2003). Forecasting Wind with Neural Networks. *Mar. structures* 16 (1), 35–49. doi:10.1016/s0951-8339(02)00053-9

Murphy, K. P. (2012). *Machine Learning: A Probabilistic Perspective*. Cambridge, Massachusetts, United States: MIT press.

Nikose, T. J., and Sonparote, R. S. (2020). Computing Dynamic Across-Wind Response of Tall Buildings Using Artificial Neural Network. *J. Supercomput* 76 (5), 3788–3813. doi:10.1007/s11227-018-2708-8

Nikose, T. J., and Sonparote, R. S. (2019a). Dynamic along Wind Response of Tall Buildings Using Artificial Neural Network. *Cluster Comput.* 22 (2), 3231–3246. doi:10.1007/s10586-018-2027-0

Nikose, T. J., and Sonparote, R. S. (2019b). Dynamic Wind Response of Tall Buildings Using Artificial Neural Network. *The Struct. Des. Tall Spec. Buildings* 28 (13), e1657. doi:10.1002/tal.1657

Oh, B. K., Glisic, B., Kim, Y., and Park, H. S. (2019). Convolutional Neural Network-Based Wind Induced Response Estimation Model for Tall Buildings. *Comput. Aided Civ. Infrastruct. Eng.* 34, 843–858. doi:10.1111/mice.12476

Oh, B. K., Kim, K. J., Kim, Y., Park, H. S., and Adeli, H. (2017). Evolutionary Learning Based Sustainable Strain Sensing Model for Structural Health Monitoring of High-Rise Buildings. *Appl. Soft Comput.* 58, 576–585. doi:10.1016/j.asoc.2017.05.029

O'Neal, A., Rodgers, B., Segler, J., Murthy, D., Lakuduva, N., Johnson, M., et al. "Training an Emergency-Response Image Classifier on Signal Data," in Proceedings of the 2018 17th IEEE International Conference on Machine Learning and Applications (ICMLA), Orlando, FL, USA, December 2018 (Piscataway, New Jersey, United States: IEEE), 751–756.

Oreskovic, C., Orf, L. G., and Savory, E. (2018). A Parametric Study of Downbursts Using a Full-Scale Cooling Source Model. *J. Wind Eng. Ind. Aerodynamics* 180, 168–181. doi:10.1016/j.jweia.2018.07.020

Oreskovic, C., and Savory, E. (2018). Evolution and Scaling of a Simulated Downburst-Producing Thunderstorm Outflow. *Wind and Structures* 26 (3), 147–161. doi:10.12989/was.2018.26.3.147

Pan, B., Xu, X., and Shi, Z. (2019). Tropical Cyclone Intensity Prediction Based on Recurrent Neural Networks. *Electron. Lett.* 55 (7), 413–415. doi:10.1049/el.2018.8178

Panofsky, H. A., and McCormick, R. A. (1960). The Spectrum of Vertical Velocity Near the Surface. *Q.J R. Met. Soc.* 86 (370), 495–503. doi:10.1002/qj.49708637006

Park, M.-S., Kim, M., Lee, M.-I., Im, J., and Park, S. (2016). Detection of Tropical Cyclone Genesis via Quantitative Satellite Ocean Surface Wind Pattern and Intensity Analyses Using Decision Trees. *Remote sensing Environ.* 183, 205–214. doi:10.1016/j.rse.2016.06.006

Pei, J. S., Wright, J. P., and Smyth, A. W. (2005). Mapping Polynomial Fitting into Feedforward Neural Networks for Modeling Nonlinear Dynamic Systems and beyond. *Comput. Methods Appl. Mech. Eng.* 194 (42-44), 4481–4505. doi:10.1016/j.cma.2004.12.010

Pi, Y., Nath, N. D., and Behzadan, A. H. (2020). Convolutional Neural Networks for Object Detection in Aerial Imagery for Disaster Response and Recovery. *Adv. Eng. Inform.* 43, 101009. doi:10.1016/j.aei.2019.101009

Potter, C. W., and Negnevitsky, M. (2006). Very Short-Term Wind Forecasting for Tasmanian Power Generation. *IEEE Trans. Power Syst.* 21 (2), 965–972. doi:10.1109/tpwrs.2006.873421

Pouyanfar, S., Sadiq, S., Yan, Y., Tian, H., Tao, Y., Reyes, M. P., et al. (2018). A Survey on Deep Learning: Algorithms, Techniques, and Applications. *ACM Comput. Surv. (Csur)* 51 (5), 1–36. doi:10.1145/3234150

Psichogios, D. C., and Ungar, L. H. (1992). A Hybrid Neural Network-First Principles Approach to Process Modeling. *Aiche J.* 38 (10), 1499–1511. doi:10.1002/aic.690381003

Raissi, M., Perdikaris, P., and Karniadakis, G. E. (2017a). Physics Informed Deep Learning (Part I): Data-Driven Solutions of Nonlinear Partial Differential Equations. *arXiv preprint*. arXiv:1711.10561.

Raissi, M., Perdikaris, P., and Karniadakis, G. E. (2017b). Physics Informed Deep Learning (Part II): Data-Driven Discovery of Nonlinear Partial Differential Equations. *arXiv* 1711, 10566.

Raissi, M., Perdikaris, P., and Karniadakis, G. E. (2019). Physics-informed Neural Networks: A Deep Learning Framework for Solving Forward and Inverse Problems Involving Nonlinear Partial Differential Equations. *J. Comput. Phys.* 378, 686–707. doi:10.1016/j.jcp.2018.10.045

Rathje, E. M., Dawson, C., Padgett, J. E., Pinelli, J.-P., Stanzione, D., Adair, A., et al. (2017). DesignSafe: New Cyberinfrastructure for Natural Hazards Engineering. *Nat. Hazards Rev.* 18 (3), 06017001. doi:10.1061/(asce)nh.1527-6996.0000246

Razavi, A., and Sarkar, P. P. (2021). Effects of Roof Geometry on Tornado-Induced Structural Actions of a Low-Rise Building. *Eng. structures* 226, 111367. doi:10.1016/j.engstruct.2020.111367

Razavi, A., and Sarkar, P. P. (2018). Laboratory Study of Topographic Effects on the Near-Surface Tornado Flow Field. *Boundary-layer Meteorol.* 168 (2), 189–212. doi:10.1007/s10546-018-0347-5

Refan, M., and Hangan, H. (2016). Characterization of Tornado-like Flow fields in a New Model Scale Wind Testing Chamber. *J. Wind Eng. Ind. Aerodynamics* 151, 107–121. doi:10.1016/j.jweia.2016.02.002

Richman, M. B., and Leslie, L. M. (2012). Adaptive Machine Learning Approaches to Seasonal Prediction of Tropical Cyclones. *Proced. Comput. Sci.* 12, 276–281. doi:10.1016/j.procs.2012.09.069

Richman, M. B., Leslie, L. M., Ramsay, H. A., and Klotzbach, P. J. (2017). Reducing Tropical Cyclone Prediction Errors Using Machine Learning Approaches. *Proced. Comput. Sci.* 114, 314–323. doi:10.1016/j.procs.2017.09.048

Riedmiller, M., and Braun, H. "A Direct Adaptive Method for Faster Backpropagation Learning: The RPROP Algorithm," in Proceedings of the IEEE international conference on neural networks, San Francisco, CA, USA, March 1993 (Piscataway, New Jersey, United States: IEEE), 586–591.

Rizzo, F., and Caracoglia, L. (2020). Artificial Neural Network Model to Predict the Flutter Velocity of Suspension Bridges. *Comput. Structures* 233, 106236. doi:10.1016/j.compstruc.2020.106236

Robertson, B. W., Johnson, M., Murthy, D., Smith, W. R., and Stephens, K. K. (2019). Using a Combination of Human Insights and 'deep Learning' for Real-Time Disaster Communication. *Prog. Disaster Sci.* 2, 100030. doi:10.1016/j.pdisas.2019.100030

Romanic, D., LoTufo, J., and Hangan, H. (2019). Transient Behavior in Impinging Jets in Crossflow with Application to Downburst Flows. *J. Wind Eng. Ind. Aerodynamics* 184, 209–227. doi:10.1016/j.jweia.2018.11.020

Rosenblatt, F. (1957). *The Perceptron, a Perceiving and Recognizing Automaton Project Para*. Buffalo, New York, United States: Cornell Aeronautical Laboratory.

Rumelhart, D. E., Hinton, G. E., and Williams, R. J. (1986). Learning Representations by Back-Propagating Errors. *nature* 323 (6088), 533–536. doi:10.1038/323533a0

Russell, S., and Norvig, P. (2016). *Artificial Intelligence: A Modern Approach*. London, United Kingdom: Pearson Education Limited.

Rüttgers, M., Lee, S., Jeon, S., and You, D. (2019). Prediction of a Typhoon Track Using a Generative Adversarial Network and Satellite Images. *Sci. Rep.* 9 (1), 1–15. doi:10.1038/s41598-019-42339-y

Salehi, H., and Burgueño, R. (2018). Emerging Artificial Intelligence Methods in Structural Engineering. *Eng. structures* 171, 170–189. doi:10.1016/j.engstruct.2018.05.084

Santosa, B. (2007). Feature Selection with Support Vector Machines Applied on Tornado Detection. *IPTEK J. Technol. Sci.* 18 (1). doi:10.12962/j20882033.v18i1.178

Sarkar, P. P., Haan, F. L., Jr., Balaramudu, V., and Sengupta, A., "Laboratory Simulation of Tornado and Microburst to Assess Wind Loads on Buildings." in Proceedings of the Structures Congress 2006: Structural Engineering and Public Safety. St. Louis, Missouri, United States. May 2006. 1–10. doi:10.1061/40889(201)11

Saunders, J. W., and Melbourne, W. H. (1980). "Buffeting Effects of Upstream Buildings," in *Wind Engineering*. Editor J. W. Saunders (Pergamon: Pergamon Press), 593–606. doi:10.1016/b978-1-4832-8367-8.50059-0

Scholkopf, B., and Smola, A. J. (2018). *Learning with Kernels: Support Vector Machines, Regularization, Optimization, and beyond. Adaptive Computation and Machine Learning Series*. Cambridge, Massachusetts, United States: MIT Press.

Sfetsos, A. (2000). A Comparison of Various Forecasting Techniques Applied to Mean Hourly Wind Speed Time Series. *Renew. Energ.* 21 (1), 23–35. doi:10.1016/s0960-1481(99)00125-1

Sharma, R., Shikhola, T., and Kohli, J. K. (2020). Modified Fuzzy Q-Learning Based Wind Speed Prediction. *J. Wind Eng. Ind. Aerodynamics* 206, 104361. doi:10.1016/j.jweia.2020.104361

Silver, D., Schrittwieser, J., Simonyan, K., Antonoglou, I., Huang, A., Guez, A., et al. (2017). Mastering the Game of Go without Human Knowledge. *nature* 550 (7676), 354–359. doi:10.1038/nature24270

Simiu, E., and Scanlan, R. H. (1978). *Wind Effects on Structures*. Hoboken, New Jersey, United States: Wiley.

Smith, T. M., Elmore, K. L., and Dulin, S. A. (2004). A Damaging Downburst Prediction and Detection Algorithm for the WSR-88D. *Wea. Forecast.* 19 (2), 240–250. doi:10.1175/1520-0434(2004)019<0240:addpad>2.0.co;2

Snaiki, R., and Wu, T. (2017b). A Linear Height-Resolving Wind Field Model for Tropical Cyclone Boundary Layer. *J. Wind Eng. Ind. Aerodynamics* 171, 248–260. doi:10.1016/j.jweia.2017.10.008

Snaiki, R., and Wu, T. (2018). A Semi-empirical Model for Mean Wind Velocity Profile of Landfalling hurricane Boundary Layers. *J. Wind Eng. Ind. Aerodynamics* 180, 249–261. doi:10.1016/j.jweia.2018.08.004

Snaiki, R., and Wu, T. (2020c). An Analytical Model for Rapid Estimation of hurricane Supergradient Winds. *J. Wind Eng. Ind. Aerodynamics* 201, 104175. doi:10.1016/j.jweia.2020.104175

Snaiki, R., and Wu, T. (2020b). Hurricane hazard Assessment along the United States Northeastern Coast: Surface Wind and Rain fields under Changing Climate. *Front. Built Environ.* 6, 573054. doi:10.3389/fbuil.2020.573054

Snaiki, R., and Wu, T. (2019). Knowledge-enhanced Deep Learning for Simulation of Tropical Cyclone Boundary-Layer Winds. *J. Wind Eng. Ind. Aerodynamics* 194, 103983. doi:10.1016/j.jweia.2019.103983

Snaiki, R., and Wu, T. (2017a). Modeling Tropical Cyclone Boundary Layer: Height-Resolving Pressure and Wind fields. *J. Wind Eng. Ind. Aerodynamics* 170, 18–27. doi:10.1016/j.jweia.2017.08.005

Snaiki, R., and Wu, T. (2020a). Revisiting hurricane Track Model for Wind Risk Assessment. *Struct. Saf.* 87, 102003. doi:10.1016/j.strusafe.2020.102003

Solari, G., Burlando, M., De Gaetano, P., and Repetto, M. P. (2015). Characteristics of Thunderstorms Relevant to the Wind Loading of Structures. *Wind and Structures* 20 (6), 763–791. doi:10.12989/was.2015.20.6.763

Solari, G. (2020). Thunderstorm Downbursts and Wind Loading of Structures: Progress and prospect. *Front. Built Environ.* 6, 63. doi:10.3389/fbuil.2020.00063

Stiles, B. W., Danielson, R. E., Poulsen, W. L., Brennan, M. J., Hristova-Veleva, S., Tsae-Pyng Shen, T. P., et al. (2014). Optimized Tropical Cyclone Winds from QuikSCAT: A Neural Network Approach. *IEEE Trans. Geosci. Remote Sensing* 52 (11), 7418–7434. doi:10.1109/tgrs.2014.2312333

Subasri, R., Suresh, S., and Natarajan, A. M. (2014). Discrete Direct Adaptive ELM Controller for Active Vibration Control of Nonlinear Base Isolation Buildings. *Neurocomputing* 129, 246–256. doi:10.1016/j.neucom.2013.09.035

Subramanian, D., Salazar, J., Duenas-Osorio, L., and Stein, R. "Constructing and Validating Geographically Refined HAZUS-MH4 hurricane Wind Risk Models: A Machine Learning Approach," in Proceedings of the Advances in hurricane engineering: Learning from our past, Miami, Florida, United States, October 2013, 1056–1066. doi:10.1061/9780784412626.092

Sun, W., Bocchini, P., and Davison, B. D. (2020). Applications of Artificial Intelligence for Disaster Management. *Nat. Hazards* 103, 2631–2689. doi:10.1007/s11069-020-04124-3

Sun, Y., Yang, L., and Wu, Y. "Wind Load Prediction of Large-Span Dry Coal Sheds Based on GRNN and its Application," in Proceedings of International Structural Engineering and Construction, Valencia, Spain, July, 2017. doi:10.14455/isec.res.2017.189

Sutton, R. S., and Barto, A. G. (2018). *Reinforcement Learning: An Introduction*. Cambridge, Massachusetts, United States: MIT press.

Tagliaferri, F., Viola, I. M., and Flay, R. G. J. (2015). Wind Direction Forecasting with Artificial Neural Networks and Support Vector Machines. *Ocean Eng.* 97, 65–73. doi:10.1016/j.oceaneng.2014.12.026

Tang, Z., Feng, C., Wu, L., Zuo, D., and James, D. L. (2018). Characteristics of Tornado-like Vortices Simulated in a Large-Scale ward-type Simulator. *Boundary-layer Meteorol.* 166 (2), 327–350. doi:10.1007/s10546-017-0305-7

Taniike, Y., and Inaoka, H. (1988). "Aeroelastic Behavior of Tall Buildings in Wakes," in *Advances in Wind Engineering*. Editors C. Kramer and H. J. Gerhardt (Amsterdam, Netherlands: Elsevier), 317–327. doi:10.1016/b978-0-444-87156-5.50043-6

Tian, J., Gurley, K. R., Diaz, M. T., Fernández-Cabán, P. L., Masters, F. J., and Fang, R. (2020). Low-rise Gable Roof Buildings Pressure Prediction Using Deep Neural Networks. *J. Wind Eng. Ind. Aerodynamics* 196, 104026. doi:10.1016/j.jweia.2019.104026

Tian, W., Huang, W., Yi, L., Wu, L., and Wang, C. (2020). A CNN-Based Hybrid Model for Tropical Cyclone Intensity Estimation in Meteorological Industry. *IEEE Access* 8, 59158–59168. doi:10.1109/access.2020.2982772

Tian, Z., Ren, Y., and Wang, G. (2020). An Application of Backtracking Search Optimization-Based Least Squares Support Vector Machine for Prediction of Short-Term Wind Speed. *Wind Eng.* 44 (3), 266–281. doi:10.1177/0309524x19849843

Trafalis, T. B., Adrianto, I., Richman, M. B., and Lakshmivarahan, S. (2014). Machine-learning Classifiers for Imbalanced Tornado Data. *Comput. Manag. Sci.* 11 (4), 403–418. doi:10.1007/s10287-013-0174-6

Turkkan, N., and Srivastava, N. K. (1995). Prediction of Wind Load Distribution for Air-Supported Structures Using Neural Networks. *Can. J. Civ. Eng.* 22 (3), 453–461. doi:10.1139/l95-053

Twisdale, L. A., and Vickery, P. J. (1992). Research on Thunderstorm Wind Design Parameters. *J. Wind Eng. Ind. Aerodynamics* 41 (1-3), 545–556. doi:10.1016/0167-6105(92)90461-i

Uematsu, Y., and Tsuruishi, R. (2008). Wind Load Evaluation System for the Design of Roof Cladding of Spherical Domes. *J. wind Eng. Ind. aerodynamics* 96 (10-11), 2054–2066. doi:10.1016/j.jweia.2008.02.051

Ukkonen, P., Manzato, A., and Mäkelä, A. (2017). Evaluation of Thunderstorm Predictors for Finland Using Reanalyses and Neural Networks. *J. Appl. Meteorology Climatology* 56 (8), 2335–2352. doi:10.1175/jamc-d-16-0361.1

Varshney, K., and Poddar, K. (2012). Prediction of Wind Properties in Urban Environments Using Artificial Neural Network. *Theor. Appl. Climatology* 107 (3-4), 579–590. doi:10.1007/s00704-011-0506-9

Vickery, P. J., Skerlj, P. F., and Twisdale, L. A. (2000). Simulation of Hurricane Risk in the U.S. Using Empirical Track Model. *J. Struct. Eng.* 126 (10), 1222–1237. doi:10.1061/(asce)0733-9445(2000)126:10(1222)

Vickery, P. J., Wadhera, D., Twisdale, L. A., Jr., and Lavelle, F. M. (2009). U.S. Hurricane Wind Speed Risk and Uncertainty. *J. Struct. Eng.* 135 (3), 301–320. doi:10.1061/(asce)0733-9445(2009)135:3(301)

Vyavahare, A. Y., Godbole, P. N., and Nikose, T. (2012). Analysis of Tall Building for across Wind Response. *Int. J. Civil Struct. Eng.* 2 (3), 679–986.

Wang, H., and Wu, T. (2021). Fast Hilbert-Wavelet Simulation of Nonstationary Wind Field Using Noniterative Simultaneous Matrix Diagonalization. *J. Eng. Mech.* 147 (3), 04020153. doi:10.1061/(asce)em.1943-7889.0001897

Wang, H., and Wu, T. (2020). Knowledge-Enhanced Deep Learning for Wind-Induced Nonlinear Structural Dynamic Analysis. *J. Struct. Eng.* 146 (11), 04020235. doi:10.1061/(asce)st.1943-541x.0002802

Wang, H., Zhang, Y.-M., Mao, J.-X., and Wan, H.-P. (2020). A Probabilistic Approach for Short-Term Prediction of Wind Gust Speed Using Ensemble Learning. *J. Wind Eng. Ind. Aerodynamics* 202, 104198. doi:10.1016/j.jweia.2020.104198

Wang, J., and Cheng, C. M. "Aero-Data Based Wind Resistant Design of Rectangular Shaped Tall Buildings," in Proceedings of the International Conference on Innovations in Civil and Structural Engineering (ICICSE'15), Istanbul, Turkey, June 2015, 148–154.

Wang, J., Cheng, C. M., and Chen, C. H. "The Study of Wind Force Coefficient Predictions for Rectangular High-Rise Buildings," in Proceedings of The eighth Asia-Pacific conference on wind engineering, Chennai, India, December 2013, 10–14.

Wang, J., and Cheng, C. M. (2017). Formulation of Estimation Models for Wind Force Coefficients of Rectangular Shaped Buildings. *J. Appl. Sci. Eng.* 20 (1), 55–62. doi:10.6180/jase.2017.20.1.07

Wang, Y., Zhang, W., and Fu, W. "Back Propogation (BP)-neural Network for Tropical Cyclone Track Forecast," in Proceedings of the 2011 19th International Conference on Geoinformatics, Shanghai, China, June 2011 (Piscataway, New Jersey, United States: IEEE), 1–4.

Watkins, C. J. C. H. (1989). *Learning from Delayed Rewards*. Cambridge, UK: King's College.

Watkins, C. J., and Dayan, P. (1992). Q-learning. *Machine Learn.* 8 (3-4), 279–292. doi:10.1023/a:1022676722315

Wei, C.-C. (2015). Forecasting Surface Wind Speeds over Offshore Islands Near Taiwan during Tropical Cyclones: Comparisons of Data-Driven Algorithms and Parametric Wind Representations. *J. Geophys. Res. Atmos.* 120 (5), 1826–1847. doi:10.1002/2014jd022568

Wei, C.-C. (2019). Study on Wind Simulations Using Deep Learning Techniques during Typhoons: a Case Study of Northern Taiwan. *Atmosphere* 10 (11), 684. doi:10.3390/atmos10110684

Wen, Y.-K., and Chu, S.-L. (1973). Tornado Risks and Design Wind Speed. *J. Struct. Div.* 99 (12), 2409–2421. doi:10.1061/jsdeag.0003666

Wiederhold, G., McCarthy, J., and Feigenbaum, E. (1990). Arthur Samuel: pioneer in Machine Learning. *Commun. ACM* 33 (11), 137–139.

Wijnands, J. S., Qian, G., and Kuleshov, Y. (2016). Variable Selection for Tropical Cyclogenesis Predictive Modeling. *Monthly Weather Rev.* 144 (12), 4605–4619. doi:10.1175/mwr-d-16-0166.1

Wijnands, J. S., Shelton, K., and Kuleshov, Y. (2014). Improving the Operational Methodology of Tropical Cyclone Seasonal Prediction in the Australian and the South Pacific Ocean Regions. *Adv. Meteorology* 2014, 838746. doi:10.1155/2014/838746

Williams, R. J. (1992). Simple Statistical Gradient-Following Algorithms for Connectionist Reinforcement Learning. *Machine Learn.* 8 (3-4), 229–256. doi:10.1007/bf00992696

Wu, R.-T., and Jahanshahi, M. R. (2019). Deep Convolutional Neural Network for Structural Dynamic Response Estimation and System Identification. *J. Eng. Mech.* 145 (1), 04018125. doi:10.1061/(asce)em.1943-7889.0001556

Wu, T., and Kareem, A. (2013). Bridge Aerodynamics and Aeroelasticity: A Comparison of Modeling Schemes. *J. Fluids Structures* 43, 347–370. doi:10.1016/j.jfluidstructs.2013.09.015

Wu, T., and Kareem, A. (2011). Modeling Hysteretic Nonlinear Behavior of Bridge Aerodynamics via Cellular Automata Nested Neural Network. *J. Wind Eng. Ind. Aerodynamics* 99 (4), 378–388. doi:10.1016/j.jweia.2010.12.011

Wu, T., Li, S., and Sivaselvan, M. (2019). Real-time Aerodynamics Hybrid Simulation: a Novel Wind-Tunnel Model for Flexible Bridges. *J. Eng. Mech.* 145 (9), 04019061. doi:10.1061/(asce)em.1943-7889.0001649

Wu, T. (2013). "Nonlinear bluff-body Aerodynamics," (Indiana, USA: University of Notre Dame). Doctoral dissertation.

Wu, T., and Song, W. (2019). Real-time Aerodynamics Hybrid Simulation: Wind-Induced Effects on a Reduced-Scale Building Equipped with Full-Scale Dampers. *J. Wind Eng. Ind. Aerodynamics* 190, 1–9. doi:10.1016/j.jweia.2019.04.005

Wu, X., Ghaboussi, J., and Garrett, J. H., Jr. (1992). Use of Neural Networks in Detection of Structural Damage. *Comput. Structures* 42 (4), 649–659. doi:10.1016/0045-7949(92)90132-j

Yakut, O., and Alli, H. (2011). Neural Based Sliding-Mode Control with Moving Sliding Surface for the Seismic Isolation of Structures. *J. Vibration Control.* 17 (14), 2103–2116. doi:10.1177/1077546310395964

Yang, Q., Gao, R., Bai, F., Li, T., and Tamura, Y. (2018). Damage to Buildings and Structures Due to Recent Devastating Wind Hazards in East Asia. *Nat. Hazards* 92 (3), 1321–1353. doi:10.1007/s11069-018-3253-8

Yasen, M. Z. Y., Al-Jundi, R. A. S., and Al-Madi, N. S. A. "Optimized ANN-ABC for Thunderstorms Prediction," in Proceedings of the 2017 International Conference on New Trends in Computing Sciences (ICTCS), Amman, Jordan, October 2017 (Piscataway, New Jersey, United States: IEEE), 98–103.

Yu, C., Li, Y., Xiang, H., and Zhang, M. (2018). Data Mining-Assisted Short-Term Wind Speed Forecasting by Wavelet Packet Decomposition and Elman Neural Network. *J. Wind Eng. Ind. Aerodynamics* 175, 136–143. doi:10.1016/j.jweia.2018.01.020

Yu, M., Huang, Q., Qin, H., Scheele, C., and Yang, C. (2019). Deep Learning for Real-Time Social media Text Classification for Situation Awareness - Using Hurricanes Sandy, Harvey, and Irma as Case Studies. *Int. J. Digital Earth* 12 (11), 1230–1247. doi:10.1080/17538947.2019.1574316

Yu, Y., Yao, H., and Liu, Y. (2020). Structural Dynamics Simulation Using a Novel Physics-Guided Machine Learning Method. *Eng. Appl. Artif. Intelligence* 96, 103947. doi:10.1016/j.engappai.2020.103947

Zambrano, T. G., and Peterka, J. A. (1978). Wind Load Interaction on an Adjacent Building. *CER* 77, 78–26.

Zhang, A., and Zhang, L. (2004). RBF Neural Networks for the Prediction of Building Interference Effects. *Comput. Structures* 82 (27), 2333–2339. doi:10.1016/j.compstruc.2004.05.014

Zhang, C., Dai, L., Ma, L., Qian, J., and Yang, B. (2017). Objective Estimation of Tropical Cyclone Innercore Surface Wind Structure Using Infrared Satellite Images. *J. Appl. Remote Sensing* 11 (4), 046030. doi:10.1117/1.jrs.11.046030

Zhang, S., and Nishijima, K. "Statistics-based Investigation on Typhoon Transition Modeling," in Proceedingsof the Seventh International Colloquium on Bluff Body Aerodynamics and Application, Shanghai, China, September 2012, 364–373.

Zhang, T., Lin, W., Lin, Y., Zhang, M., Yu, H., Cao, K., et al. (2019). Prediction of Tropical Cyclone Genesis from Mesoscale Convective Systems Using Machine Learning. *Weather Forecast.* 34 (4), 1035–1049. doi:10.1175/waf-d-18-0201.1

Zhang, W., Fu, B., Peng, M. S., and Li, T. (2015). Discriminating Developing versus Nondeveloping Tropical Disturbances in the Western North Pacific through Decision Tree Analysis. *Weather Forecast.* 30 (2), 446–454. doi:10.1175/waf-d-14-00023.1

Zhang, Y., Chandra, R., and Gao, J. "Cyclone Track Prediction with Matrix Neural Networks," in Proceedings of the 2018 International Joint Conference on Neural Networks (IJCNN), Rio de Janeiro, Brazil, July 2018 (Piscataway, New Jersey, United States: IEEE), 1–8.

Zhao, M., Held, I. M., and Lin, S.-J. (2012). Some Counterintuitive Dependencies of Tropical Cyclone Frequency on Parameters in a GCM. *J. Atmos. Sci.* 69 (7), 2272–2283. doi:10.1175/jas-d-11-0238.1

Zhu, J., and Zhang, W. (2018). Probabilistic Fatigue Damage Assessment of Coastal Slender Bridges under Coupled Dynamic Loads. *Eng. Structures* 166, 274–285. doi:10.1016/j.engstruct.2018.03.073

Conflict of Interest: The authors declare that the research was conducted in the absence of any commercial or financial relationships that could be construed as a potential conflict of interest.

Publisher's Note: All claims expressed in this article are solely those of the authors and do not necessarily represent those of their affiliated organizations, or those of the publisher, the editors and the reviewers. Any product that may be evaluated in this article, or claim that may be made by its manufacturer, is not guaranteed or endorsed by the publisher.

APPENDIX A: LIST OF REVIEWED MACHINE LEARNING ALGORITHMS (NOTE: ACRONYMS WITH * REPRESENT THOSE REVIEWED IN THIS CONTRIBUTION).

A2C advantage actor critic
AdaBoost* adaptive boosting
AE* autoencoder
ALEN* adaptive linear element network
ANFIS* adaptive neuro-fuzzy inference system
ANN* artificial neural network
AWN* adaptive wavelet network
BNB* Bernoulli naive Bayes
BNN* Bayesian neural network
CGAN conditional GAN
CNN* convolutional neural network
CNN-AE* convolutional neural network-based autoencoder
ConvLSTM* convolutional Long Short-Term Memory
DCGAN deep convolutional GAN
DDPG* deep deterministic policy gradient
DDQN double deep Q-network
DNN* deep neural network
DQN deep Q-network
DRL* deep reinforcement learning
DRNN* diagonal recurrent neural networks
DT* decision tree
ENN* Elman neural network
ERBFN* radial basis function neural network
ERNN* Elman recurrent neural networks
FIS* fuzzy inference system
FNN* fuzzy neural network
GAN* generative adversarial network
GBRT* gradient boosted regression trees
GBTE* gradient-boosted tree ensembles
GMDH* group method of data handling
GNB* gaussian naïve Bayes
GPR* gaussian process regression
GRU* gated recurrent unit network
GRNN* generalized regression neural network
ICA independent component analysis
IIRANN* infinite impulse response artificial neural network
JRNN* Jordan recurrent neural networks
KEDL* knowledge-enhanced deep learning
KE-DRL* knowledge-enhanced deep reinforcement learning
KE-LSTM* knowledge enhanced long short-term memory
KM k-means
KNN* k-nearest neighbors
LAFMN* local activation feedback multilayer network
LDA* linear discriminant analysis
LNN* linear neural network
LR* logistic regression
LSSVM* least squares support vector machine
LSTM* long short-term memory
MC* multiple correlation
MFQL* modified fuzzy Q-learning
MLR* multiple linear regression
MNB* multinomial naive Bayes
MNN* matrix neural network
MSC mean-shift clustering
NB* naïve Bayes
NESN* nonlinear echo state networks
NLN* neural logic network
OLR* ordinary linear regression
PCA principal component analysis
PI* Physics-informed
PPO proximal policy optimization
QDA* quadratic discriminant analysis
QL* Q-learning
RBF* radial basis function
RBFNN* radial basis function neural network
RF* random forest
RL* reinforcement learning
RNN* recurrent neural networks
RR* ridge regression
SC spectral clustering
SD-AE* stacked denoising autoencoder
SLDA* supervised latent Dirichlet Allocation
SGD* stochastic gradient descent
SVM* support vector machines
SVR* support vector regression
TRPO trust region policy optimization
WGAN Wasserstein GAN
XGBoost* extreme gradient boosting